# ACIDIZING SANDSTONE RESERVOIRS USING DIFFERENT ACID SYSTEMS

A Dissertation

by

QIN JI

Submitted to the Office of Graduate and Professional Studies of
Texas A&M University
in partial fulfillment of the requirements for the degree of

DOCTOR OF PHILOSOPHY

| | |
|---|---|
| Chair of Committee, | Hisham A. Nasr-El-Din |
| Committee Members, | Mahmoud El-Halwagi |
| | Stephen A. Holditch |
| | Zoya Heidari |
| Head of Department, | Daniel A. Hill |

August 2017

Major Subject: Petroleum Engineering

# ABSTRACT

$AlCl_3$ has been long used as a retarding agent for mud acid, its applications studied in the lab and tested in the field. The theory and mechanism of $AlCl_3$ retardation have been investigated in many projects involving mud acidizing and reservoir permeability enhancement. This dissertation advances this investigation by using solubility tests, coreflood tests, and $^{19}F$ Nuclear Magnetic Resonance (NMR) to better understand the mechanism of $AlCl_3$ working as a retarding agent in mud acid. To enhance the acid performance and to minimize formation damage, this study provides a systematic investigation of the interactions between the Al-based retarded mud acid and clay minerals in sandstone reservoirs. Furthermore, for the first time, $^{19}F$ NMR spectroscopy was used to follow the reactions of Al-based retarded mud acid with clay minerals.

Solubility tests were performed to evaluate the retardation of the Al-based retarded mud acid when reacted with kaolinite, bentonite, and illite. Inductively Coupled Plasma (ICP) and $^{19}F$ NMR were used to analyze the concentrations of key cations and components in the supernatant while the Scanning Electron Microscopy (SEM) and Energy Dispersive X-ray Spectroscopy (EDS) techniques were used to identify the reaction products and detect any precipitation.

This study shows that $AlCl_3$ can retard the reaction of HF with kaolinite, bentonite, or illite at 75 and 200°F in Al-based retarded mud acid. Even with 5 wt% $AlCl_3 \cdot 6H_2O$ added to the acid system, no $AlF_3$ precipitate was observed in any of the solubility tests.

Coreflood tests showed significant permeability improvement in the Berea sandstone when Al-based retarded mud acid was used. The enhancement diminished when the temperature increased to 300°F. CT scan showed deeper penetration of Al-based retarded mud acid than mud acid at 75°F, and the penetration reduced when temperature increased to 200°F. Based on these results, new mechanisms were developed to better understand the reaction of Al-based retarded mud acid and clay minerals.

Field tests were followed in this study. The optimal acidizing plan was found for the Katz field after a series of coreflood experiments. This study provides the guidelines for designing the acidizing jobs in the Katz field.

# DEDICATION

This dissertation is dedicated to my brilliant and outrageously loving and supportive husband, Allen Xin Li, our exuberant, sweet, and kind-hearted little girl, Hannah Jie Li, and to my always encouraging, ever faithful parents, Qin Jiang and Hong Ji.

# ACKNOWLEDGEMENTS

I would like to thank my advisor Dr. Nasr-El-Din for accepting me into his research group, teaching me how to do research, and making me become a real petroleum engineer.

I would like to thank my committee members, Dr. Heidari, Dr. Holditch, and Dr. El-Halwagi, for their guidance and support throughout the course of this research.

I would like to thank Dr. McCain and Dr. Sun for funding me as a teaching assistant. I have been teaching assistant for Dr. McCain for seven semesters and I have learned so much from him. Thank you for giving me the chance to enjoy teaching and sharing my knowledge. You are also one of the best teachers I have ever had.

I would like to thank the stuff members and colleagues in Texas A&M University. Thanks also go to Kinder Morgan $CO_2$ Company for funding the Katz field study project. Thanks Mark Deer, Mark Linroth, Randyln Welch, Edwin Egbobawaye, Buddy Goodgame, Stevie Nosekabel and all the Kinder Morgan Katz team for helping me through the lab experiments and field study.

Finally and most importantly, I would like to thank my families both in China and the United States for their love, encouragement and endless support. Without your support and guidance, I won't be able to grow up to a strong woman. I need to thank my husband Allen for his love and my daughter Hannah for the endless happiness she brings to me. I am so lucky to have you in my life.

## CONTRIBUTORS AND FUNDING SOURCES

This work is supported by a dissertation committee consisting of Professors Dr. Nasr-El-Din and Dr. Holditch of the Department of Petroleum Engineering, Professor Dr. El-Halwagi from the Department of Chemical Engineering, and Professor Dr. Heidari from University of Texas Austin , Department of Petroleum Engineering.

Chapters 4 and 5 were funded by Kinder Morgan $CO_2$ Company. The injection data were provided by Stevie Nosekabel, the reservoir engineer from Kinder Morgan. Figure 75 and 76 were provided by Edwin Egbobawaye, the geologist from Kinder Morgan.

All other work conducted for the dissertation was completed by Qin Ji independently.

# NOMENCLATURE

| | |
|---|---|
| ABF | Ammonium Bifluride, $NH_4HF_2$ |
| ALMA | Al-based Retarded Mud Acid |
| BPM | Barrel per Minute |
| CT | X-ray Computed Tomography |
| EGMBE | Ethylene Glycol Monobutyl Ether |
| FWS | Free Water System |
| GPT | Gallon per Thousand Gallons |
| ICP | Inductively Coupled Plasma |
| II | Injection Index |
| MA | Mud Acid |
| NEFL | Non-emulsified Iron Control Hydrochloric Acid |
| OOIP | Original Oil in Place |
| PPG | Pound per Gallon |
| PV | Pore Volume |
| SEM | Scanning Electron Microscopy |
| SPF | Shot per Foot |
| WAG | Water-alternative-gas |
| XRD | X-ray Diffraction |

TABLE OF CONTENTS

Page

LIST OF FIGURES

Page

LIST OF TABLES

Page

# 1 INTRODUCTION*

Acidizing is a process that involves an unsteady, nonisothermal 3D flow in porous media reacting with chemicals. Acidizing can lead to continuous variation in the porosity and permeability of the porous medium because of dissolution of the rock matrix and precipitation of the reaction products. The goal of acidizing is to remove the formation damage caused by drilling, workover, or completion processes, as it can restore the original formation permeability of the sandstone reservoir.

Three steps are needed when acidizing sandstone reservoirs: preflush, main treatment, and post-flush. The mixture of hydrochloric acid (HCl) and hydrofluoric acid (HF), known as mud acid, has been extensively used as the main treatment (Gidley 1985; Smith and Hendrickson 1965). In sandstone reservoirs, HF can dissolve aluminosilicates and silica (Gdanski 1998, 1999, 2000), while HCl keeps the pH low enough to prevent the reaction products from precipitating in spent acid.

Three reactions were involved when HF reacted with feldspars (Gdanski 1998, 1999, 2000). Zhou et al. (2013) summarized the primary, secondary, and tertiary reactions.

Primary reaction (Gdanski 1998):

$$(5+\mathrm{x})\mathrm{HF} + \mathrm{M}-\mathrm{Al}-\mathrm{Si} + (3-\mathrm{x}+1)\mathrm{H}^{+} \rightarrow \mathrm{HSiF_5} + \mathrm{AlF_x^{(3-x)}} + \mathrm{M}^{+} + \mathrm{H_2O}, \quad \ldots\ldots (1)$$

*Part of this chapter is reprinted with permission from "Acidizing Sandstone Reservoirs With Aluminum-Based Retarded Mud Acid" by Ji, Q., Zhou, L., and Nasr-El-Din, H.A. 2015. SPE Journal (In press: posted 1 December 2015, SPE-169395-PA) © [2015] by Society of Petroleum Engineers.

Secondary reaction (Gdanski 1999):

$$x/5\,HSiF_5 + M - Al - Si + (3 - x + 1)H^+ + H_2O \rightarrow AlF_x^{(3-x)} + M^+ +$$

silica gel ↓, ……...…...…. (2)

the reaction rate constant was found to be sensitive to temperature. Below 125°F, this reaction was very slow, but the reaction rate above 125°F was fast and quickly went to completion (Gdanski 1998).

Tertiary reaction (Gdanski 2000):

$$yAlF_x^{(3-x)} + (x - y)Al - Si + 3(x - y)H^+ \rightarrow xAlF_y^{(3-y)} + (x - y)\text{silica gel} \downarrow \quad .$$

…… (3)

Where *y* is the number of fluorides coordinated with Al after tertiary reaction, $0 < y < x$. The rate constant was determined under various temperatures and the reaction with clays was found to be very slow below 200°F (Gdanski 1998).

The success rate of using mud acid to acidize sandstone reservoirs varies. Simon and Anderson (1990) reported field cases of formation damage caused by mud acid. The following problems and their causes constitute the disadvantages of mud acid application. First, the complex acid/rock interactions in the presence of HCl-sensitive clays (e.g., illite) may cause serious problems by choking the pore throats and decreasing the permeability. Second, a high risk of secondary and tertiary reactions may appear in the zones that are not adequately covered by the preflush, especially at elevated temperatures. Third, under high temperatures, the high reaction and corrosion rates of HCl spend the acid at a fast rate (Gdanski and Shuchart 1996; Simon and Anderson 1990; Thomas et al. 2002).

### *1.1 Al-Based Retarded Mud Acid*

In 1985, Gdanski introduced the Al-based retarded mud acid (15 wt% HCl, 1.5 wt% HF, and 5 wt% $AlCl_3 \cdot 6H_2O$, ALMA) as a retarded mud acid system. He proposed that $AlCl_3$ reacts with HF as per Eq. 4,

$$AlCl_3 + 4HF \leftrightarrow AlF_4^- + H^+ + 3HCl \quad \text{.....(4)}$$

Then, $AlF_4^-$ hydrolyzes deep in the formation and regenerates HF, such that

$$AlF_4^- + 3H^+ \overset{slow}{\longleftrightarrow} AlF^{2+} + 3HF. \quad \text{.....(5)}$$

Gdanski (1985) found its retardation to quartz powder at temperature up to 300°F in the solubility tests. However it does not retarded the reaction with clays that much. He also performed subsequent coreflood tests at 150°F using 1.75 in. × 6 in. Berea cores (80% quartz, 10% feldspar, and 10% kaolinite). Using four cores, Gdanski applied the retarded mud acid system through them in sequence. Due to the pressure drop from each core to the next, Al-based retarded mud acid was proved to be able to penetration deeper than that obtained with the 12:3 and 13.5:1.5 mud acid systems was achieved. He found the $AlCl_3$ can retard HF effectively at temperatures up to 300°F. When it is mixed with brine, it has fewer tendencies to form precipitates. Gdanski's started the research on the ALMA, however he didn't provide integral results to support his conclusions.

### *1.2 Previous Studies*

Al-Dahlan et al. (2001) added 5913 mg/l Al in the form of $AlCl_3$ to the 12:3 mud acid system and did solubility tests on quartz and clays at 77 and 167°F. This acid system was found to be retarded within the first 0.5 hr with kaolinite and chlorite and to be retarded within the first 1 hr with illite and bentonite. The effect of Fe concentration

and pH on the $AlCl_3$ acid system was investigated by Nasr-El-Din et al. (2002), who found that aluminum compounds (sodium hexafluoroaluminate) precipitated at pH from 1.6 to 7.1, while iron compounds (sodium hexafluoroferrate) precipitated at pH values dependent on the initial iron (Fe III) and HF acid concentrations. A successful field treatment at 150°F using Al-based retarded mud acid was conducted in an oil-production well in Central Saudi Arabia (Nasr-El-Din et al. 1998). Very few studies about the Al-based retarded mud acid system were found.

### *1.3 Objectives*

The characteristics of Al-based retarded mud acid (15 wt% HCl, 1.5 wt% HF, and 5 wt% $AlCl_3 \cdot 6H_2O$) were only studied in solubility tests when reacts with quartz and in coreflood tests with Berea cores at 150°F (Gdanski 1985). The objectives of the present study are to: (1) investigate the mechanisms of how $AlCl_3$ acts as the retarding agent in the mud acid in reaction with aluminosilicates at different temperatures, (2) better compare the Al-based retarded mud acid with mud acid, using solubility tests (with kaolinite, illite, and bentonite at 75 and 200°F), (3) conduct coreflood tests (at 75, 200, and 300°F) using Berea sandstone cores to test the Al-based retarded mud acid performance in sandstone formation, and (4) examine the effect of $AlCl_3$ concentration on the retardation of the acid system.

# 2 EXPERIMENTAL STUDIES*

## *2.1 Materials*

The Al-based retarded mud acid was prepared in the lab with concentrations of 15 wt% HCl, 1.5 wt% HF, and 5 wt% $AlCl_3 \cdot 6H_2O$, and the mole ratio of F/Al is 3.62. HF acid was prepared using ammonium bifluoride ($NH_4HF_2$) and HCl. HCl was purchased from Macron Fine Chemicals in the concentration of 37 wt% while $AlCl_3 \cdot 6H_2O$ and $NH_4HF_2$ were provided by a local service company. $AlCl_3 \cdot 6H_2O$ is in the form of 32° Baumé (50 wt%) solution and $NH_4HF_2$ is solid particles. **Table 1** gives the formula of mud acid and Al-based retarded mud acid. All solutions were prepared by deionized water with the conductivity of 18.3 MΩ·cm. The details of how to prepare these acid systems are shown in Appendix A.

| Acid Type | HCl, g | $NH_4HF_2$, g | $AlCl_3 \cdot 6H_2O$ solution (Baumé=32°), g | DI Water, g |
|---|---|---|---|---|
| Mud Acid (15 wt% HCl, 1.5 wt% HF) | 447.5 | 21.38 | 0 | 531.12 |
| Al-based Retarded Mud Acid (15 wt% HCl, 1.5 wt% HF, and 5 wt% $AlCl_3 \cdot 6H_2O$) | 447.5 | 21.38 | 100 | 431.12 |

Table 1—Formulas for mud acid and Al-based retarded mud acid (1000 g).

*Part of this chapter is reprinted with permission from "Acidizing Sandstone Reservoirs With Aluminum-Based Retarded Mud Acid" by Ji, Q., Zhou, L., and Nasr-El-Din, H.A. 2015. SPE Journal (In press: posted 1 December 2015, SPE-169395-PA) © [2015] by Society of Petroleum Engineers.

Clay minerals were obtained from WARD's Natural Science Company, Florida, USA.

Berea core plugs were cut from Berea sandstone blocks, and each core size was 1.5 in. in diameter and 6 in. in length. The pore volume of each core was between 30 to 32 $cm^3$ and the permeability varied from 20 to 30 md. Ammonium chloride ($NH_4Cl$) used in the core flood was purchased from Macron Fine Chemicals with purity more than 99.5%. The corrosion inhibitor and intensifier were provided by a local service company.

### *2.2 Solubility Test*

The solubility tests (batch) were performed at room temperature and 200°F. Before the test, clays were heated up to 250°F for 4 hr in the oven to remove water. After that the clays were moved into a desiccator to cool done to room temperature. Then at room temperature, 4 g of clay minerals (kaolinite, bentonite, and illite with the particle sizes of 32-45 µm, 32-45 µm, and 90-106 µm, respectively) were mixed to 40 g of 15 wt% HCl, 1.5 wt% HF, and 5 wt% $AlCl_3 \cdot 6H_2O$ solution (Al-based retarded mud acid) or 40 g of 15 wt% HCl and 1.5 wt% HF solution (mud acid) in a plastic beaker. No glass beaker was used because HF reacts with glass. After agitating for 10, 20, or 30 min, and 1, 2, 3, 4, or 6 hr, the suspension was filtered using a 1 µm filter paper. The concentrations of Si, Al, Ca, Mg, and Fe in the filtrate were analyzed by the inductively coupled plasma (ICP) analysis using an Optima 7000 DV ICP-OES system and WinLab $32^{TM}$ software. The solid residues were dried at 250°F for 4 hr and then crushed into powder and mixed well. Three samples were collected and analyzed by the Scanning

Electron Microscopy (SEM) and the Energy-Dispersive X-ray Spectroscopy (EDS) to determine concentrations of Al and Si with the remaining solid.

For the solubility tests at 200°F, an oven was preheated to 200°F. 10 g of clay minerals and 100 g of Al-based retarded mud acid or mud acid were mixed and put into a Teflon liner. To prevent corrosion, 1 vol% corrosion inhibitor and 0.5 vol% intensifier (formic acid) were also added to the mixed acid. The Teflon liner was then pressurized to 300 psi into an aging cell using a nitrogen source, put into the oven, and rotated for 1, 2, 3, 4, or 6 hr. After it reacted for the designated time period, the aging cell was taken from the oven and cooled for approximately 30 min to depressurize. The supernatants and solids were analyzed through the same procedures as those at the room temperature condition. Fresh acid was prepared at the beginning of each solubility test with different reaction times to make the experiment more accurate.

### *2.3 NMR Analysis*

$^{19}F$ Nuclear Magnetic Resonance (NMR) spectroscopy was used to determine the fluoride species following the reaction of the Al-based retarded mud acid with clay minerals. The aluminum fluoride complexes and silicon fluoride complexes from live and spent acids were analyzed by an Agilent Inova 400 NMR spectrometer. Samples were not prepared in the normal glass liners but the FEP (fluorinated ethylene polypropylene copolymer) tube liners to prevent the reaction between HF and glass. 0.5 ml of the live or spent acid was added into the tube liner, and then deuterium oxide ($D_2O$) was added to each sample to provide a reference lock. All samples were run with the internal reference trichloro-fluoro-methane ($CFCl_3$). All of the chemical shifts were

reported in parts per million (ppm, δ) relative to $CFCl_3$ (δ = 0 ppm) using trifluorotulence ($C_5H_5CF_3$, δ = - 63.72 ppm) as an external reference.

### *2.4 Coreflood Experiment*

Berea sandstone cores were used, **Table 2**. The cores were first dried at 250°F for 5 hr and then saturated with 5 wt% ammonium chloride for 4 hr under vacuum. In the coreflood experiment, the overburden pressure was set to 2,000 psi, and the back pressure was 1,000 psi. The injection rate was 2 $cm^3$/min. Then, 5 wt% of $NH_4Cl$ solution was injected into the core. When the pressure drop became stable, this value was used to calculate the initial permeability of the core. If the coreflood experiments were performed at high temperatures, then the temperature was increased to 200 or 300°F. The heating jacket that wrapped the core holder and the heating tapes mounted on the injection line and production lines were used to keep the temperature of the reaction at designate temperature. The diagram of the coreflood experiment is shown as **Fig. 1**. After the pressure drop became stable again, preflush, main treatment, and post-flush fluids were injected in sequence. The system was cooled after the post-flush. When the pressure drop became stable at 75°F, its value was used to calculate the permeability of the treated core. The initial and final permeability of the core were measured at 75°F when the viscosity of the brine (5 wt% of $NH_4Cl$ solution) was 0.907 cp. The core effluent samples were collected every 5 minutes during the experiment and analyzed by ICP to determine the concentrations of Ca, Mg, Fe, Al, and Si. The core was scanned by X-ray computed tomography (CT) both before and after the coreflood experiment, and

the CT results were analyzed utilizing ImageJ software. The model of the CT is Toshiba Aquilion RXL and the resolution is 0.5 mm.

| Grey Berea | Concentration, wt% |
|---|---|
| Quartz | 86 |
| Kaolinite | 5 |
| Feldspar | 3 |
| Illite | 1 |
| Calcite | 2 |
| Dolomite | 1 |
| Chlorite | 2 |

Table 2—Composition of Berea sandstone.

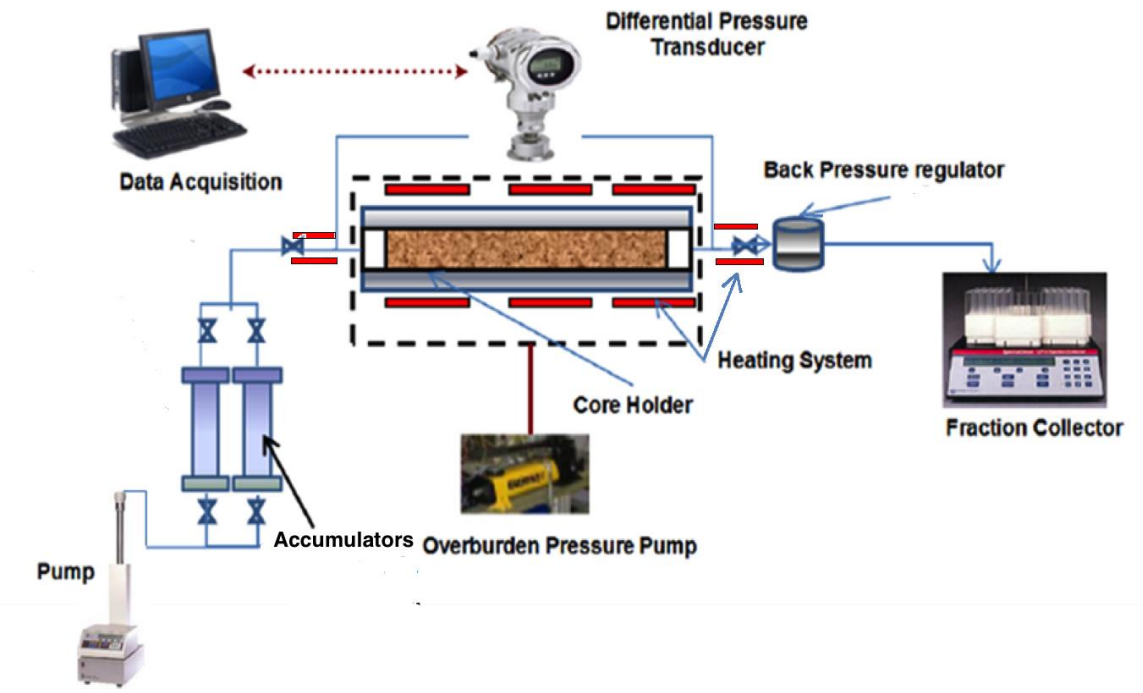


**Fig. 1—Diagram of the coreflood experiment**

# 3 RESULTS AND DISCUSSION*

## *3.1 $^{19}F$ NMR Results*

### 3.1.1 Effect of Reaction Time

**Table 3** gives the chemical shifts of F complexes in samples (1) to (8) from **Fig. 2.** Fig. 2a shows the chemical shifts of $^{19}F$ NMR in the live and spent Al-based retarded mud acid, which reacted with kaolinite for 0.5, 4, and 6 hr. Based on the reports of Shuchart and Buster (1995), Yang et al. (2012), Reyes et al. (2013) and Zhou and Nasr-El-Din (2013), the chemical shifts at -128 to -130 ppm belong to silicon fluoride complexes where as the chemical shifts at -155 to -157 ppm belong to aluminum fluoride complexes. The chemical shift belonging to HF should be at -160 ppm. In all live and spent Al-based retarded mud acid, no HF was observed in the solution. There are two chemical shifts in the range of -128 to -130 ppm, which belong to $H_2SiF_6$ and $HSiF_5$ (Finney et al. 2006). In the live Al-based retarded mud acid system, the Al:F mole ratio is 3.62. Based on the equilibrium constants from Brosset and Orring (1943), the main aluminum fluoride complexes in the solution should be $AlF_3$ and $AlF_4^-$. Bodor et al. (2000) suggested that the more F combining with Al, the less negative the chemical shift will be in the $^{19}F$ NMR. In this case (Figs. 2a (1) to (4)), the chemical shift at -155 ppm was $AlF_4^-$, and at -156 ppm was $AlF_3$. **Figs. 2a** (1) and (2) show that after Al-based

*Part of this chapter is reprinted with permission from "Acidizing Sandstone Reservoirs With Aluminum-Based Retarded Mud Acid" by Ji, Q., Zhou, L., and Nasr-El-Din, H.A. 2015. SPE Journal (In press: posted 1 December 2015, SPE-169395-PA) © [2015] by Society of Petroleum Engineers.

retarded mud acid reacted with kaolinite for 0.5 hr, 53.58 mol% of F separated from Al-F and combined with Si. As the reaction time increased from 0.5 to 6 hr, parts of the F ions were released from Si and back to Al (Figs. 2a (2) and (4)). This effect is because of the precipitation of Si. In this case, the longer the reaction time is, the greater the potential damaged caused by the Al-based retarded mud acid, similar to that of mud acid.

| Sample # | $SiF_5^-$ | $SiF_6^{2-}$ | $AlF_4^-$ | $AlF_3$ |
|---|---|---|---|---|
| 1 | | | -155.202 | -156.202 |
| 2 | -128.229 | -129.102 | -155.151 | -156.084 |
| 3 | -128.268 | -129.034 | -154.927 | -155.877 |
| 4 | -128.213 | -129.078 | -155.128 | -156.053 |
| 5 | -128.919 | -129.782 | -156.022 | -156.933 |
| 6 | -129.131 | -129.922 | -155.804 | -156.806 |
| 7 | -129.256 | -130.039 | -156.137 | -157.146 |
| 8 | | | -154.881 | -155.829 |

Table 3—Chemical shifts of fluoride complexes from the samples in Fig. 1, ppm.

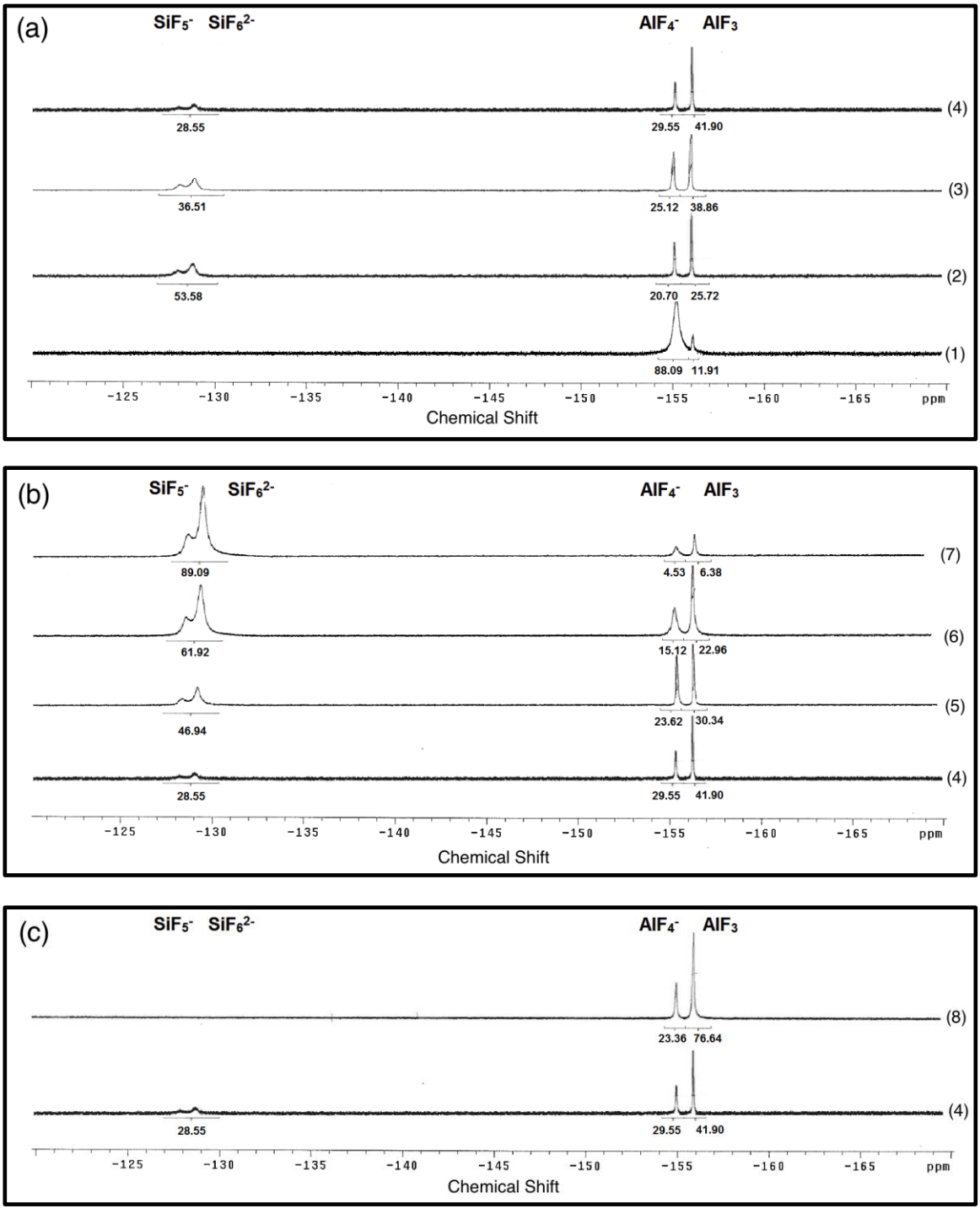


**Fig. 2—$^{19}$F NMR spectra of (a) different reaction time of Al-based retarded mud acid with kaolinite at 75°F (1) 0 hr, (2) 0.5 hr, (3) 4 hr, and (4) 6 hr; (b) different spent acids and clays after reacting for 6 hr at 75°F (4) Al-based retarded mud acid with kaolinite, (5) mud acid with kaolinite, (6) Al-based retarded mud acid with bentonite, and (7) mud acid with bentonite; (c) different temperatures of spent Al-based retarded mud acid with kaolinite after reacting for 6 hr at (4) 75°F and (8) 200°F.**

### 3.1.2 Effect of Clay and Acid Types

**Fig. 2b** (4) and (5) show the chemical shifts of $^{19}F$ NMR in the spent Al-based retarded mud acid and mud acid that reacted with kaolinite for 6 hr while Fig. 1b (6) and (7) show the chemical shifts of $^{19}F$ NMR in the spent Al-based retarded mud acid and mud acid reacted with bentonite for 6 hr. Two shifts at -128 and -129 ppm belong to $HSiF_5$ and $H_2SiF_6$ and two shifts at -155 and -156 ppm belong to $AlF_4^-$ and $AlF_3$. Comparing Fig. 2b (4) and (5), the ratios of aluminum fluoride complexes decreased from 71.45 to 53.96%, while comparing Fig. 2b (6) and (7), the ratios of aluminum fluoride complexes decreased from 38.08 to 10.91%. Clearly, more F was bonded with Al in the spent Al-based retarded mud acid system than the spent mud acid system, which indicates that Al-based retarded mud acid can bond with more F. This effect can keep a low F concentration in the spent acid, which could buffer the system much better. The aluminum fluoride complex ratios in Fig. 2b (4) and (5) (71.45 and 53.96%) were much higher than those in Fig. 2b (6) and (7) (38.08 and 10.91%), which can be explained by the higher Al concentration in kaolinite than bentonite. In both kaolinite and bentonite solubility tests, $^{19}F$ NMR results show greater amounts of Si (in the form of $H_2SiF_6$ and $HSiF_5$) dissolved in the mud acid than the Al-based retarded mud acid system. This observation is consistent with the ICP results, which also indicates $AlCl_3$ can be added as a retarder for the mud acid.

### 3.1.3 Effect of Temperature

**Fig. 2c** shows the chemical shifts of $^{19}F$ NMR in the spent Al-based retarded mud acid reacted at 75 and 200°F, and the final products of aluminum fluoride complexes were still $AlF_4^-$ and $AlF_3$. The difference between Fig. 2c (4) and (8) is that when the temperature rose to 200°F, there was no silicon fluoride complex in the $^{19}F$ NMR results. This indicates the precipitation of all the Si at 200°F, which is consistent with Reyes et al. (2013). Later in the EDS results, the clay residue did not contain F. Therefore, all Si had precipitated in the form of $Si(OH)_4$.

### 3.1.4 New Mechanism of Al-based Retarded Mud Acid

Gdanski (1985) proposed the mechanism of how $AlCl_3$ can act as a retarding agent in the mud acid in Eqs. 1 and 2. After $AlF_4^-$ is produced in Eq. (4), it will slowly release $F^-$ until it becomes $AlF^{2+}$ as HF is keep consuming by reacting with aluminosilicates shown in Eqs. (6) to (8).

$$AlF_4^- + H^+ \overset{slow}{\longleftrightarrow} AlF_3 + HF, \quad \text{.....(6)}$$

$$AlF_3 + H^+ \overset{slow}{\longleftrightarrow} AlF_2^+ + HF \quad \text{.....(7)}$$

$$AlF_2^+ + H^+ \overset{slow}{\longleftrightarrow} AlF^{2+} + HF \quad \text{..... (8)}$$

However, from all the $^{19}F$ NMR results, only $AlF_4^-$ and $AlF_3$ were observed in the spent mud acid or Al-based retarded mud acid at both 75 and 200°F, with no observation of $AlF^{2+}$ or $AlF_2^+$. In this case, the concentrations of $AlF^{2+}$ or $AlF_2^+$ are below the $^{19}F$ NMR detection limit. Therefore most of the $AlF_4^-$ will only be able to hydrolyze with

one $H^+$ and only $AlF_4^-$ can release $F^-$ rather than other Al-F complexes. In this case, the sequence of the reaction will end at Eq. 6. Eqs. 7 and 8 will never exist in the Al-based retarded mud acid system. Therefore, the initial F/Al in the acid system must be above 3 to obtain a better retardation effect. Al-based retarded mud acid has the F/Al mole ratio equal to 3.62, which means most of the Al-F species are in the form of $AlF_4^-$ and the amount of $AlCl_3$ is sufficient to act as the retarding agent in the mud acid system. $^{27}Al$ NMR was not useful in this study as explained by Zhou et al. (2013).

### *3.2 ICP and EDS Result*

**Figs. 3** through **5** show that for all three clay minerals (kaolinite, bentonite, and illite), mud acid can dissolve approximately 1,500 ppm Si more than Al-based retarded mud acid. For both kaolinite and bentonite, the concentration of Si in the spent acid increased at the beginning of the reaction and after nearly 0.5 to 1 hr started to decrease. This indicates that for Si the precipitation rate is greater than the dissolving rate from the clays later in the reaction. For illite, the concentrations of Si in the spent acid increased with the increase in the reaction time, which indicates that the precipitation rate of Si is less than the dissolving rate of illite.

**Figs. 6** through **8** show that mud acid can dissolve approximately 1,500 to 2,000 ppm more of Al than Al-based retarded mud acid when reacting with kaolinite, bentonite, and illite. In Al-based retarded mud acid systems, 7010 ppm of Al has already been added into the system as the retarder. Thus, when the dissolved Al was calculated,

7010 ppm of Al was subtracted. For all three clay minerals, the concentrations of Al in the spent acid increased with the increase in reaction time.

**Figs. 9** and **10** show that mud acid can dissolve approximately 200 and 400 ppm more of Fe than Al-based retarded mud acid when reacted with illite and bentonite, respectively, and the concentration of Fe in the spent acid increased with the reaction time.

For both illite and bentonite, mud acid can dissolve approximately 100 ppm more of Mg than Al-based retarded mud acid, and the concentrations of Mg in the spent acid increased with the reaction time (**Figs. 11** and **12**).

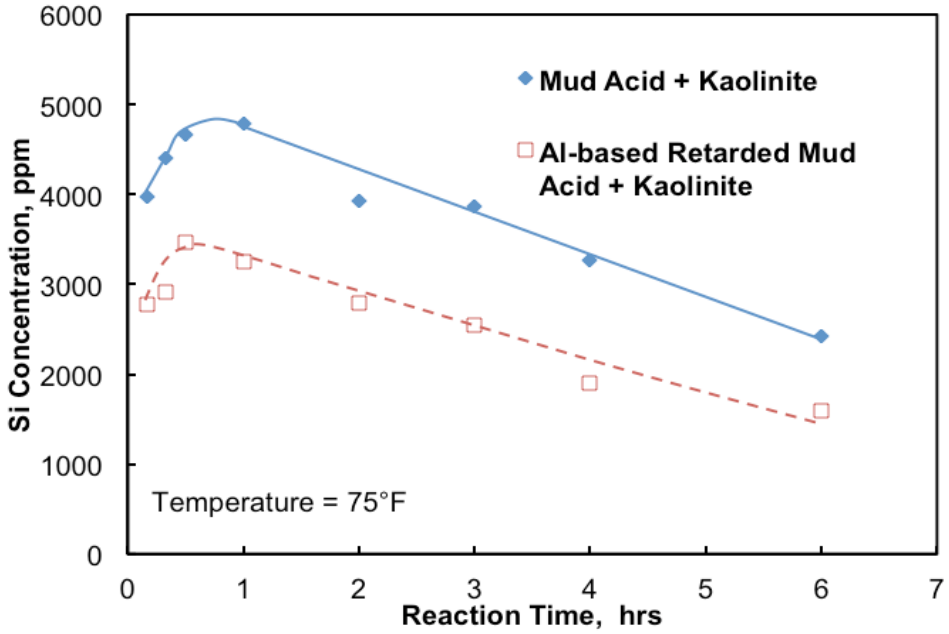


**Fig. 3—Silicon concentration in spent mud and Al-based retarded mud acids as a function of time when react with kaolinite at 75°F.**

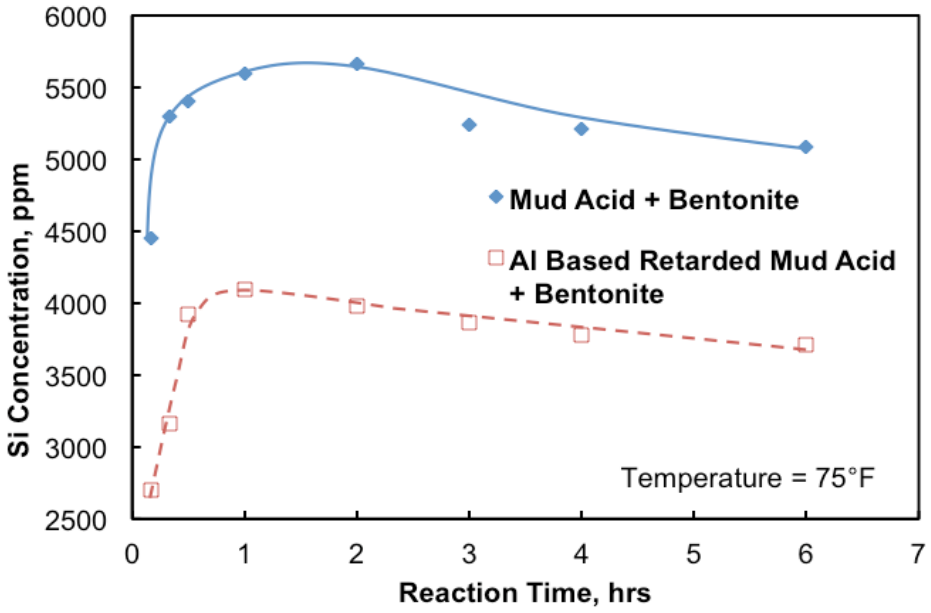


**Fig. 4—Silicon concentration in spent mud and Al-based retarded mud acids as a function of time when react with bentonite at 75°F.**

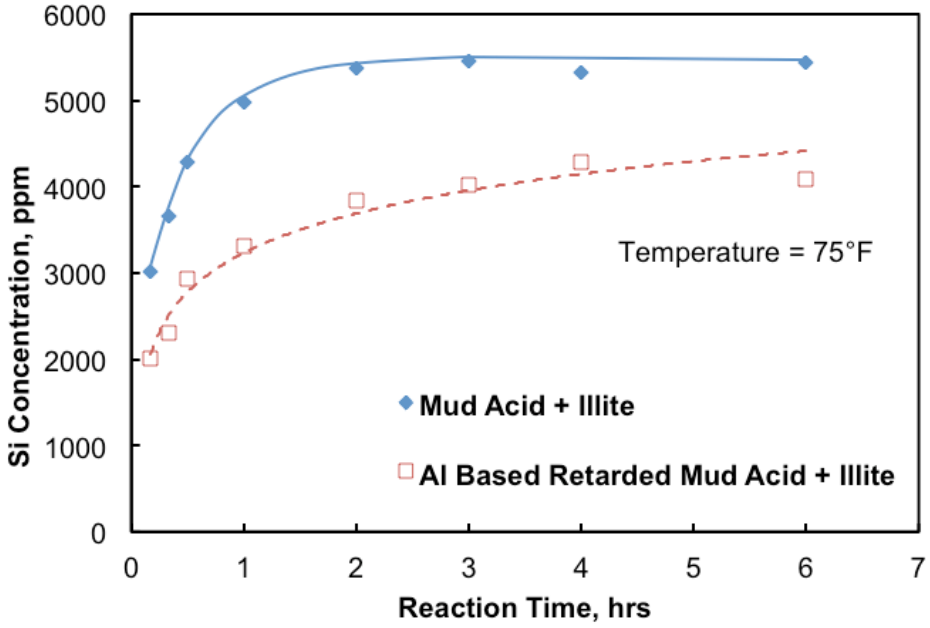


**Fig. 5—Silicon concentration in spent mud and Al-based retarded mud acids as a function of time when react with illite at 75°F.**

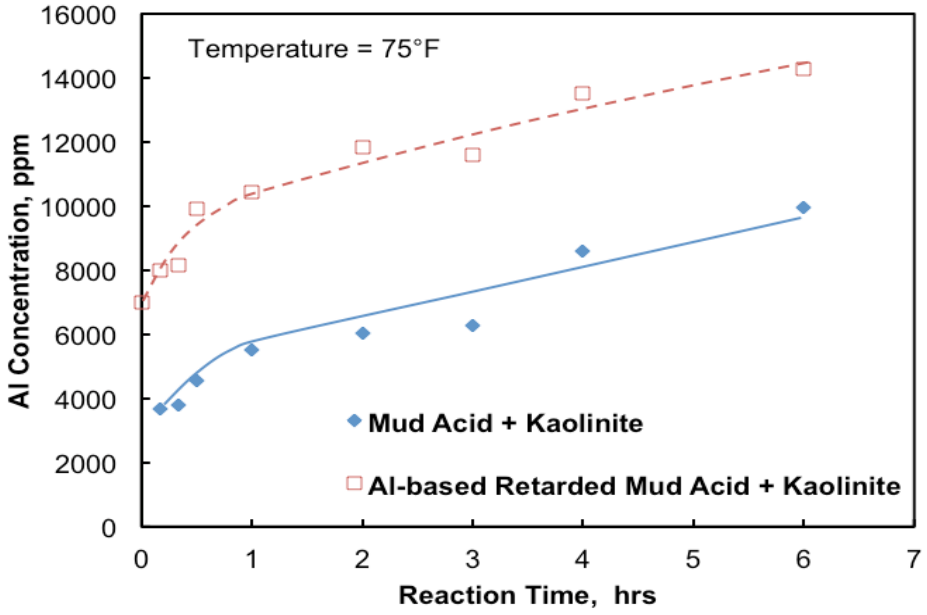


**Fig. 6—Aluminum concentration in spent mud and Al-based retarded mud acids as a function of time when react with kaolinite at 75°F.**

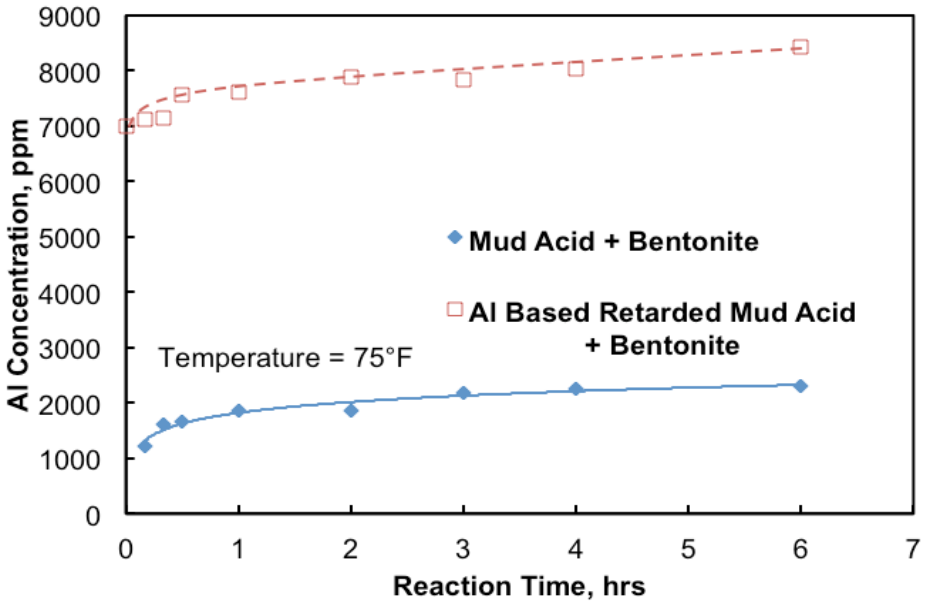


**Fig. 7—Aluminum concentration in spent mud and Al-based retarded mud acids as a function of time when react with bentonite at 75°F.**

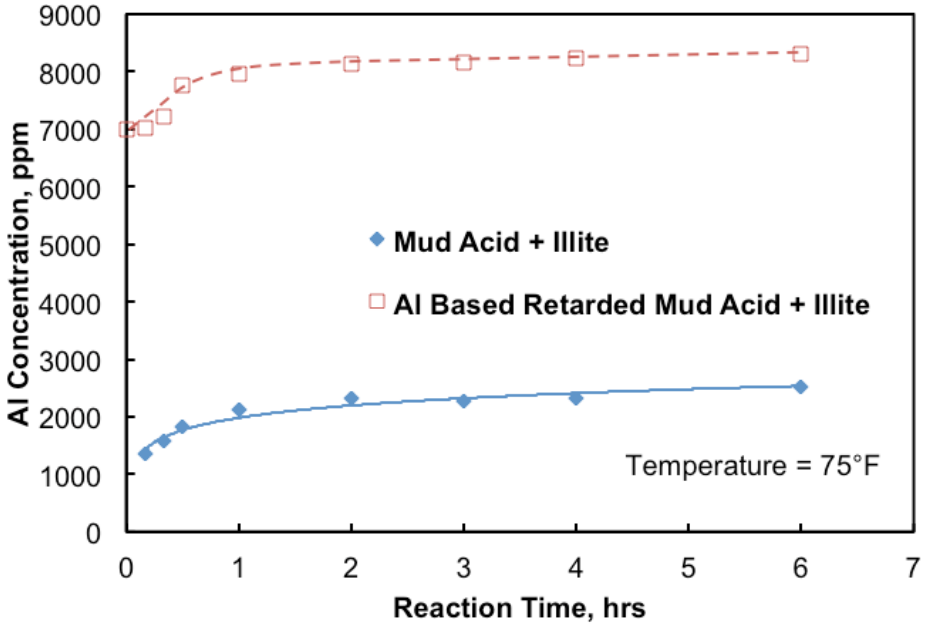


**Fig. 8—Aluminum concentration in spent mud and Al-based retarded mud acids as a function of time when react with illite at 75°F.**

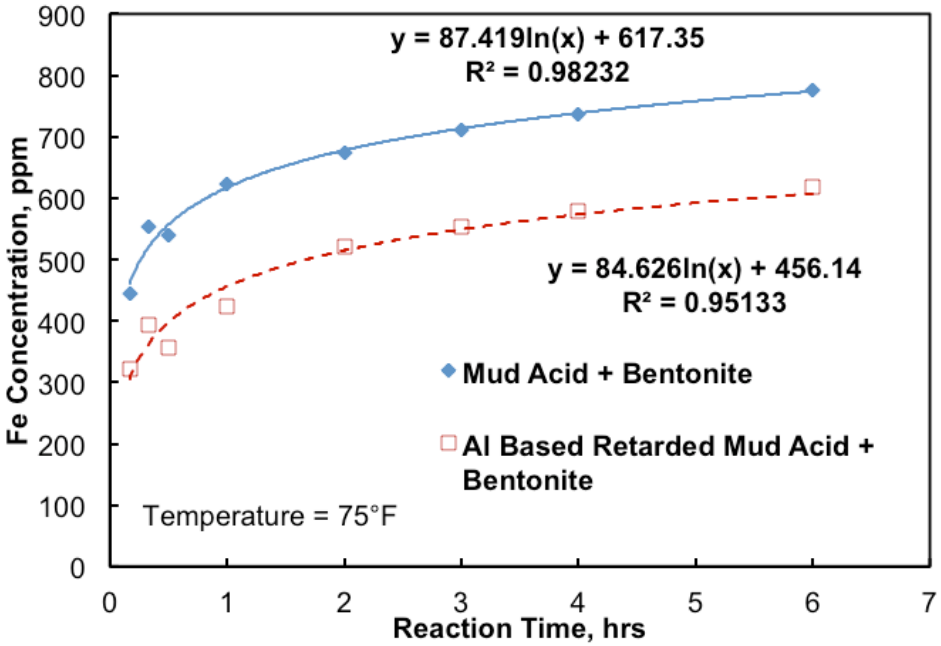


**Fig. 9—Iron concentration in spent mud and Al-based retarded mud acids as a function of time when react with bentonite at 75°F.**

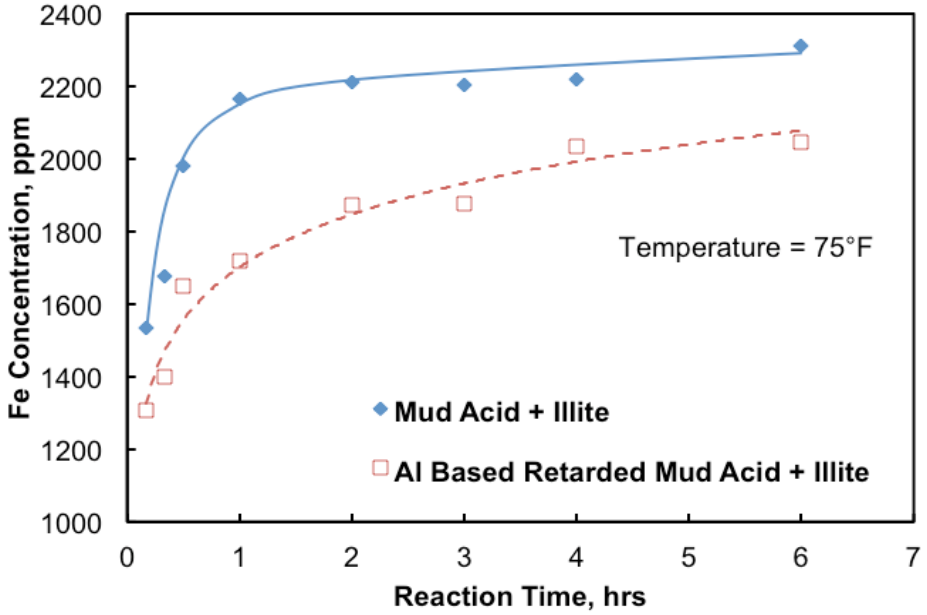


**Fig. 10—Iron concentration in spent mud and Al-based retarded mud acids as a function of time when react with illite at 75°F.**

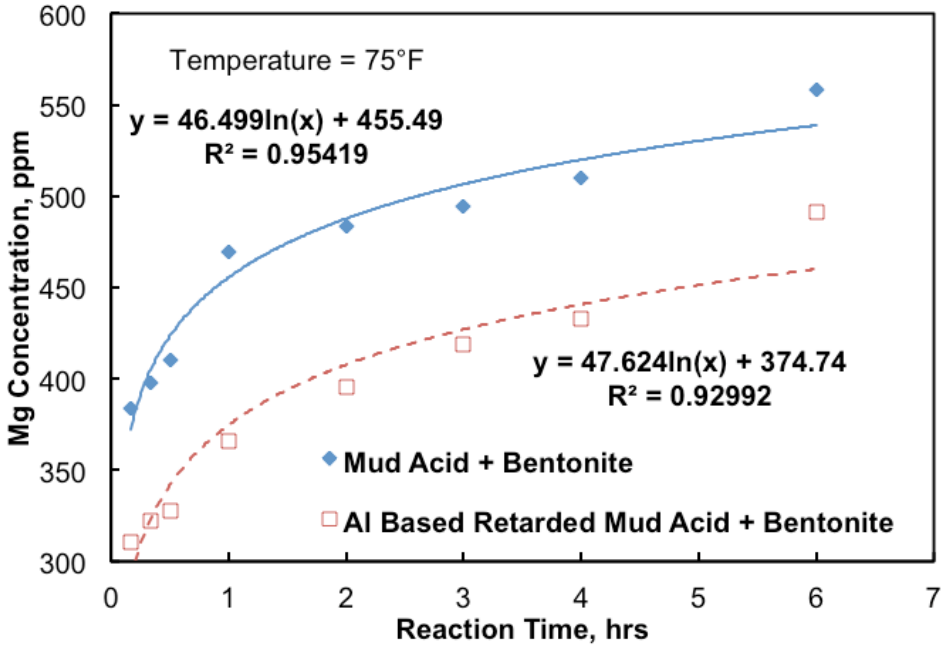


**Fig. 11—Magnesium concentration in spent mud and Al-based retarded mud acids as a function of time when react with bentonite at 75°F.**

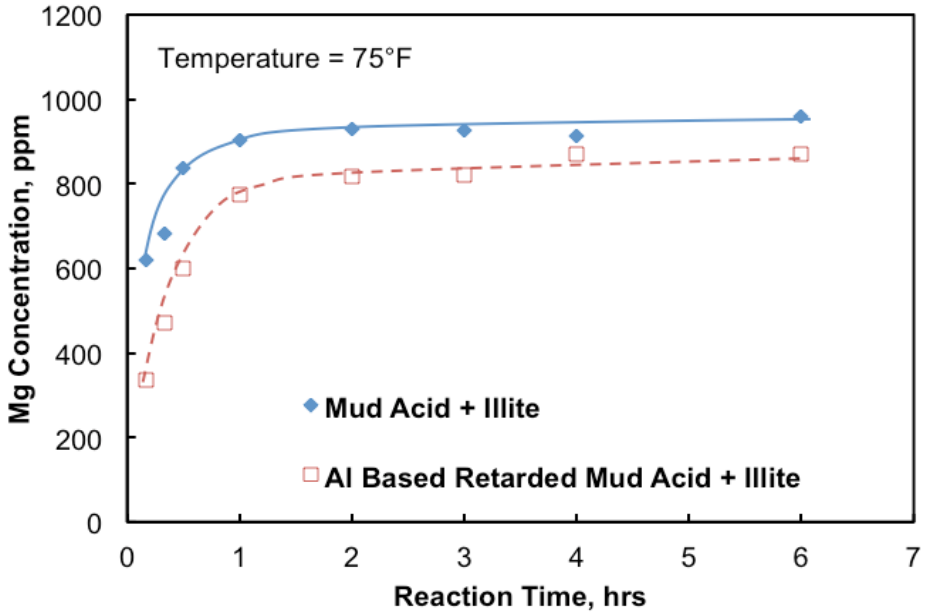


**Fig. 12—Magnesium concentration in spent mud and Al-based retarded mud acids as a function of time when react with illite at 75°F.**

**Fig. 13** shows the EDS results of Si and Al concentrations in the solids after the reaction of Al-based retarded mud acid or mud acid with kaolinite. The concentration of Si increased faster in the solid after the reaction of the mud acid than the Al-based retarded mud acid. This means Si precipitates faster in the mud acid system, which is consistent with the results from ICP. The concentration of Al in the solid parts decreased faster in the mud acid system than in the Al-based retarded mud acid system, which indicates mud acid can dissolve kaolinite faster than Al-based retarded mud acid. So the combined results of ICP and EDS, at room temperature, indicate that $AlCl_3$ can be added into the mud acid system as a retarder.

At 200°F, Si precipitated very fast in the solubility test (**Fig. 14**). After 1 hr, the concentrations of Si were only 140 and 80 ppm in the spent mud acid and Al-based retarded mud acid, respectively. The concentration of Al in the spent mud acid, **Fig. 15**,

is about 2,000 ppm higher than that in the spent Al-based retarded mud acid, which indicated the retardation of the Al-based retarded mud acid at 200°F. However, when compared to the Al concentration at room temperature (Fig. 6), the difference of the results between mud acid and Al-based retarded mud acid shows the retardation effect decreased when temperature increased. This might because when temperature increased, the energy of molecules increased and the bond of Al-F is less strong which cause the buffering effect of Al decreased. EDS never showed any indication of F in the solid residual either at 200°F. So at 200°F, $AlCl_3$ can also be added into the mud acid system as the retarder but less effective than at room temperature.

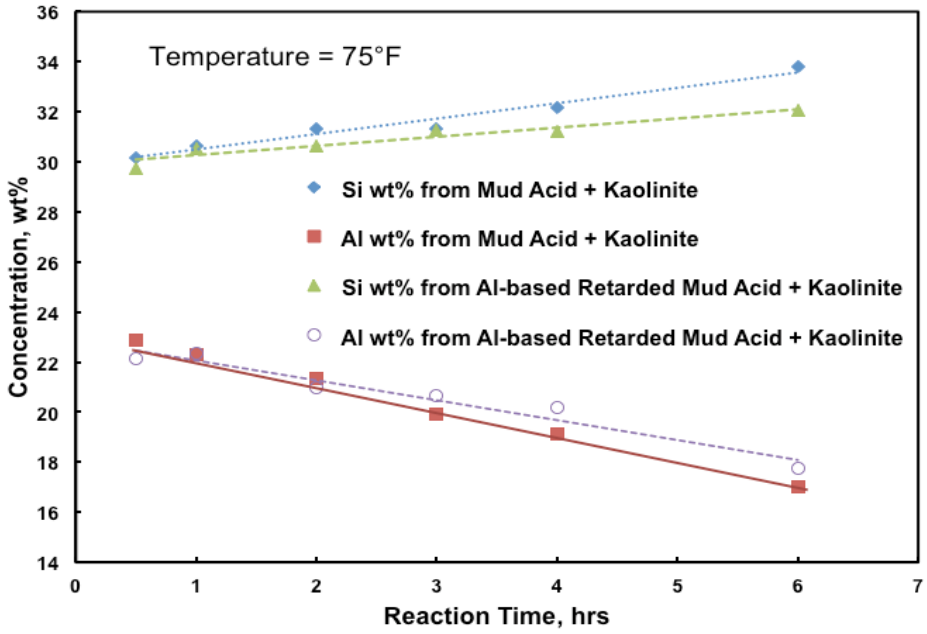


**Fig. 13—Silicon and aluminum concentrations in clay residual of mud and Al-based retarded mud acids as a function of time when react with kaolinite at 75°F.**

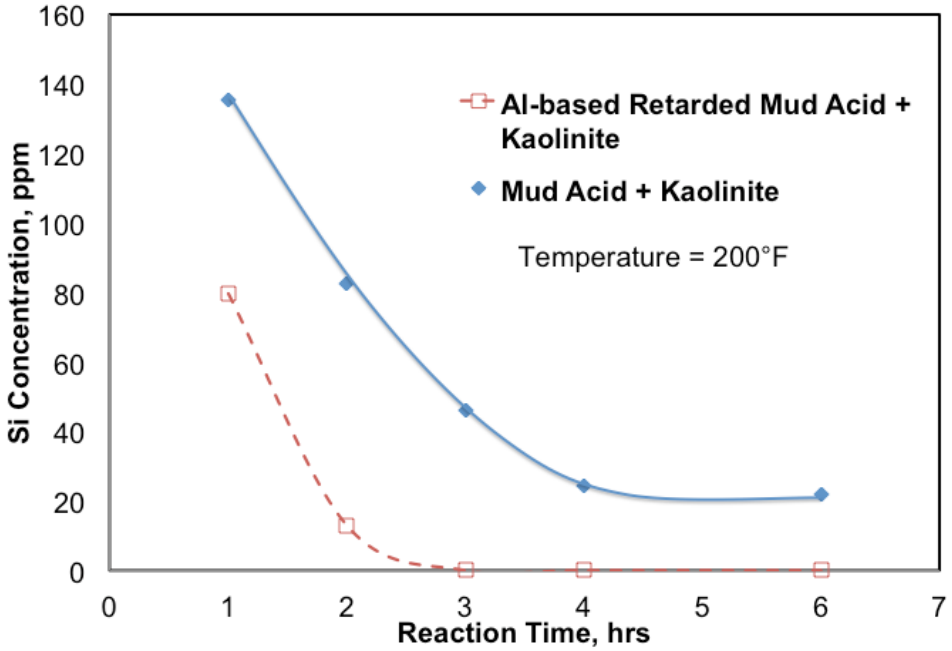


**Fig. 14—Silicon concentration in spent mud and Al-based retarded mud acids as a function of time when react with kaolinite at 200°F.**

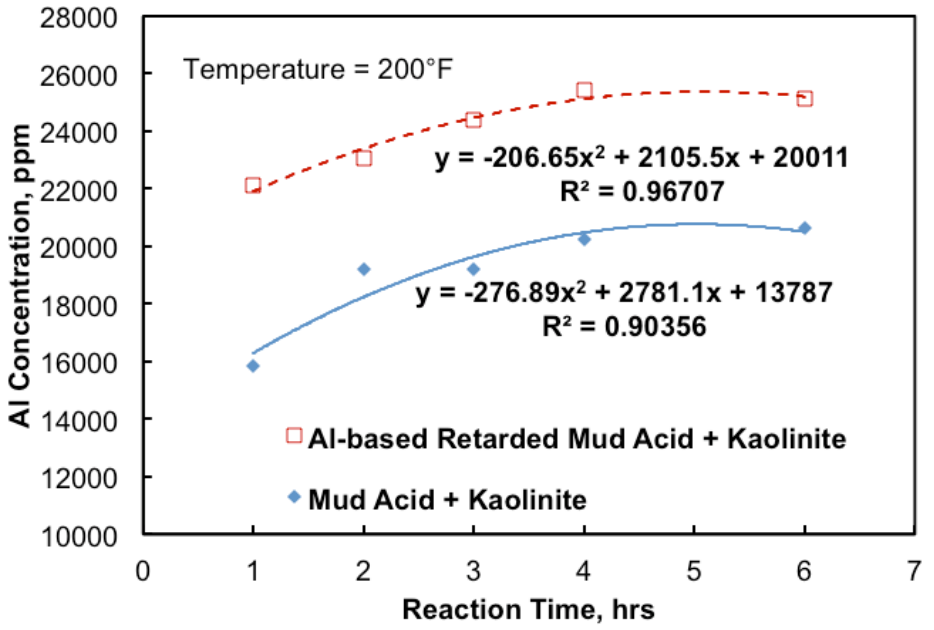


**Fig. 15—Aluminum concentration in spent mud and Al-based retarded mud acids as a function of time when react with kaolinite at 200°F.**

### *3.3 Coreflood Results*

Three steps were performed in the coreflood test. The Berea core was first preflushed with 4 pore volume (PV) of 5 wt% HCl and followed by the main treatment with 3 PV of the Al-based retarded mud acid or mud acid. After reacting with the acids, the core was post-treated with the 5 wt% $NH_4Cl$ until the pressure drop became stable. Based on the pressure drop (**Figs. 16** and **17**) before and after the coreflood experiment, the permeability of the Berea core, calculated by Darcy's law, increased from 23.7 to 73.9 md when Al-based retarded mud acid was used in the main treatment. Permeability increased from 21.1 to 45.5 md when mud acid was used in the main treatment; significant improvement of the permeability has been observed. The increase of permeability for Al-based retarded mud acid and mud acid were 212.6 and 115.4%, respectively. In this case, at 75°F, Al-based retarded mud acid had an enhanced performance in the Berea coreflood test.

The concentrations of Ca, Mg, Al, Si, and Fe in the core effluent samples collected during the Berea coreflood experiments are shown in the **Figs. 18** and **19**. At 75°F the low concentrations of Si and Al in the preflush stage indicated that HCl did not react with alunminosilicates. During the main treatment stage, the concentrations of Al and Si were almost equivalent as shown in Fig. 19. The concentrations of Si and Al (after subtracting 7010 ppm from the Al-based retarded mud acid) in Fig. 18 were both lower than those in Fig. 19, which showed the retardation of Al-based retarded mud acid at room temperature; this was consistent with the solubility test results.

Figs. 18 and 19 show that in the post treatment stage, the Al and Si concentrations were still at a high level for the first PV, which means the main treatment acids were still dissolving aluminum silicates such as clays and feldspars.

In the preflush stage, most of the Ca was dissolved in the first 2 PV of HCl injections in both cases. The removal of Ca in the preflush minimized the precipitation of $CaF_2$ in the main treatment stage, which might have damaged the core. Based on Figs. 18 and 19, 2 PV of HCl preflush is sufficient to remove Ca and Mg, but still have Fe left. In this case, a larger volume of preflush is proposed for the future study.

In the coreflood experiment, it took approximately 0.5 hr to change acids between the preflush stage and the main treatment stage. The first pick of Fe, Al, and Mg in the main treatment stage would be caused by the Al-based retarded mud acid or mud acid reaction with aluminosilicates and also the long soaking time of the preflush acid. The high concentration of Fe was caused by the dissolved chlorite from HF.

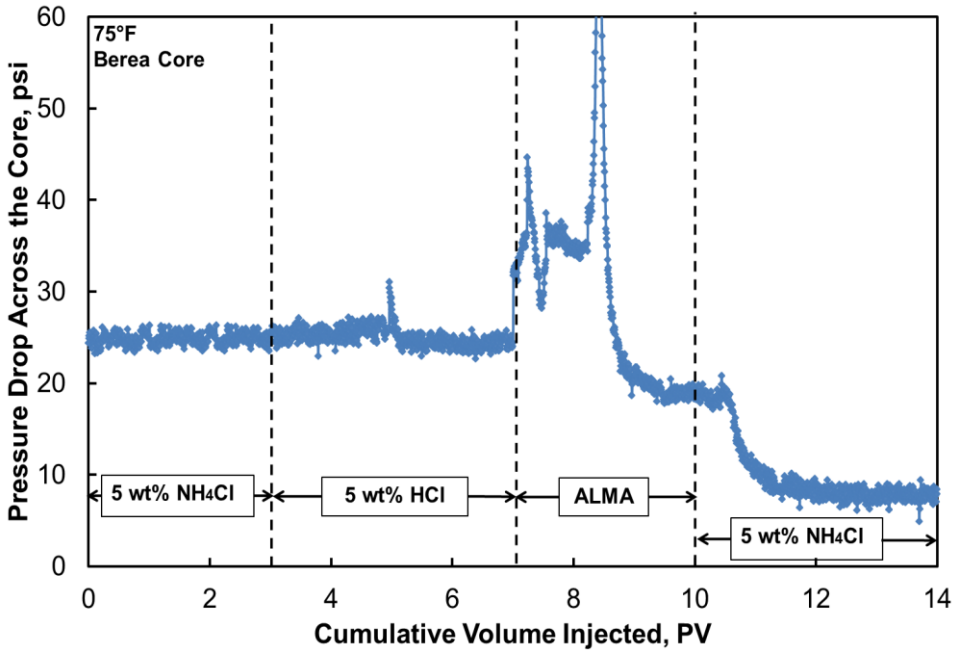


**Fig. 16—Pressure drop across the Berea core, 2 cm$^3$/min, 3 PV of Al-based retarded mud acid.**

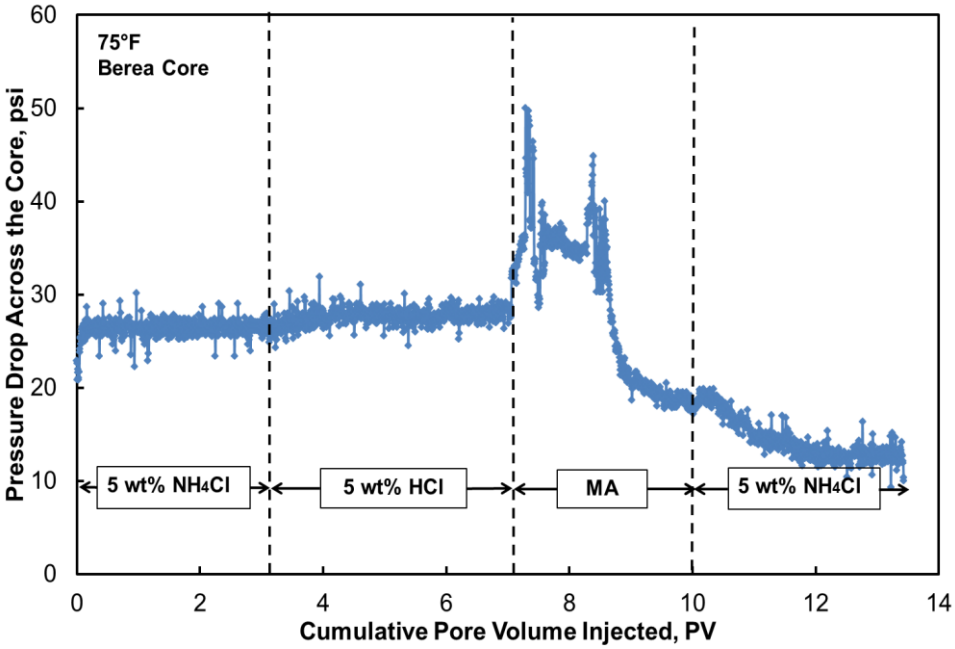


**Fig. 17—Pressure drop across the Berea core, 2 cm$^3$/min, 3 PV of mud acid.**

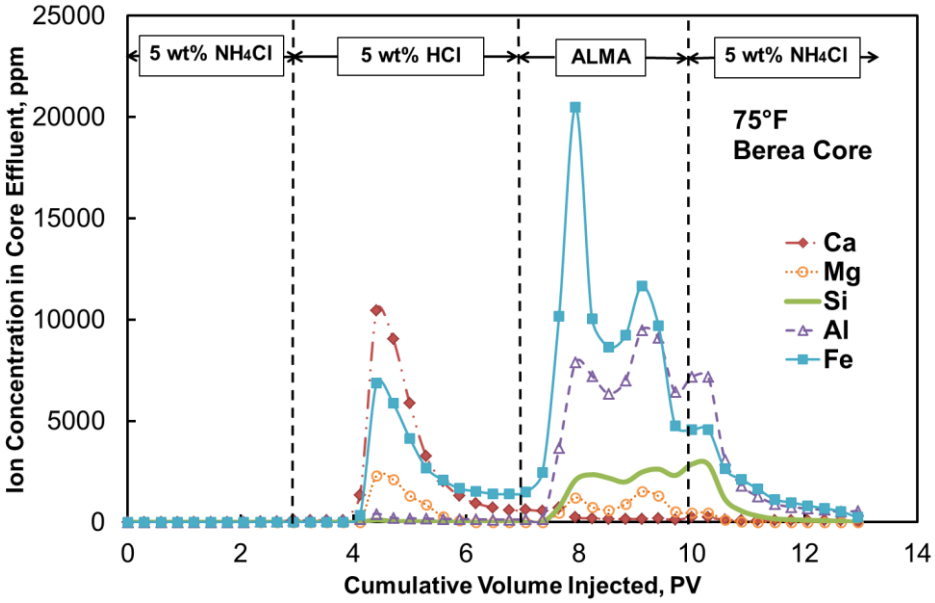


**Fig. 18—Ion concentration in the core effluent samples. Flow rate was 2 $cm^3$/min and the volume of Al-based retarded mud acid was 3 PV.**

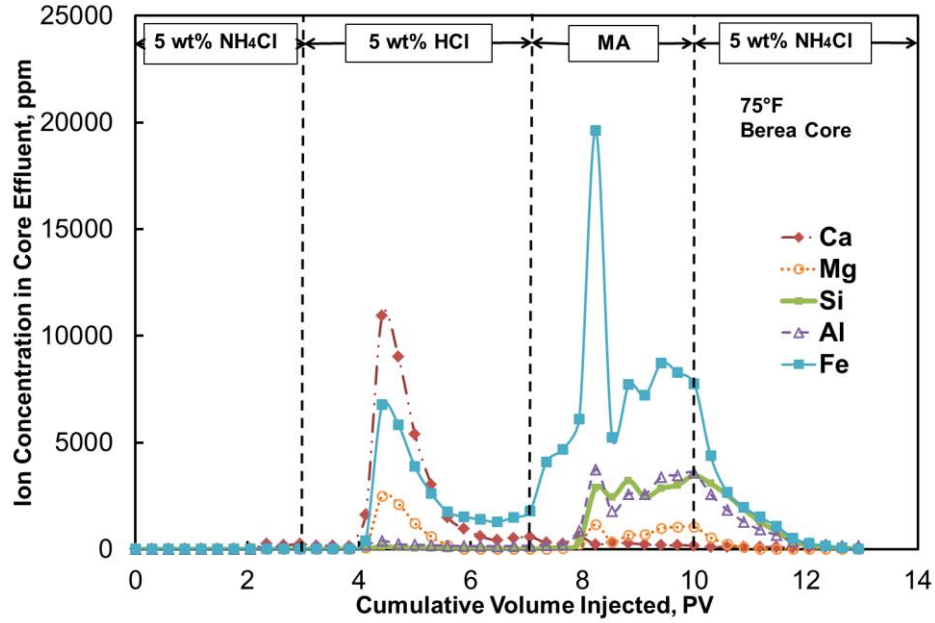


**Fig. 19—Ion concentration in the core effluent samples. Flow rate was 2 $cm^3$/min and the volume of mud acid was 3 PV.**

At 200°F, based on the pressure drop in **Figs. 20** and **21,** the permeability of the Berea core increased from 23.9 to 45.7 md when Al-based retarded mud acid was used in the main treatment, while it increased only from 18.6 to 27.0 md when mud acid was used in the main treatment; hence, significant improvement of the permeability was observed. The increase of permeability for Al-based retarded mud acid and mud acid were 91.6 and 45.4%, respectively. In this case, at 200°F, Al-based retarded mud acid also had a better performance in the Berea coreflood test than mud acid, but compared to the results from75°F, the performance of Al-based retarded mud acid declined.

**Figs. 22** and **23** show that, at 200°F, in the main treatment stage, the concentration of Si and Al was 3000 and 10000 ppm when use Al-based retarded mud acid was used and 4000 and 5500 ppm when mud acid was used. Taking into account the 7010 ppm of Al, which is contributed by the Al-based retarded mud acid, the concentration of Al dissolved from the Berea core was about 2990 ppm. This indicated that the clay minerals in the core reacted with HF in the main treatment stage, and that Al-based retarded mud acid dissolved less clays than mud acid. In the mud acid system, the Si concentration did not show the increment as the same amount of Al as the Al-based retarded mud acid, which indicated more Si precipitated as the silica gel; this could be the reason why the permeability improvement is less than the Al-based retarded mud acid system. An optimistic balance between dissolving aluminum silicates and silica gel precipitation should be found by testing different pore volumes in the main treatment stage in the coreflood test.

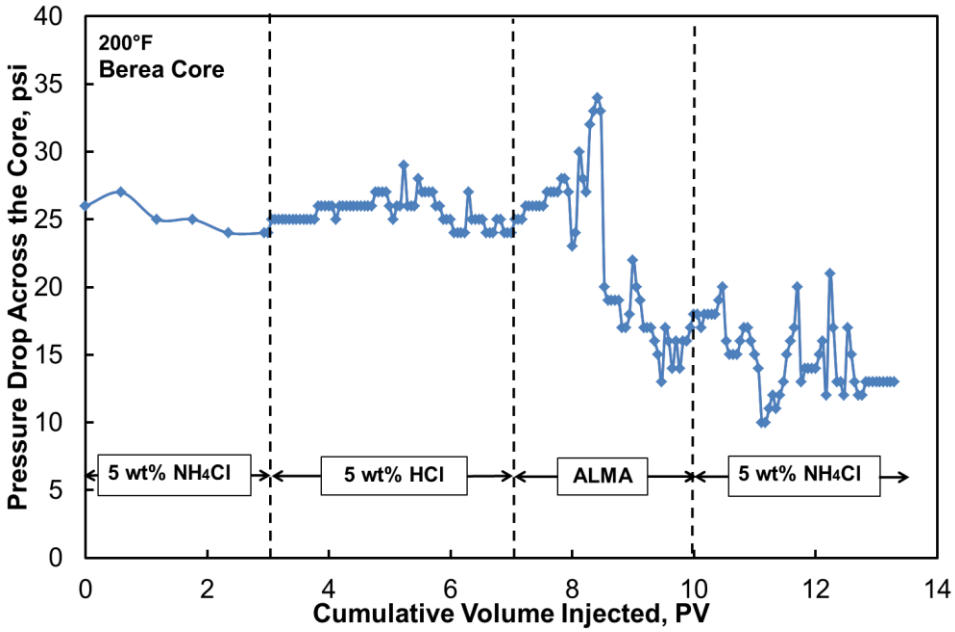


**Fig. 20—Pressure drop across the Berea core, 2 cm$^3$/min, 3 PV of Al-based retarded mud acid.**

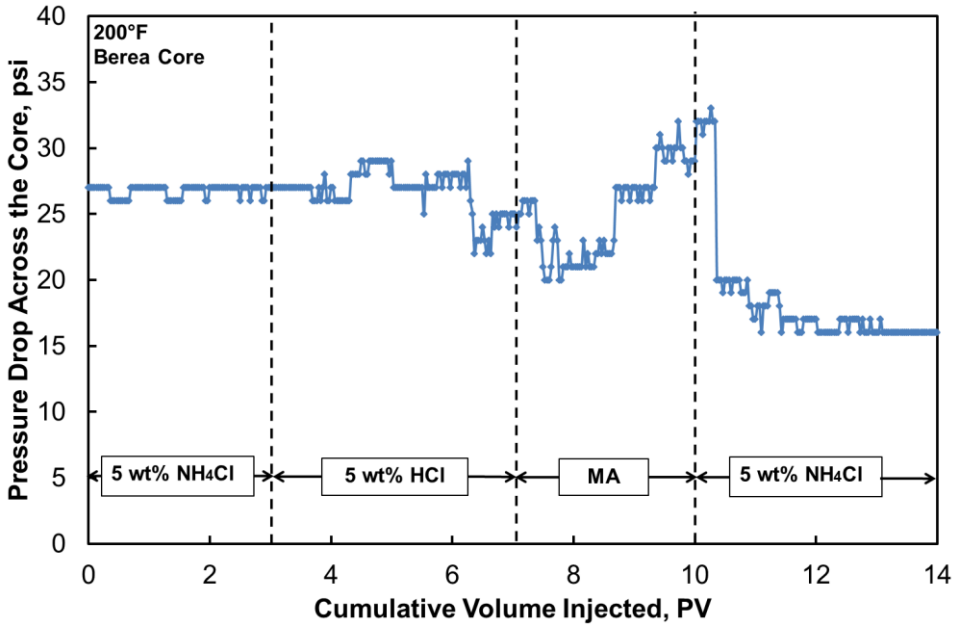


**Fig. 21—Pressure drop across the Berea core, 2 cm$^3$/min, 3 PV of mud acid.**

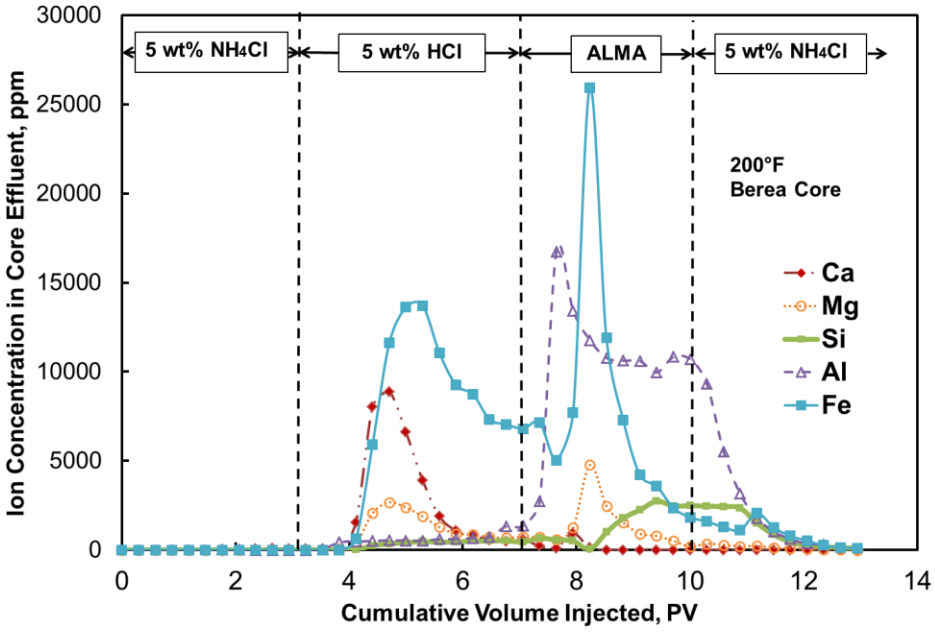


**Fig. 22—Ion concentration in the core effluent samples. Flow rate was 2 cm$^3$/min and the volume of Al-based retarded mud acid was 3 PV.**

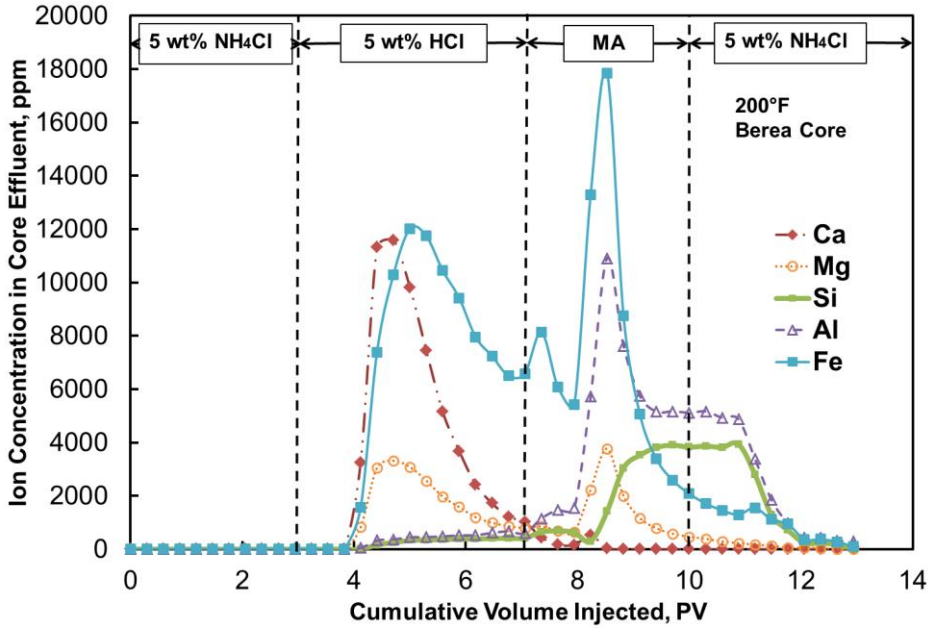


**Fig. 23—Ion concentration in the core effluent samples. Flow rate was 2 cm$^3$/min and the volume of mud acid was 3 PV.**

CT scans were also performed on the cores before and after the coreflood experiments. For the CT images, each pixel has a relative value of linear attenuation coefficient after image reconstruction. The CT number is converted by the attenuation coefficient and can be used as the indicator of the change of density and porosity (Akin and Kovscek 2003). **Figs. 24** and **25** show the CT number across the dry Berea cores before and after the coreflood test at 75 and 200°F with the flow rate of 2 $cm^3$/min, respectively. The CT number is the average value for each cross section. Fig. 24 shows that before acidizing the Berea cores, the CT number for both cores were similar. After acidizing, the CT number for both cores dropped. For the first 0.5 in., the core with the mud acid in the main treatment had a lower CT number than the core with Al-based retarded mud acid in the main treatment. However, after the first 0.5 in., as the results show, the opposite happened, and it lasts until the end of the core. This indicates that at 75°F, Al-based retarded mud acid has a better performance than the mud acid and it can slow down the reaction with aluminosilicates so that to penetrate deeper into the core. Fig. 25 shows that at 200°F, after acidizing, the CT number of each core has smaller difference comparing with that at 75°F condition. For the first 0.5 in., the CT numbers of the core with mud acid in the main treatment are slightly lower than the core with Al-based retarded mud acid in the main treatment which indicates that mud acid spent faster than the Al-based retarded mud acid at the first 0.5 in. After the first 0.5 in., the CT numbers of both cores became similar. The retarding effect of Al-based retarded mud acid reduced after temperature increased to 200°F.

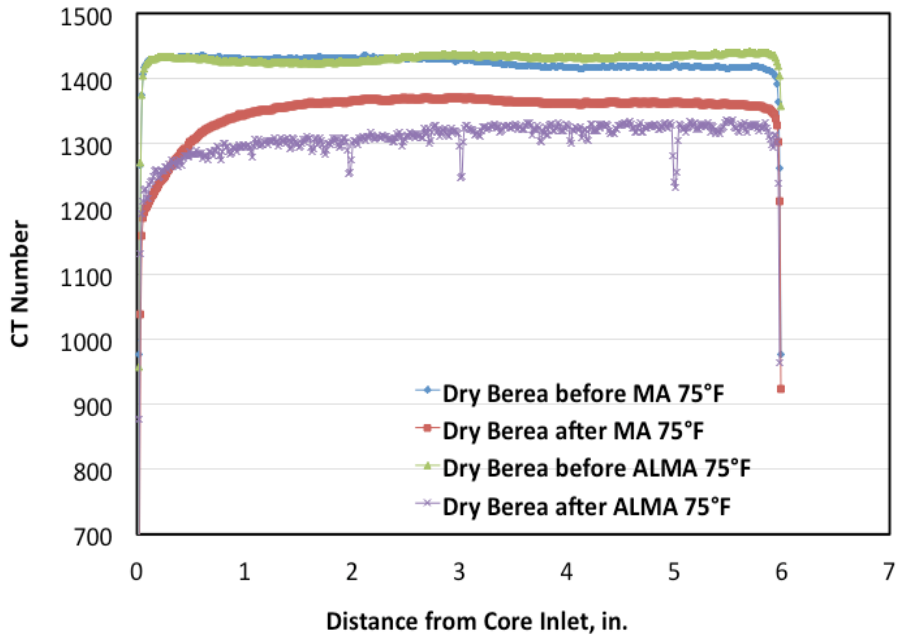


**Fig. 24— CT number across the Berea core after the coreflood test with 2 cm$^3$/min 3 PV of Al-based retarded mud acid and mud acid in the main acid at 75°F.**

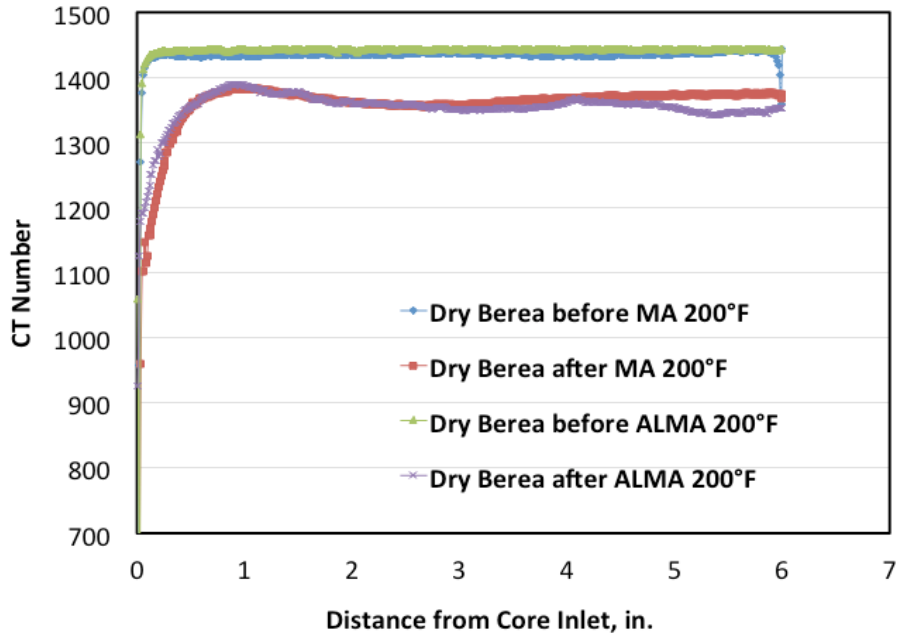


**Fig. 25— CT number across the Berea core after the coreflood test with 2 cm$^3$/min 3 PV of Al-based retarded mud acid and mud acid in the main acid at 200°F.**

**Figs. 26** through **29** show the pressure drop across the core and ion concentrations in the coreflood effluent when Berea core was treated by Al-based retarded mud acid or mud acid at 300°F. The permeability of the Berea core maintain the value of 31.3 md when Al-based retarded mud acid was used in the main treatment, while decreased from 59.5 to 31.2 md when mud acid was used in the main treatment; no improvement of the permeability has been observed. At 300°F, Al-based retarded mud acid has a better stimulation result compared to mud acid, however the retardation of the acid decreased when temperature increased from 75 to 300°F. This observation is also consistent with the results from solubility test. The initial and final permeabilities of Berea sandstone cores in all the coreflood experiments are presented in **Table 4**.

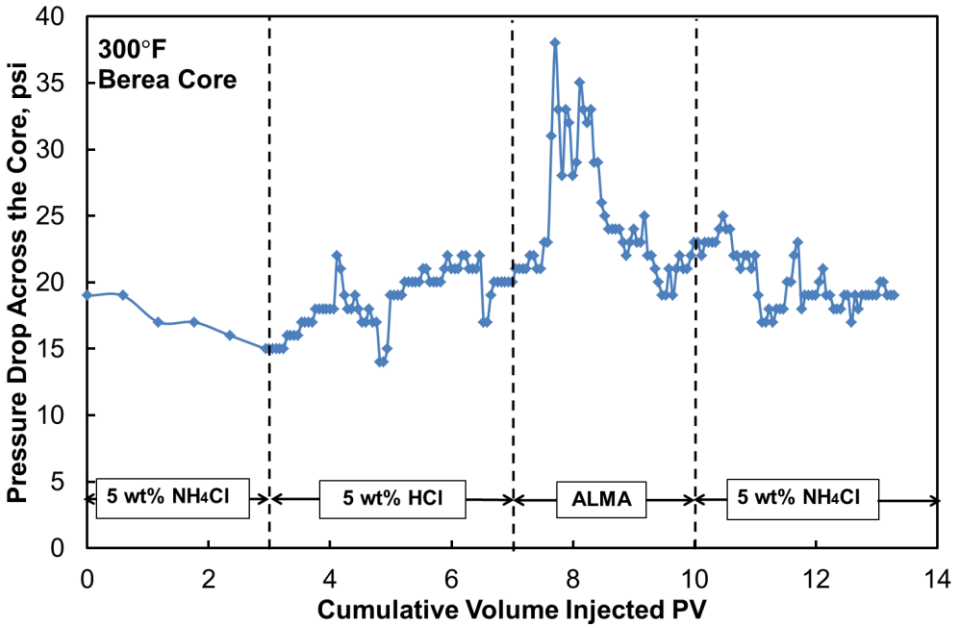


**Fig. 26—Pressure drop across the Berea core, 2 cm$^3$/min, 3 PV of Al-based retarded mud acid.**

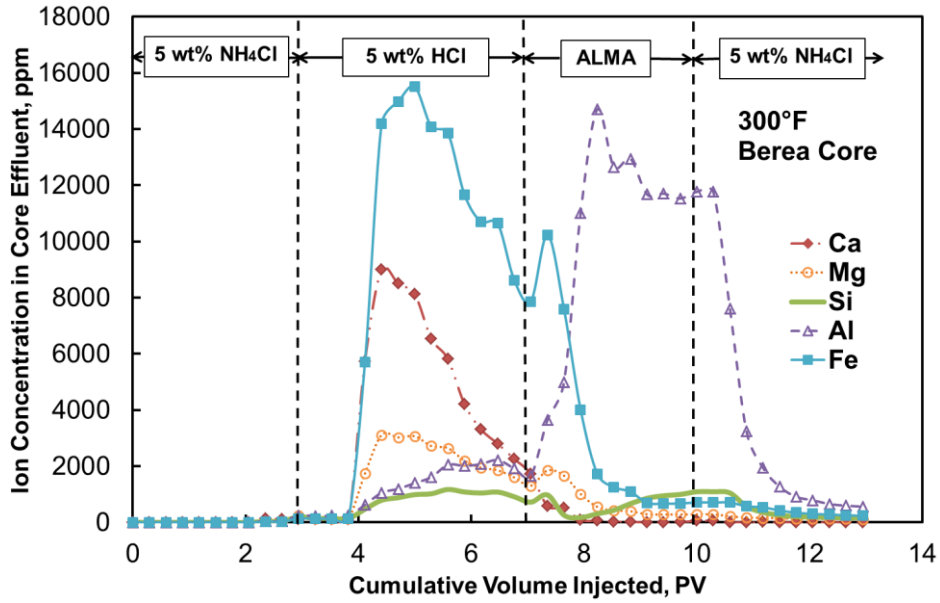


**Fig. 27—Ion concentration in the core effluent samples. Flow rate was 2 cm$^3$/min and the volume of Al-based retarded mud acid was 3 PV.**

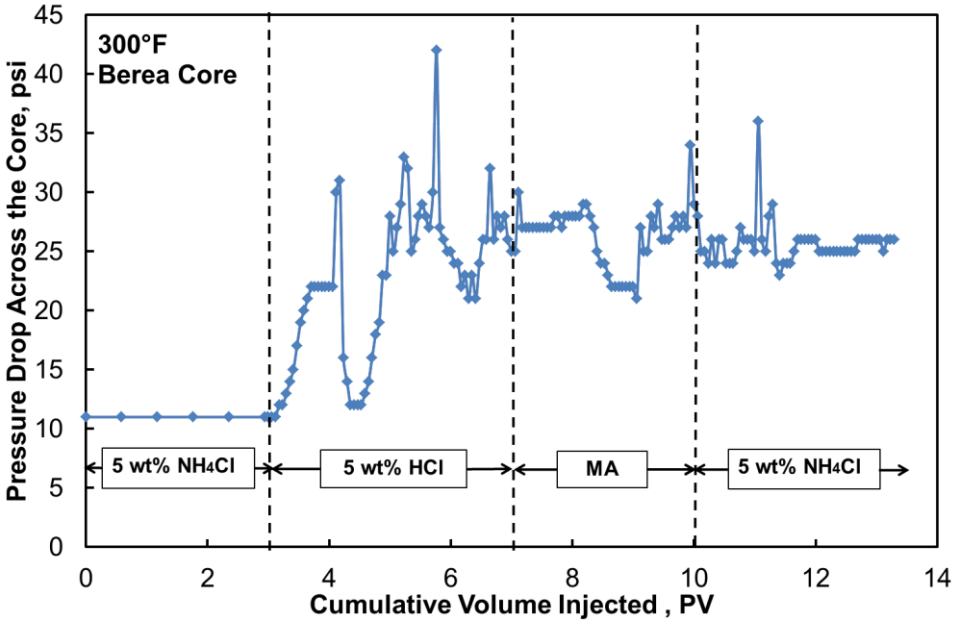


**Fig. 28—Pressure drop across the Berea core, 2 cm$^3$/min, 3 PV of mud acid.**

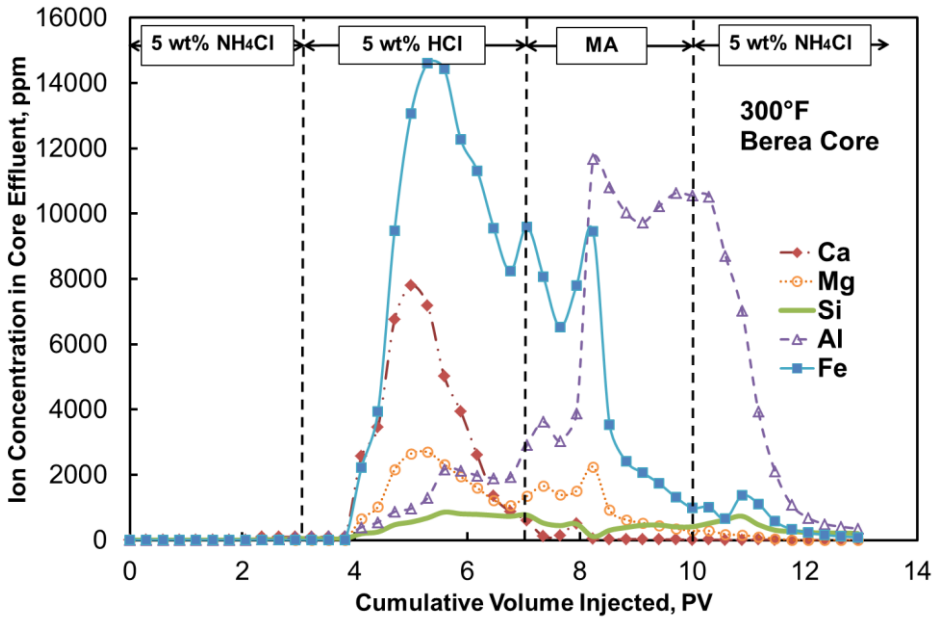


**Fig. 29—Ion concentration in the core effluent samples. Flow rate was 2 cm$^3$/min and the volume of mud acid was 3 PV.**

| Temperature, °F | ALMA | | | MA | | |
|---|---|---|---|---|---|---|
| | $K_{initial}$, md | $K_{final}$, md | Increased K, % | $K_{initial}$, md | $K_{final}$, md | Increased K, % |
| 75 | 23.7 | 73.9 | 212.6 | 21.1 | 45.5 | 115.4 |
| 200 | 23.9 | 45.7 | 91.2 | 18.6 | 27 | 45.2 |
| 300 | 31.3 | 31.3 | 0.0 | 59.5 | 31.2 | -47.6 |

Table 4—Initial and final permeability of Berea sandstone cores after the coreflood test with Al-based retarded mud acid or mud acid at different temperatures.

### *3.4 Conclusions*

Solubility tests of Al-based retarded mud acid (15 wt% HCl, 1.5 wt% HF, and 5 wt% $AlCl_3 \cdot 6H_2O$) and mud acid (15 wt% HCl and 1.5 wt% HF) with kaolinite, illite, and bentonite were performed at both 75 and 200°F. Al-based retarded mud acid with

different concentration of $AlCl_3 \cdot 6H_2O$ has also been tested. Supernatants were analyzed by $^{19}F$ NMR and the concentrations of variance cations were measured by ICP. These tests were followed by coreflood tests at 75, 200, and 300°F.

1. $AlCl_3$ can be added into the mud acid system as a retarder to react with clay minerals at 75 and 200°F. The retarding effect decreased as temperature increased.
2. At 75°F, the higher the $AlCl_3$ concentration is in the Al-based retarded mud acid system, the less clays it can dissolve.
3. $^{19}F$ NMR showed that $AlF_3$ and $AlF_4^-$ in the spent acid were the only two aluminum fluoride complexes, $AlF_4^-$ slowly hydrolyzes with $H^+$ to release HF, which keep the low $F^-$ concentration in the system.
4. $^{19}F$ NMR results also showed that more $F^-$ can complex with Al in the Al-based retarded mud acid system than in the mud acid system, which could lead to a deeper penetration of the acid into the formation.
5. No $AlF_3$ precipitate was observed in any of the Al-based retarded mud acid solubility tests at both 75 and 200°F.
6. At high temperatures, $Si(OH)_4$ precipitates very fast, which might cause formation damage.
7. CT scans showed deeper penetration of Al-based retarded mud acid than mud acid at 75°F, but the penetration reduced when temperature increased to 200°F.

8. Al-based retarded mud acid can better improve the permeability of a Berea sandstone core than mud acid. The lower the temperature is, the better the potential retardation effect of Al-based retarded mud acid could have. The retarding effect diminished at 300°F.

# 4 KATZ FIELD CASE STUDY (LABORATORY STUDY)

## *4.1 Introduction*

Katz field, located in the northeast area in Stonewall County, Texas with small portions in Haskell, King, and Knox counties is a sandstone formation currently in production status with both production and injection wells (**Fig. 30**). Katz Oil Company originally discovered this field in January 1951. Kinder Morgan Production Co. became the major operator in May 2006. Three pay zones were identified in this field and from top to bottom they are called the 1st, 2nd, and 3rd Sand, respectively. The 1st Sand has an average net thickness of 24.4 ft with an average porosity of 16% and average permeability of 53 md. It is located at the depth of around 4800 ft. The Second Sand has an average net thickness of 31.4 ft with an average porosity of 17% and average permeability of 124 md. It is located at the depth of around 4900 ft. The Third Sand has an average net thickness of 26.7 ft with an average porosity of 16% and average permeability of 55 md. It is located at the depth of around 5100 ft (Smith et al. 2012). $CO_2$ water-alternative-gas (WAG) injection was started in December 2010.

The total OOIP for the Katz field is approximately 206.1 MMSTB. The 1st, 2nd, and 3rd Sand OOIPs are calculated to be 64.1, 92.3, and 49.7 MMSTB, respectively. The actual flooded OOIPs (area under the $CO_2$ flooded patterns) are 46.2, 72.5, and 40.4 MMSTB, respectively (Smith et al. 2012).

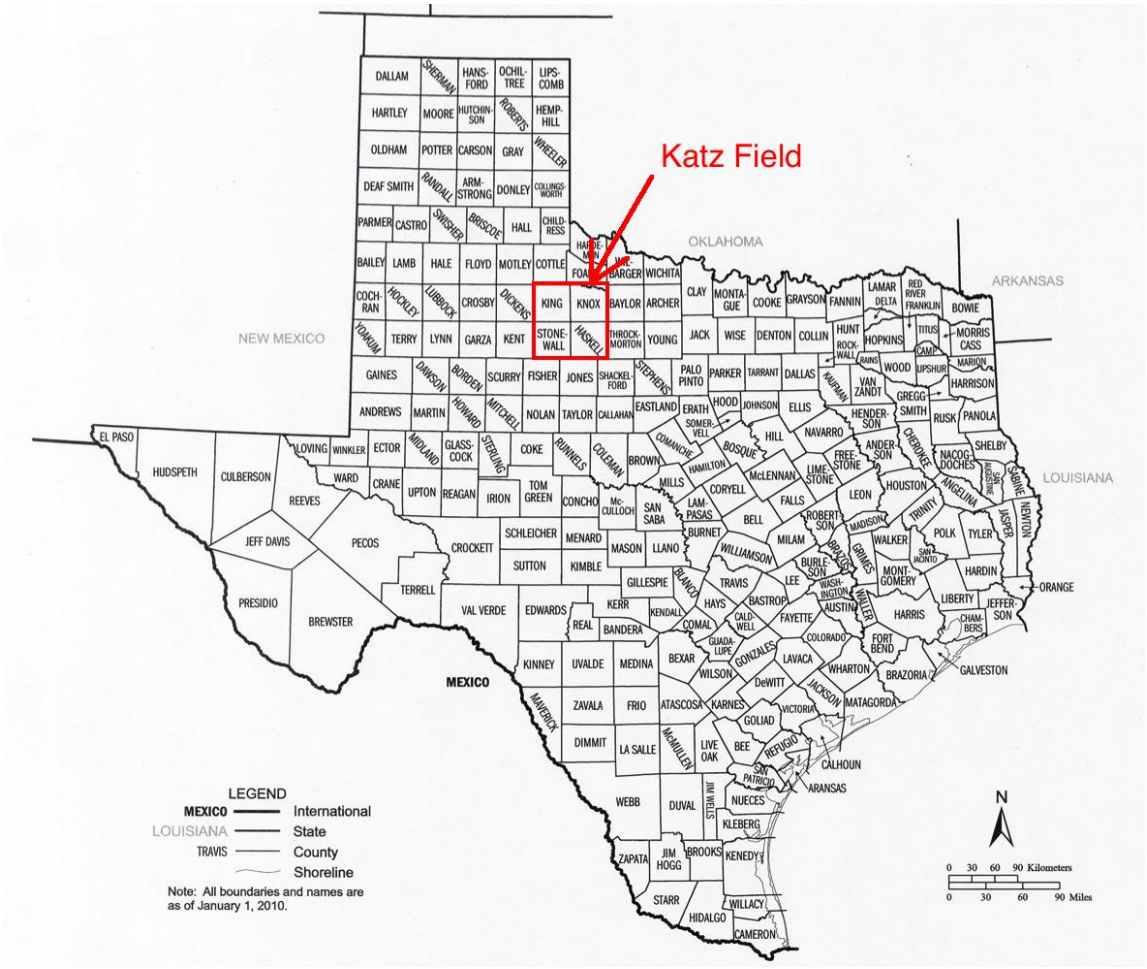


**Fig. 30—Location of the Katz field in Texas**

The temperature of the Katz reservoir is 115 to 120°F. However, for the injection wells, the temperature decreases to 100 to 105°F due to the water injection or $CO_2$ injection, or both. There are 70 injectors and 67 producers in the field (**Fig. 31**). Fifty of the injectors are in the WAG process and the rest are only in waterflooding. Twenty to thirty acidizing jobs are done each year. Approximately 50% of the acidizing jobs are for the producers, and 50% are for injectors. When acidizing the wells, equipment will be pulled out, packers will be used to isolate each zone. Sometimes the 2nd Sand can be

divided into three zones (2A, 2B, and 2C) depending on the formation structure. EGMBE (ethylene glycol monobutyl ether) is also injected into the reservoir to change the wettability from oil wet to water wet during the WAG process. The density of perforation is 6 spf in completion.

Three different types of acidizing jobs have been applied to stimulate the Katz formation; and they are named as acidizing plan A, B, and C in this study. Acidizing plan A is for the producing wells, and it is used to remove the damage caused by the perforation or other steps from the completion. The main acid for acidizing plan A is 15 vol% HCl. The other two acidizing plans are for the injection wells to restore the injection rate during waterflooding or $CO_2$ flooding during the WAG process. The main acid for these two acidizing plans are 20 vol% HCl. The processes of current three acidizing plans are shown in Appendix B.

However, without thorough investigation of the formation lithology and a systematic experimental study of the acidizing methods, injecting 15 or 20 vol% HCl might not be the optimized technique. In this project, X-ray Diffraction (XRD) and Scanning Electron Microscopy (SEM) were used to analyze the cuttings from Katz wells KSU 326 and KSU 231. Based on the XRD mineralogy data from the Katz core end pieces, outcrops with similar mineral composition were selected to test the current acidizing plans. Cores from the 1$^{st}$ and 2$^{nd}$ Sand of KSU 326 and the 3$^{rd}$ Sand of KSU 231 were also selected to test the current acidizing plan. **Table 5** shows the depth ranges of the 1st and 2nd Sand in Well KSU 326 and the 3$^{rd}$ Sand in Well KSU 231. The 2$^{nd}$ Sand in KSU 326 is divided into 2A, 2B, and 2C. The 3$^{rd}$ Sand is divided into the Upper

3rd Sand and the Lower 3rd Sand. Furthermore, the new acidizing plans were designed and performed on cores from outcrops and Katz reservoirs to investigate the recommended optimal acidizing plan for the Katz formation.

| Well | Location | Depth, ft |
|---|---|---|
| KSU 326 | 1st Sand top | 4895 |
| | 1st Sand base | 4923.5 |
| | 2A Sand top | 4943.1 |
| | 2A Sand Base/2B Sand top | 4975.6 |
| | 2B Sand Base | 5001.7 |
| | 2C Sand top | 5010.7 |
| | 2C Sand Base | 5078 |
| KSU 231 | Upper 3rd Sand top | 5080 |
| | Upper 3rd Sand base | 5153.8 |
| | Lower 3rd Sand top | 5164.6 |
| | Lower 3rd Sand base | 5249.8 |

Table 5—The depth ranges of the 1st and 2nd Sand in Well KSU 326 and the 3rd Sand in Well KSU 231. The 2nd Sand in KSU 326 is divided into 2A, 2B, and 2C. The 3rd Sand is divided into the Upper 3rd Sand and the Lower 3rd Sand.

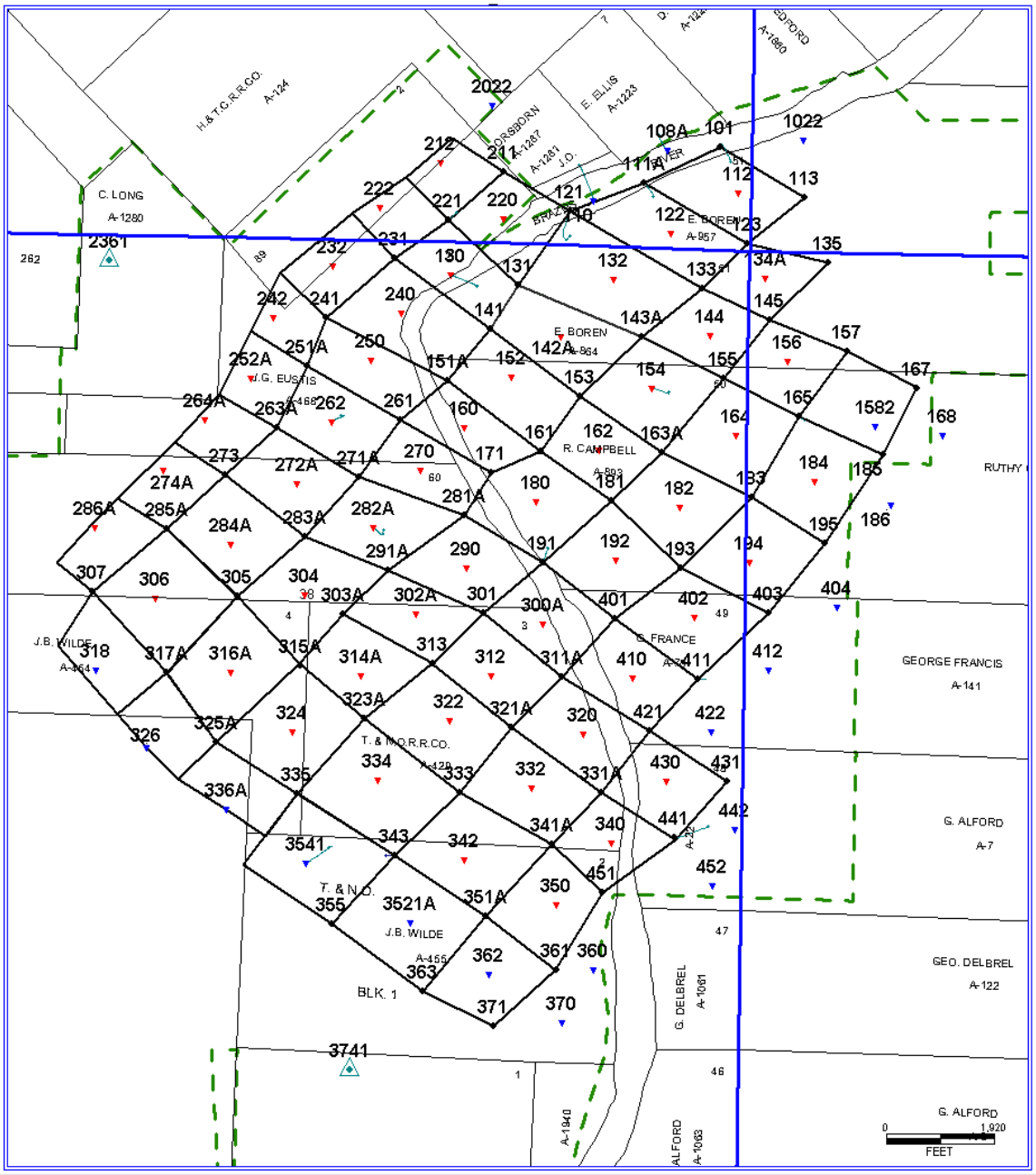


**Fig. 31—Map of Katz field with all of the wells including KSU 231 and KSU 326. The black round dots indicate producers and the upside-down triangle indicate injectors. Those red triangles indicate the wells are in the WAG process while those blue triangles indicate the wells are in the waterflooding process only.**

### *4.2 Experimental Studies*

Coreflood Experiments. XRD data of Katz cores from KSU 326 and KSU 231 varies significantly at different depths, **Table 6**. The mineral composition of the formation includes calcite, dolomite, ankerite, feldspar, kaolinite, illite, and chlorite. Due to the limited access to the Katz cores, Parker and Bandera sandstone cores were selected in this study as well. **Table 7** shows the mineralogy composition of Parker and Bandera sandstone. The Parker sandstone is from the Edwards Plateau with an average permeability of 6 md and average porosity of 17%. The Bandera is from Kansas with an average permeability of 12 md and average porosity of 21%. All the core plugs were cut into the same size of 1.5 in. × 3 in. They are shown in **Fig. 32**.


**Fig. 32—Figures of Katz cores from KSU 326 and KSU 231 in the size of 1.5 in. × 3 in.**

| Well | Depth, ft | Quartz, % | Plagioclase, % | K-feldspar, % | Calcite, % | Dolomite, % | Ankerite, % | Illite + Mica, % | Illite/ Smectite, % | Kaolinite, % | Chlorite, % | Total Clay, % |
|---|---|---|---|---|---|---|---|---|---|---|---|---|
| | 4903.8 | 53.04 | 5.97 | 4.28 | - | - | 26.08 | 6.42 | 1.52 | 2.68 | - | 10.6 |
| | 4910.3 | 74.7 | 2.5 | 8 | - | - | 2.9 | 8.01 | 0.15 | 3.7 | - | 11.9 |
| | 4914.8 | 60.57 | 13.87 | 12.97 | - | - | 1.99 | 6.96 | - | 3.63 | - | 10.6 |
| KSU | 4918.4 | 47 | 28.1 | 9 | - | - | 2.8 | 7.39 | 1.12 | 0.98 | 3.29 | 12.8 |
| 326 | 4924.3 | 37.8 | 24.94 | 20.94 | - | 5.58 | - | 6.55 | 0.12 | 2.77 | 1.27 | 10.7 |
| | 4927.2 | 29.68 | 8.32 | - | 7.52 | 15.04 | - | 26.94 | 1.38 | - | 11.08 | 39.4 |
| | 4961.9 | 13.1 | 12 | - | 68.3 | - | 4.4 | 2.15 | - | - | - | 2.2 |
| | 4969.2 | 16.5 | 10 | - | 53.9 | - | 13.6 | 5.29 | - | - | 0.71 | 6.0 |
| | 5106.4 | 77.9 | 2.5 | 6 | - | - | 0.9 | 10.5 | 0.26 | 1.16 | 0.75 | 12.7 |
| | 5111.4 | 86.4 | 3.3 | - | - | 0.06 | - | 6.09 | 1.88 | 2.32 | - | 10.3 |
| KSU | 5121.2 | 59.3 | 9.3 | 21 | - | - | 3.7 | 2.4 | 0.15 | 3.73 | - | 6.3 |
| 231 | 5136.7 | 68.8 | 18.9 | - | - | - | 1.8 | 6.64 | 1.29 | - | 1.46 | 9.4 |
| | 5144.1 | 70 | 15.3 | - | - | - | 5 | 5.63 | 1.11 | 0.56 | 0.42 | 7.7 |
| | 5147.8 | 86.1 | 2.5 | 4.2 | - | - | 2.7 | 3.53 | 0.007 | 0.95 | - | 4.5 |

Table 6—XRD results of core samples from the Katz well KSU 326 and KSU 231. The samples from the 1st and 2nd Sand are from KSU 326 and the samples from the 3rd Sand are from KSU 231.

| Mineral | Parker | Bandera |
|---|---|---|
| Quartz | 86 | 57 |
| Plagioclase | 4 | 12 |
| K-Feldspar | 1 | - |
| Mica+Illite | 6 | 10 |
| Kaolinite | 2 | 3 |
| Chlorite | Trace | 1 |
| Dolomite | - | 16 |
| Pyrite | - | Trace |

Table 7—Sandstone mineral composition, wt%

The cores were first cleaned by using the Dean-Stark method and then dried in an oven at 250°F for 5 hr. Later, the clean and dry cores were saturated with fresh-made synthetic brine for 4 hr under vacuum. The synthetic brine had the same composition as the produced water from the Katz field, and its composition is showed in **Table 8**. In the coreflood experiment, the overburden pressure was set to 2,000 psi, and the back pressure was 1,000 psi. The injection rate was 5 $cm^3$/min. Then, synthetic brine was injected into the core. When the pressure drop became stable, this value was used to calculate the initial permeability of the core. Then, the temperature of the core holder was increased to the designated temperature. The bottom hole temperatures of producing wells and injection wells are about 115°F and 110°F, respectively. Therefore, the acidizing plans for different types of wells have different designated temperatures. After the pressure drop became stable again, different fluids as shown in the Appendix B were injected in sequence. The system was cooled after the post-flush. When the pressure drop became stable at 75°F, this value was used to calculate the permeability of the treated core. The initial and final permeability of the core were measured at 75°F when the viscosity of the synthetic brine was 1.5 cp. The core effluent samples were collected every two minutes during the experiment and analyzed by ICP using an Optima 7000 DV ICP-OES system and WinLab 32™ software to determine the concentrations of Ca, Mg, Fe, Al, and Si. The core was scanned by X-ray computed tomography (CT) both before and after the coreflood experiment, and the CT results were analyzed using ImageJ software. The model of the CT is Toshiba Aquilion RXL and the resolution is 0.5 mm.

| Ion | Concentration, ppm |
|---|---|
| $Na^+$ | 46532 |
| $K^+$ | 513.5 |
| $Ca^{2+}$ | 17430 |
| $Fe^{3+}$ | 108.4 |
| $Mg^{2+}$ | 3028 |
| $Ba^{2+}$ | 33.86 |
| $Sr^{2+}$ | 1390 |
| $HCO_3^-$ | 512.4 |

Table 8—Ion concentration of Katz producing water or the synthetic brine

For simulate the current acidizing plan in our coreflood experiments, the amount of fluids in each step of different acidizing plans can be calculated based on volume balance. For the Katz field, the diameter of the injectors or producers wellbore is $7\,^7/_8$ in. and the penetration depth of the stimulation fluid is assumed to be 1 ft. Therefore, 50 gal/ft of fluid in the Katz current acidizing plan is equivalent to about 8.7 pore volume (PV) in the coreflood experiment. The details of the calculation are shown in Appendix C. The volumes of different fluids in the current acidizing plan A, B, and C are shown in Appendix D.

## *4.3 Coreflood Experiment Results*

### 4.3.1 Evaluation of Current Acidizing Plans

Coreflood experiments No. 1 to 5 examined the performance of the current acidizing plan A on Parker core #4, Bandera core #1, and three Katz cores at depths of 4903.25, 4948.75, and 5138.75 ft. The three Katz cores are from the 1st, 2nd, and 3rd Sand,

respectively. The experiment temperature was 115°F. The preflush and post-flush treatment fluids were both 2 vol% KCl with additives, and the main treatment fluid was 15 vol% HCl with additives. Formulas for the different types of fluids are shown in **Table 9**. **Table 10** shows all 14 sets of coreflood experiment results. **Figs. 33** through **37** show the pressure drop across the cores of coreflood experiment No. 1 to 5, respectively. In these five figures, during the 15 vol% HCl stage, the pressure drop fluctuated a lot which indicates HCl were reacting with the core vigorously. The permeability of Parker #4 sandstone increased from 5.0 to 5.76 md (increased 15.2%) and the permeability of Bandera #1 increased from 13.95 to 19.48 md (increased 39.6%) after the stimulation. Bandera has 16 wt% dolomite, HCl can dissolve the dolomite and increase the porosity and permeability. ICP results of Bandera core #1 shows high concentration of Ca after starting to inject HCl. For the cores from the 1st, 2nd, and 3rd Sand of Katz, the permeability decreased 45.8%, 13.8%, and 11.48% respectively. This is because Katz formation includes a large amount of illite. When HCl was injected into the formation, HCl attacked the Al from the illite. Illite precipitated in the form of amorphous silica gel ($Si(OH)_4$) to damage the formation (Thomas et al. 2001). **Figs. 38** through **42** show the ion concentration in the core effluent samples of coreflood experiment No. 1 to 5, respectively. For coreflood No. 3 through 5, after the 15 vol% HCl stage, the pressure drop across the core increased, which means the cores were damaged during the 15 vol% HCl stage. During the stage when using 2 wt% KCl fluid, the concentrations of Ca and Mg were approximately 17000 and 3000 ppm, respectively. The synthetic brine, which

was used to make for the 2 wt% KCl fluid, contributes this and it does not react with the core. The synthetic brine has 17430 ppm of Ca and 3048 ppm of Mg (Table 8).

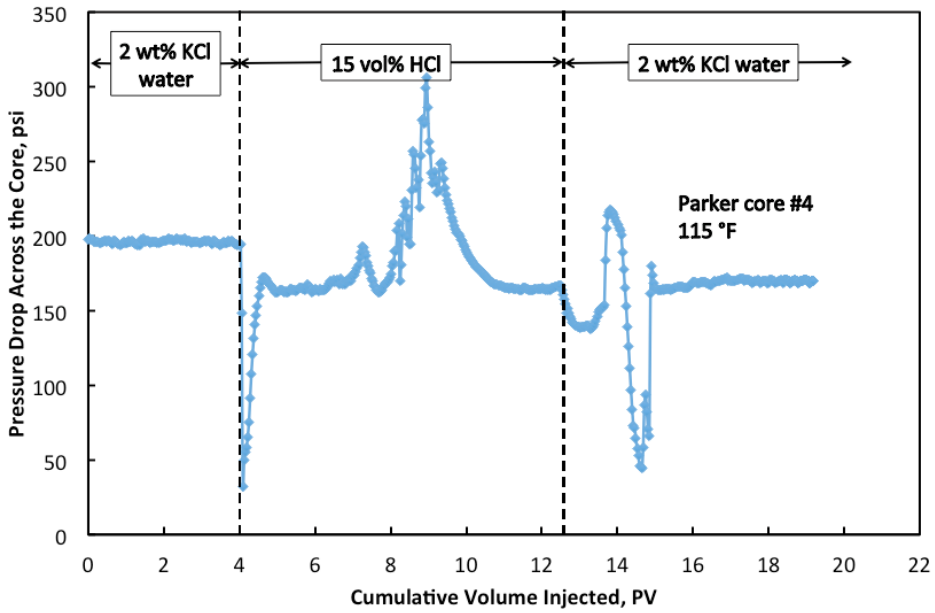


**Fig. 33—Pressure drop across the Parker core #4, 5 cm$^3$/min, 8.7 PV of 15 vol% HCl.**

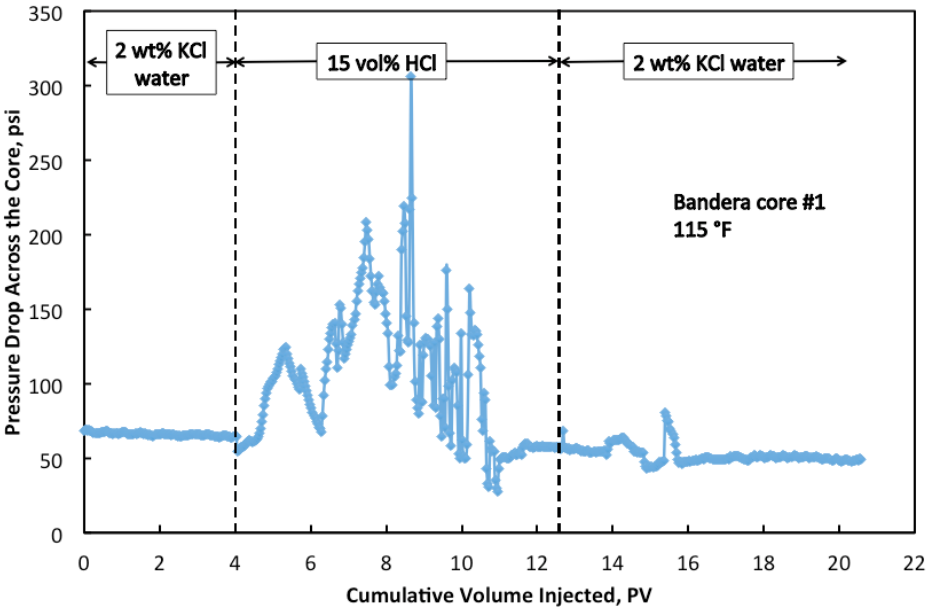


**Fig. 34—Pressure drop across the Bandera core #1, 5 cm$^3$/min, acidizing plan 1, 8.7 PV of 15 vol% HCl.**

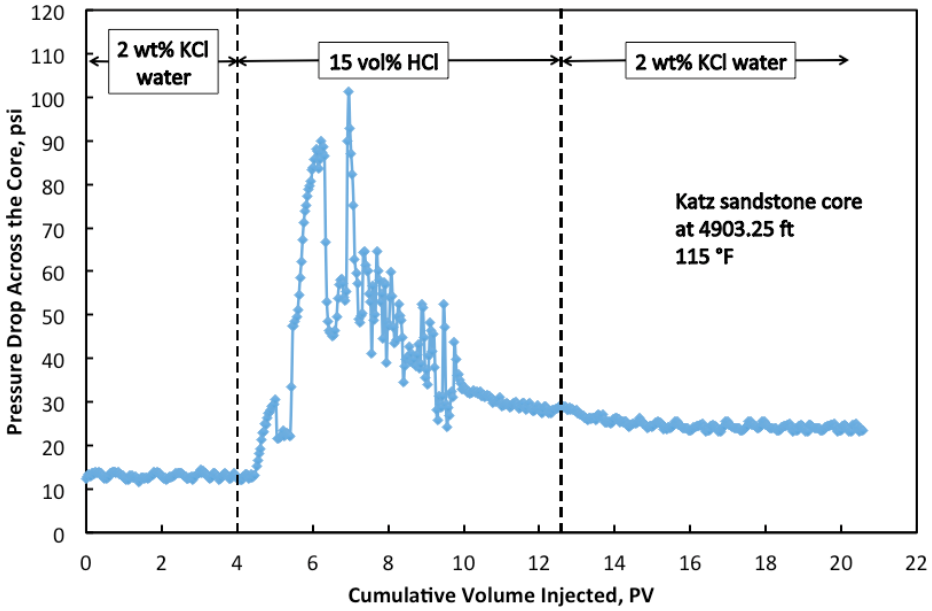


**Fig. 35—Pressure drop across the Katz core at 4903.25 ft, 5 cm$^3$/min, acidizing plan 1, 8.7 PV of 15 vol% HCl.**

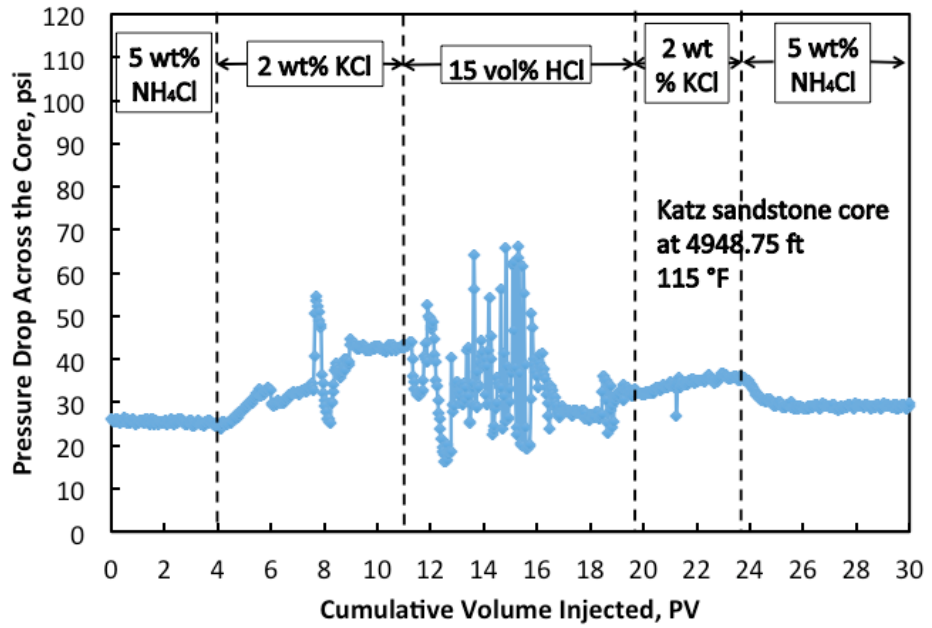


**Fig. 36—Pressure drop across the Katz core at 4948.75 ft, 5 cm$^3$/min, acidizing plan 1, 8.7 PV of 15 vol% HCl.**

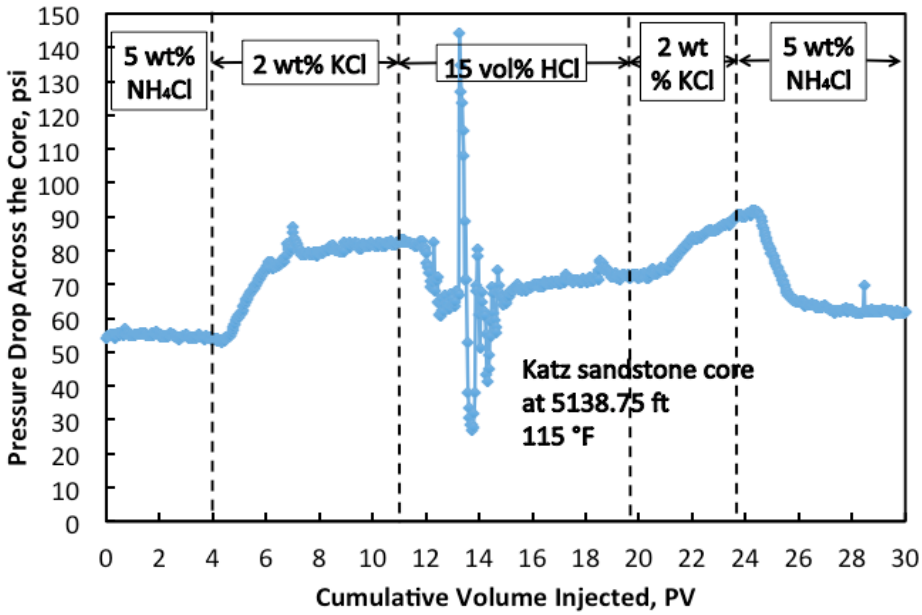


**Fig. 37—Pressure drop across the Katz core at 5138.75 ft, 5 cm$^3$/min, acidizing plan 1, 8.7 PV of 15 vol% HCl.**

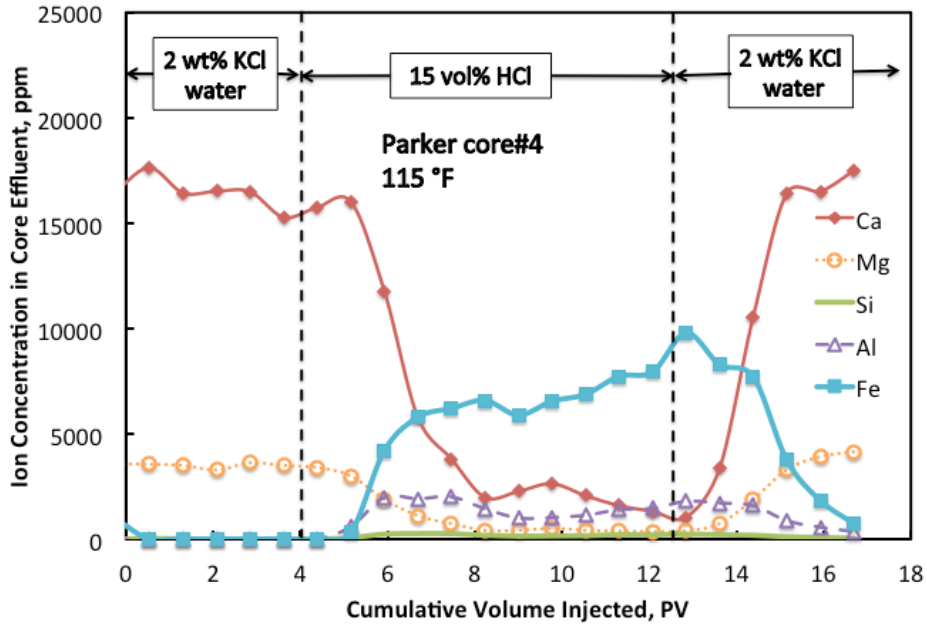


**Fig. 38—Ion concentration in the core effluent samples. Flow rate was 5 cm$^3$/min and the volume of 15 vol% HCl was 8.7 PV.**

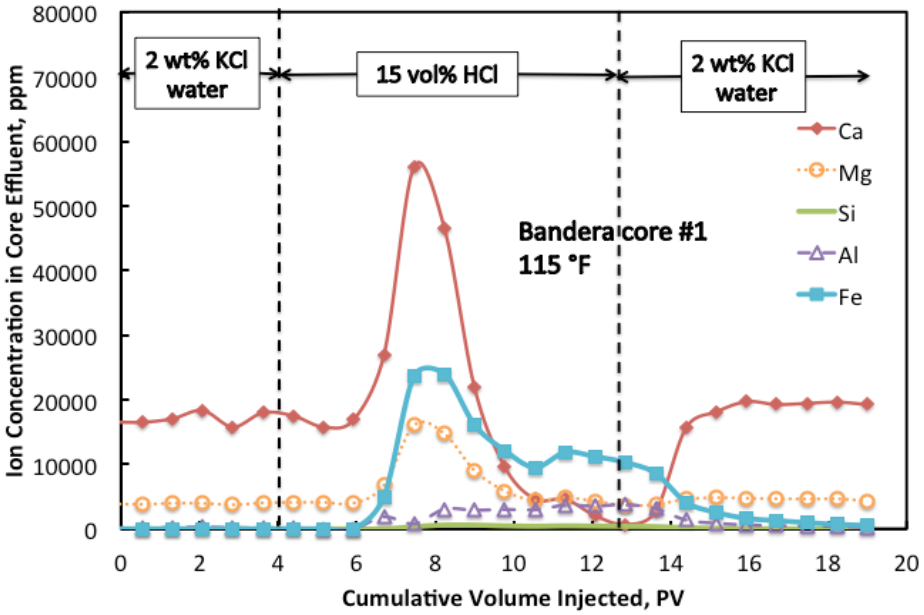


**Fig. 39—Ion concentration in the core effluent samples of Bandera core #1. Flow rate was 5 cm$^3$/min and the volume of 15 vol% HCl was 8.7 PV.**

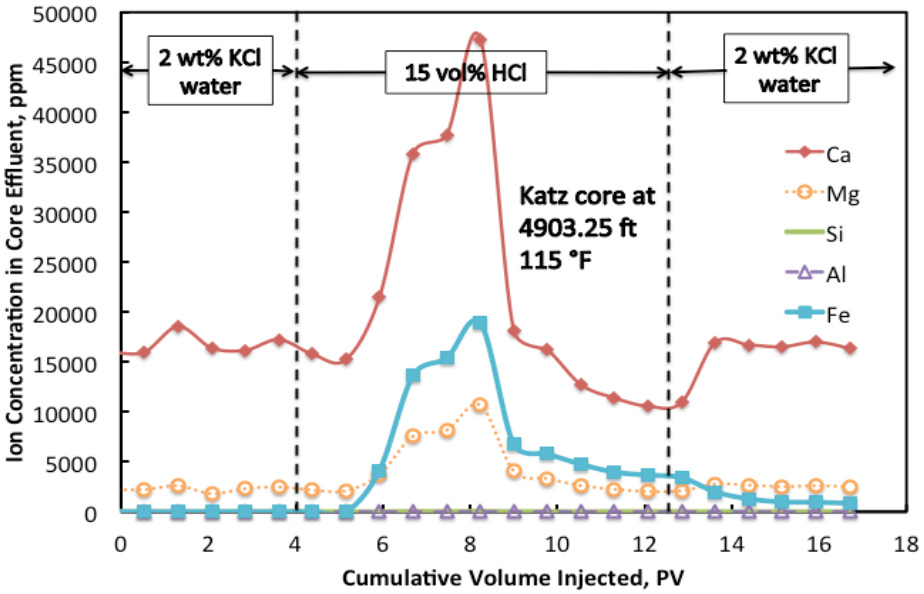


**Fig. 40—Ion concentration in the core effluent samples of Katz core at 4903.25 ft. Flow rate was 5 cm$^3$/min and the volume of 15 vol% HCl was 8.7 PV.**

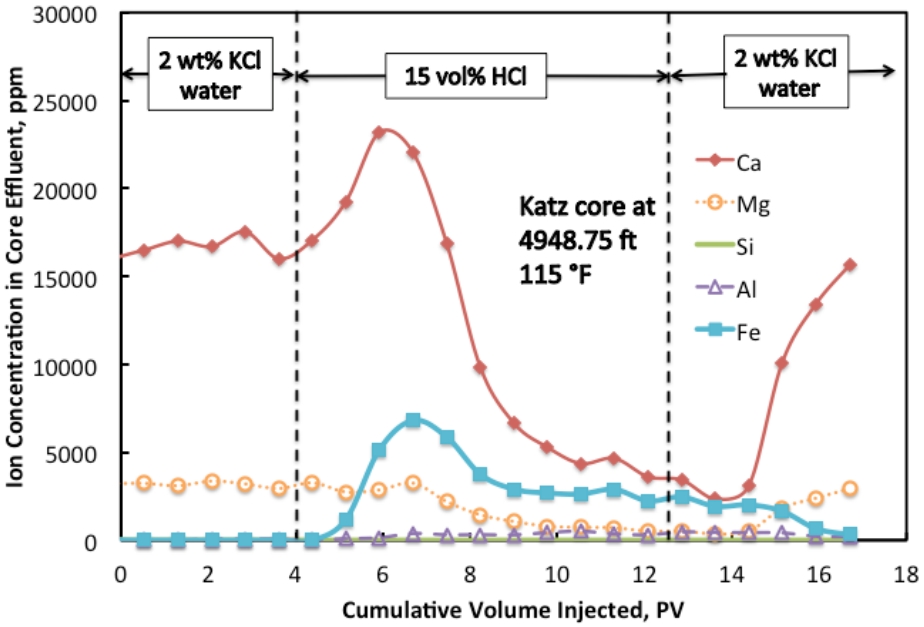


**Fig. 41—Ion concentration in the core effluent samples of Katz core at 4948.75 ft. Flow rate was 5 cm$^3$/min and the volume of 15 vol% HCl was 8.7 PV.**

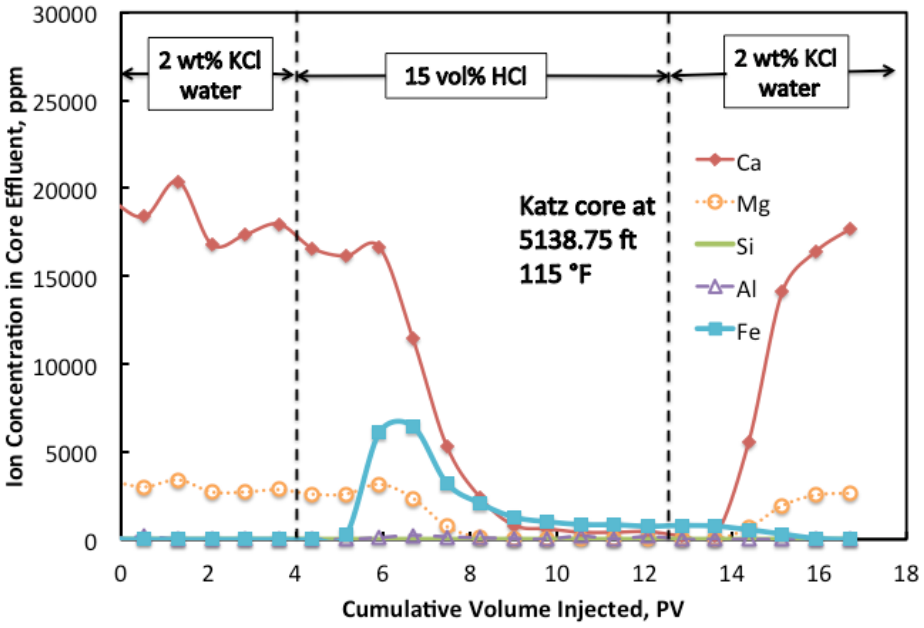


**Fig. 42—Ion concentration in the core effluent samples of Katz core at 5138.75 ft. Flow rate was 5 cm$^3$/min and the volume of 15 vol% HCl was 8.7 PV.**

| Fluid | Volume, ml | Chemplx name | Description |
|---|---|---|---|
| 15 vol% HCl + Additives | 2 | Plexhib 166 | Corrosion inhibitor |
| | 2 | Plexbreak 116 | Non-emulsifier |
| | 4 | Reducer | Iron reducer |
| | 992 | 15 vol% HCl | Acid |
| FWS - 2 wt% KCl +Additives | 2 | Clayplex 600 | Clay stabilizer |
| | 0.25 | Plexcide 24L | Biocide |
| | 1 | Plexsurf 210E | Non-ionic surfactant |
| | 2.5 | Plexgel 907L-EB | Gel agent friction reducer |
| | 50 | EGMBE | Mutual solvent |
| | 944.75 | Brine | Synthetic brine |
| 20 vol% HCl Acidtol 80:20 | 730 | 20 vol% HCl | Acid |
| | 50 | EGMBE | Mutual solvent |
| | 10 | Acidlink 711 | Solvent dispersant emulsifier |
| | 2 | Plexhib 166 | Corrosion inhibitor |
| | 4 | Reducer | Iron reducer |
| | 200 | Xylene | White water xylene |
| Water White Xylene + Additivies | 50 | EGMBE | Mutual solvent |
| | 950 | Xylene | White water xylene |

Table 9—Formulas for different fluids in the coreflood experiment (1000 ml).

CT scans were also performed on the cores before and after the coreflood experiments. For the CT images, each pixel has a relative value of linear attenuation coefficient after image reconstruction. The CT number is converted by the attenuation coefficient and can be used as the indicator of the change of density and porosity (Akin and Kovscek 2003). **Figs. 43** through **47** show the averaged cross-section CT numbers through the cores before and after the stimulation from coreflood experiment No. 1 through 5, respectively. The CT scan shows that after the stimulation, the CT numbers of the core decreased, this does not mean the permeability of the core is increased. In our

study, the amorphous silica gel has a density of 2.196 g/cm$^3$ which is much lower than the density of quartz, which is 2.65 g/cm$^3$. Therefore, precipitated amorphous silica gel can decrease the CT numbers of the cores.

| Coreflood # | Core | Acidizing plan | Initial effective porosity, % | Initial permeability, md | Final permeability, md | Increased permeability, % |
|---|---|---|---|---|---|---|
| 1 | Parker #4 | Plan A | 15.62 | 5.00 | 5.76 | 15.20 |
| 2 | Bandera #1 | Plan A | 18.05 | 13.95 | 19.48 | 39.64 |
| 3 | Katz@4903.25 ft | Plan A | 14.86 | 74.93 | 40.59 | -45.83 |
| 4 | Katz@4948.75 ft | Plan A | 14.83 | 29.57 | 25.49 | -13.80 |
| 5 | Katz@5138.75 ft | Plan A | 7.48 | 13.69 | 12.12 | -11.48 |
| 6 | Parker #1 | Plan B | 15.45 | 4.50 | 1.11 | -75.26 |
| 7 | Katz@4903.4 ft | Plan B | 16.15 | 46.39 | 31.42 | -32.26 |
| 8 | Parker #3 | Plan C | 15.94 | 4.30 | 1.19 | -72.29 |
| 9 | Katz@4948.1 ft | Plan C | 15.60 | 27.38 | 23.19 | -15.28 |
| 10 | Katz@4915.6 ft | 1 PV 1 wt% HF | 8.72 | 3.58 | 2.63 | -26.48 |
| 11 | Katz@4915.9 ft | 2 PV 1 wt% HF | 15.41 | 3.56 | 0.88 | -75.36 |
| 12 | Katz@4903.1 ft | 3 PV 0.5 wt% HF | 12.47 | 29.52 | 43.48 | 47.31 |
| 13 | Katz@5126.7 ft | 1.5 PV 0.5 wt% HF | 13.05 | 53.90 | 56.89 | 5.55 |
| 14 | Katz@4948.4 ft | 3 PV 0.5 wt% HF | 13.14 | 18.76* | 34.77* | 85.34* |
| 15 | Katz@5138.4 ft | 3 PV 5 wt% HCl + 3 PV 1 wt% HF | 13.17 | 16.71 | 2.76 | -83.5 |

* indicates the effective permeability of the synthetic brine.

Table 10—Coreflood results of outcrops and Katz cores, absolute permeability changed after the experiments.

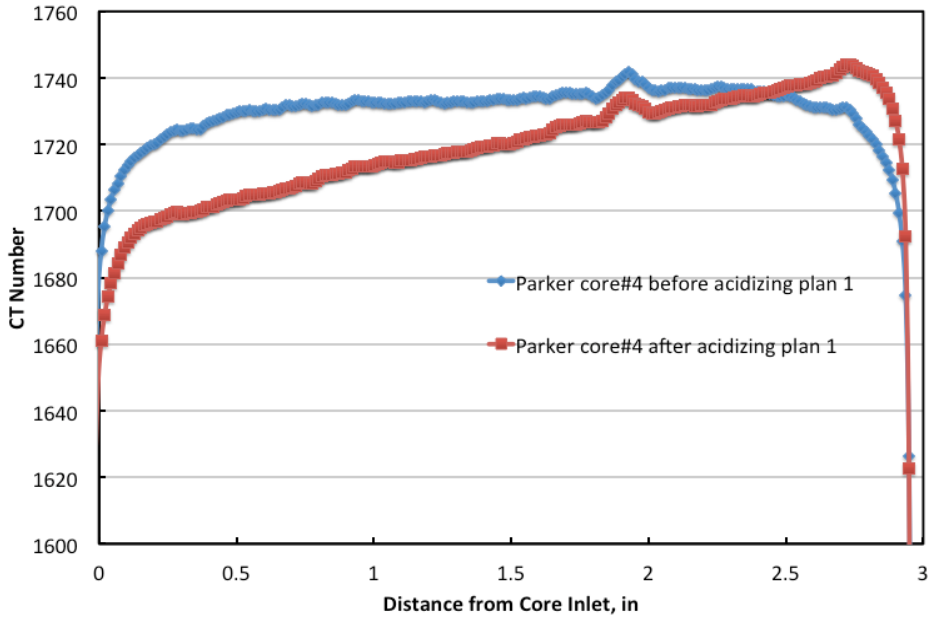


**Fig. 43—CT numbers across the Parker core #4 after the coreflood test with 5 cm$^3$/min 8.7 PV of 15 vol% HCl at 115°F.**

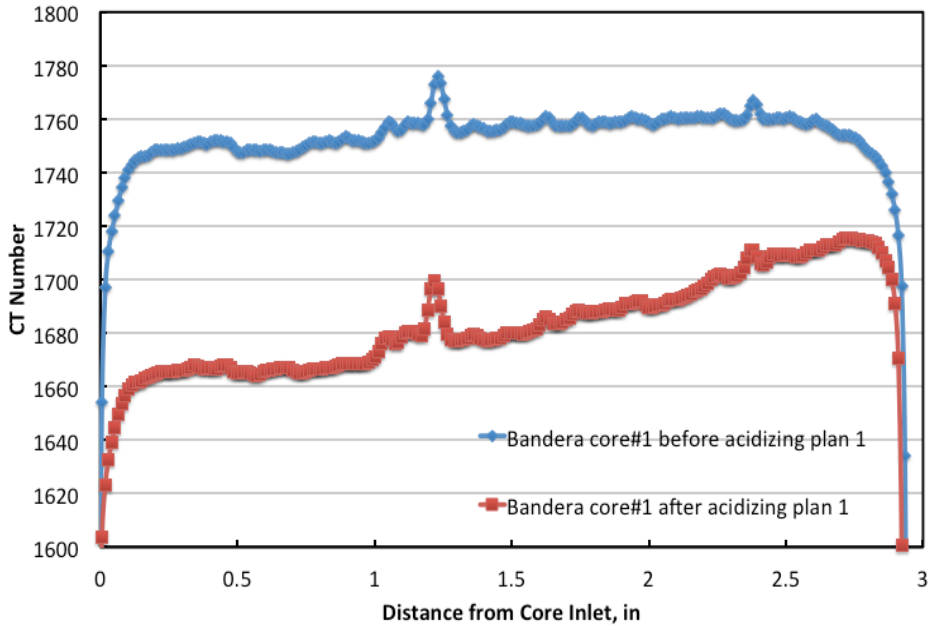


**Fig. 44—CT numbers across the Bandera core #1 after the coreflood test with 5 cm$^3$/min 8.7 PV of 15 vol% HCl at 115°F.**

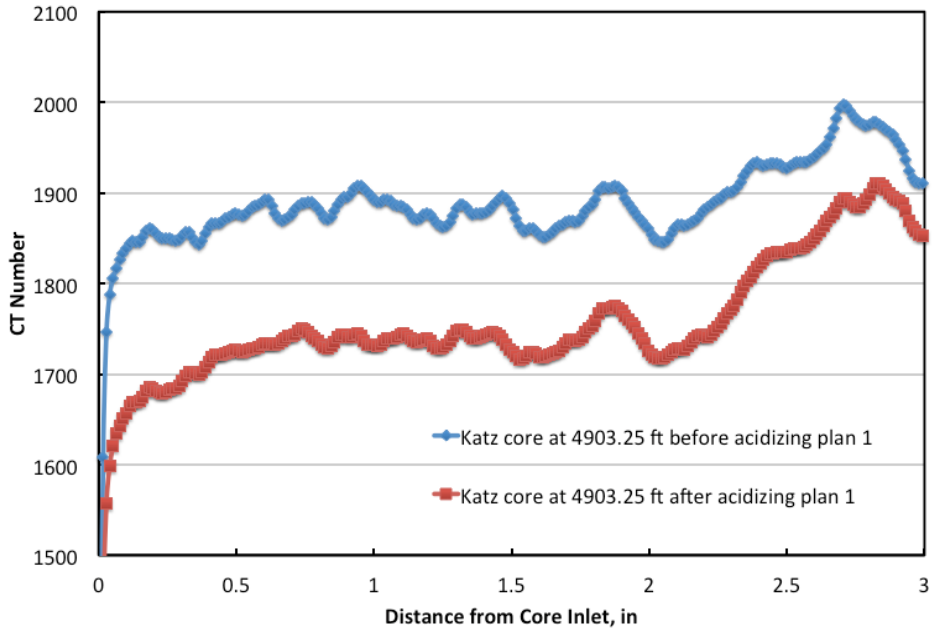


**Fig. 45—CT numbers across the Katz core at 4903.25 ft after the coreflood test with 5 cm$^3$/min 8.7 PV of 15 vol% HCl at 115°F.**

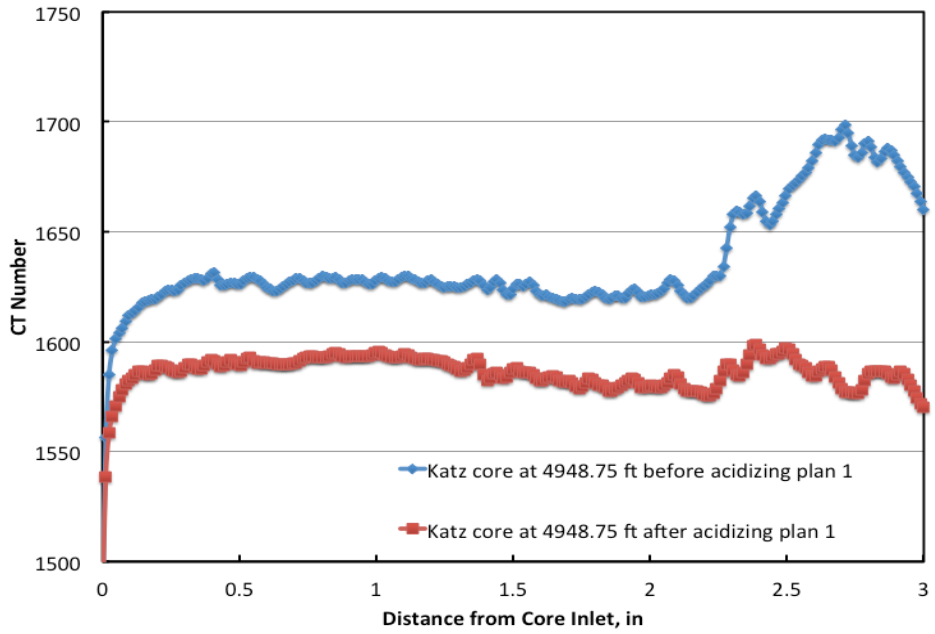


**Fig. 46—CT numbers across the Katz core at 4948.75 ft after the coreflood test with 5 cm$^3$/min 8.7 PV of 15 vol% HCl at 115°F.**

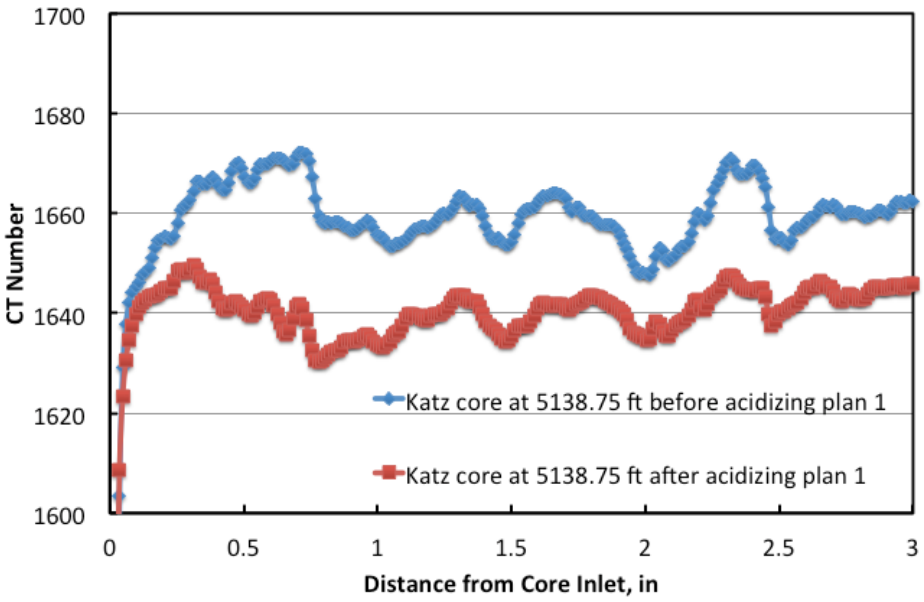


**Fig. 47—CT numbers across the Katz core at 5138.75 ft after the coreflood test with 5 cm$^3$/min 8.7 PV of 15 vol% HCl at 115°F.**

Acidizing plan B has been tested on Parker core #1 and the Katz core at depth 4903.4 ft. Both cores were damaged after the stimulation. **Figs. 48** and **49** show the pressure drop across the cores during coreflood experiment No. 6 and 7, respectively. The permeability of Parker core #1 decreased 75.26% while the permeability of the Katz core at depth 4903.4 ft decreased 32.26%. There are two acid steps with 3.8 PV 20 vol% HCl in the acidizing plan B. Fig. 48 shows that after each HCl step, the pressure drop increased which indicates the 20 vol% HCl damaged the Parker core #1 twice in the whole acidizing plan B. Fig. 49 shows that the pressure drop only increased after the first HCl step, which indicates that all illite has reacted with the first 3.8 PV 20 vol% HCl. During the second acid step, there was no damage observed from the core. **Figs. 50** and **51** show the CT numbers through the cores before and after the stimulation for coreflood experiment No. 6 and 7. Fig. 50 shows that after the stimulation, the CT numbers at the

inlet and outlet portion of the core increased. Therefore, high-density reaction productions precipitated in these two parts. Fig. 51 shows the CT numbers decreased through the core, which means the density of the Katz core at depth 4903.4 ft decreased; however the permeability of the core decreased. This indicates the low-density reaction products such as silica gel precipitate through the core.

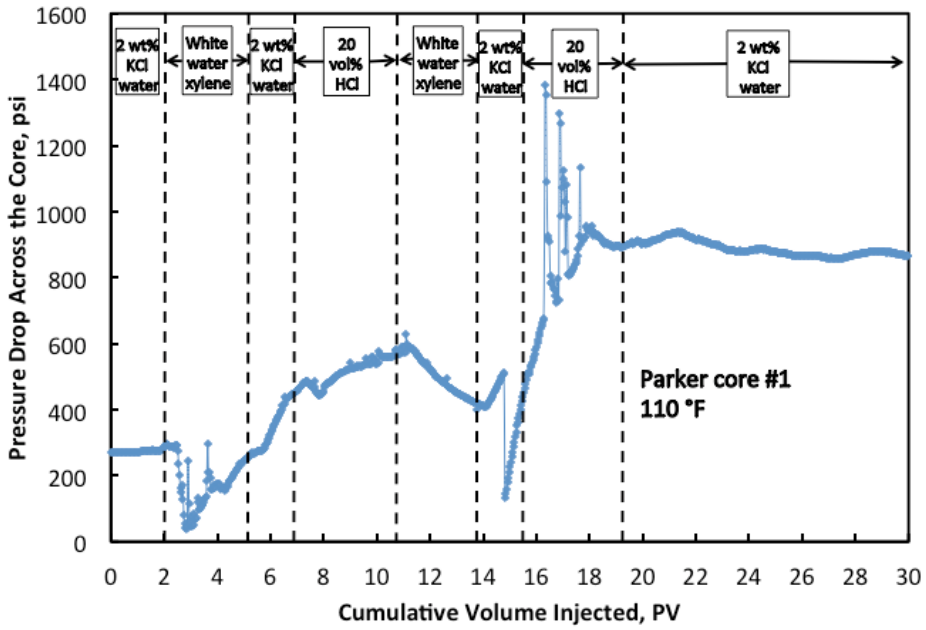


**Fig. 48—Pressure drop across the Parker core #1, 5 cm$^3$/min, acidizing plan B.**

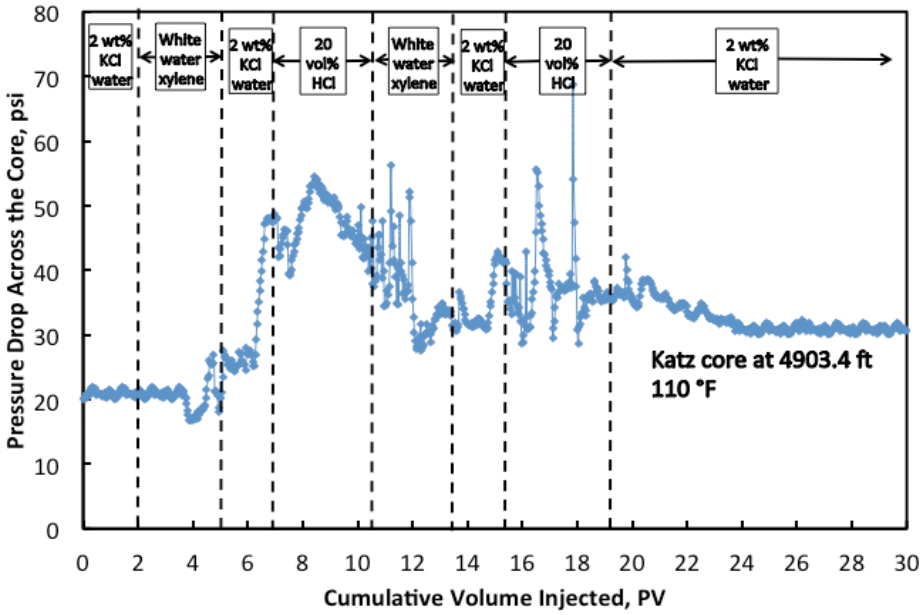


**Fig. 49—Pressure drop across the Katz core at 4903.4 ft, 5 cm$^3$/min, acidizing plan B.**

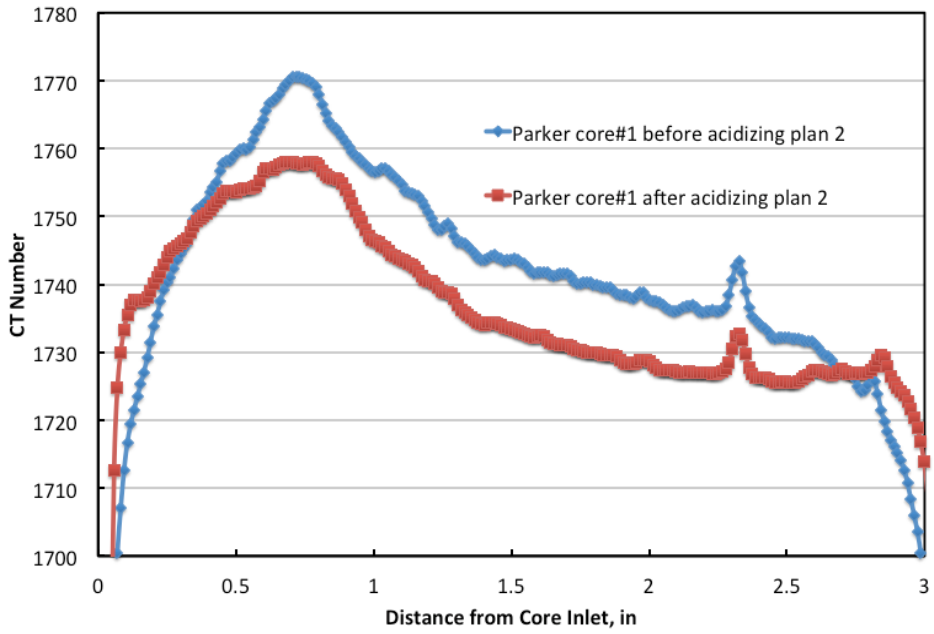


**Fig. 50—CT number across the Parker core #1, 5 cm$^3$/min acidizing plan B, 110°F.**

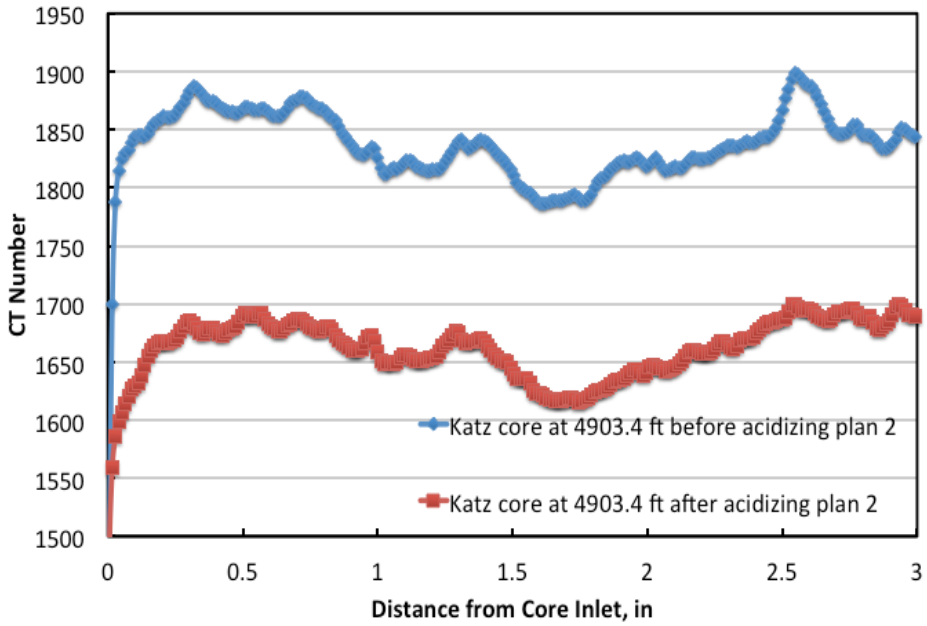


**Fig. 51—CT number across the Katz core at 4903.4 ft , 5 $cm^3$/min acidizing plan B, 110°F.**

Acidizing plan C has been tested on Parker core #3 and the Katz core at depth 4948.1 ft. Both cores were also damaged after the stimulation**. Figs. 52** and **53** show the pressure drop across the cores during coreflood experiment No. 8 and 9 respectively. The permeability of Parker core #3 decreased 72.29% while the permeability of Katz core at depth 4948.1 ft decreased 15.28%. **Figs. 54** and **55** show the CT numbers through the cores before and after the stimulation for coreflood experiment No. 8 and 9. The results were similar as that of acidizing plan B. After the stimulation, the CT numbers of Parker core #3 at the inlet and outlet portion of the core increased, which is the same as Fig. 50. CT numbers of Katz core at depth 4948.1 ft also showed the same results as the Fig. 51. Based on these results, 20 vol% HCl in acidizing B and C can damage the Parker core more severe than 15 vol% HCl in acidizing A. The effective porosity of Katz cores varies, and the range is between 7 to 16%, while the effective porosity of Parker

sandstone cores are in the range of 15 to 16%. Compared with Katz cores, Parker sandstone cores have much lower permeability, which indicates Parker sandstone might have much smaller pore throat than Katz cores and it is easier to get damaged.

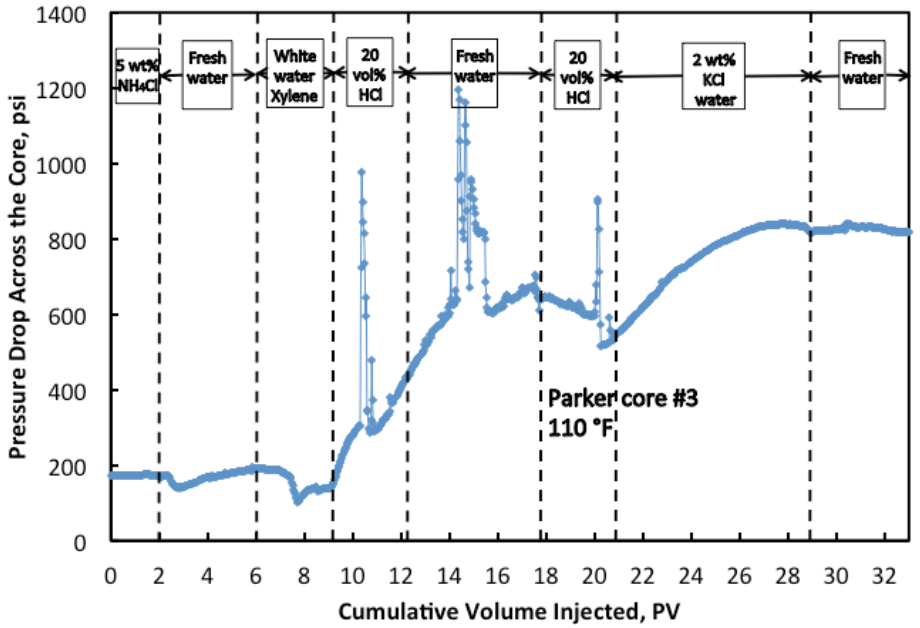


**Fig. 52—Pressure drop across the Parker core #3, 5 cm$^3$/min, acidizing plan 3.**

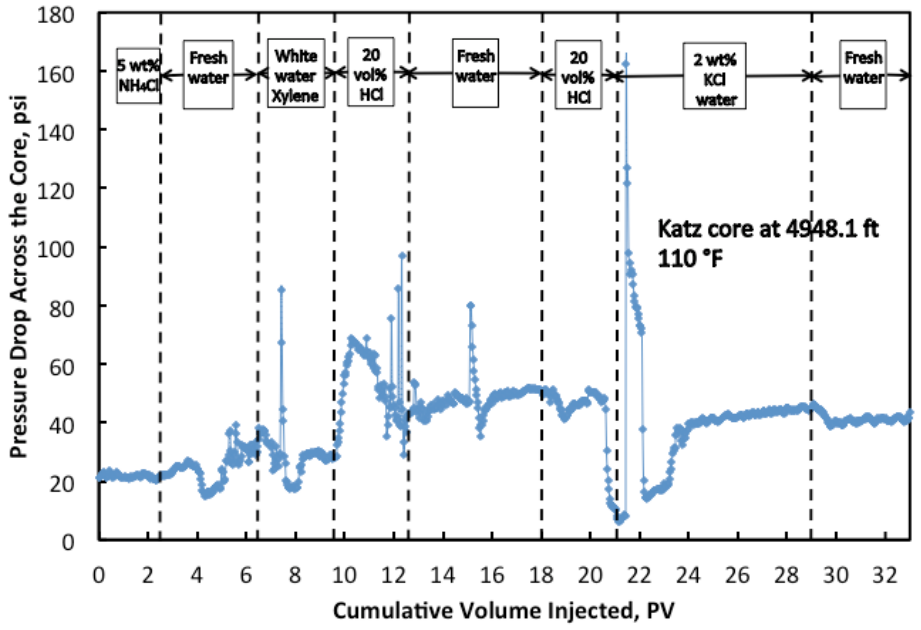


**Fig. 53—Pressure drop across the Katz core at 4948.1 ft, 5 cm$^3$/min, acidizing plan 3.**

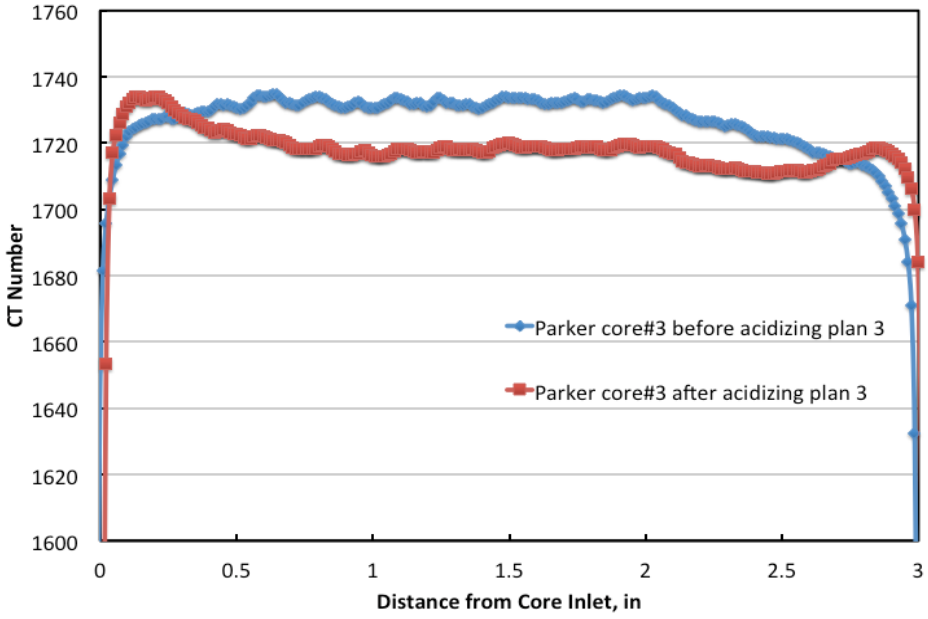


**Fig. 54—CT number across the Parker core #3, 5 cm$^3$/min acidizing plan 3, 110°F.**

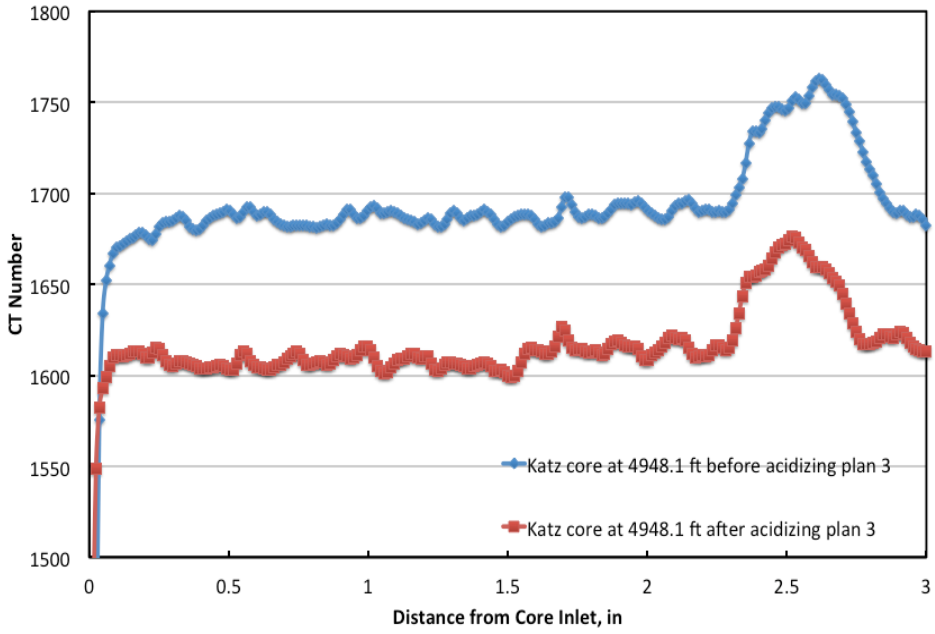


**Fig. 55—CT number across the Katz core at 4948.1 ft, 5 cm$^3$/min acidizing plan 3, 110°F.**

### 4.3.2 New Acidizing Plan

Based on the previous XRD report from a local service company (Scal Inc. Table 1), illite is observed in all three Katz reservoirs. The concentration of illite varies, and the highest concentration in the pay zones can be up to 10 wt%. Illite is a type of HCl-sensitive clay, which can cause formation damage (Thomas et al. 2001; Al-Harbi et al. 2013; Mahmoud et al. 2015). In the original acidizing plan A, B, and C in the Katz field, 15 or 20 vol% HCl is added to clean the damage caused by the previous stage, such as perforation for the Katz field. Therefore, a new acid system need to be chosen to take the place of HCl. Study showed that organic-HF could be a good alternative in formation containing HCl-sensitive clays (Abrams et al. 1983). Organic-HF acids also have a

retarded nature with sand and clay minerals when compared to regular HCl-HF mixtures (Al-Harbi et al. 2011).

Simon (1990) found the permeability could increase effectively by the 12 wt% acetic-3 wt% HF in a sandstone coreflood test. Wehunt et al. (1993) tested three organic acid systems, which were acetic acid, propanoic acid, and butanoic acid, and they found that acetic acid is the most effective one. Their study also showed that the low HF concentration from 0.05 to 0.1 wt% blended with 10 wt% acetic acid could remove the damage successfully in the coreflood experiment. Da Motta et al. (1996) did a series of coreflood experiments and found acetic-HF acids are capable of stimulating damaged injection and production wells while preserving the zonal isolation provided by cement. Shuchart and Gdanski (1996) studied two field tests which were using acetic-HF and formic-HF acid system. They found quick $AlF_3$ precipitation which could cause severe near-wellbore damage. Shuchart (1997) stated that formic acid offered better results in preventing $AlF_3$ precipitation. Wang et al. (2000) studied a new low-damage acetic-HF system and found its strong chelating effect with aluminum fluoride complexes to prevent $AlF_3$ precipitation. They did both short-core (2 in.) and long-core (8 in.) coreflood experiment, and found the acetic-HF system can be used for deeper damage removal. Their field study results showed the new acid system could increase a water injection well from 0 to 100 $m^3$/day and the good performance lasting more than 6 months. Al-Harbi et al. (2011) found that the formic-HF acid system showed retarded reaction when reacting with illite when compare with the regular mud acid system. They have not observed any silica gel precipitation or $AlF_3$ precipitation. However, when the

formic-HF acid system reacted with chlorite, more $AlF_3$ precipitated because the Fe ions prevent the chelating effect to Al ions. But the precipitation is still low when comparing with acetic-HF acid system. Yang et al. (2012) did the solubility test of different clays (kaolinite, illite, and chlorite) with 9 wt% formic-6 wt% HF or 13 wt% acetic-6 wt% HF under room temperature for 0.5 hour, no $AlF_3$ was observed. They also did the coreflood tests with Berea sandstone cores, and found that the optimal concentration for HF in the 9 wt % formic acid is 0.5 wt%.

In the present study, formic-HF was chosen instead of HCl to eliminate the formation damage because the existence of illite in the Katz formation. Coreflood experiments No. 10 to 14 were using this acidizing plan. The preflush and the post-flush were the same for these 5 coreflood experiments, only the main flush stage was different. Preflush was using 10 PV of 9 wt% formic acid and the post-flush is 3 PV of 9 wt% formic acid. Coreflood No. 10 and 11 used the Katz core at depth 4915.6 and 4915.9 ft (1st sand), respectively. The main flush for these two experiments was 1 and 2 PV of 9 wt% formic-1 wt% HF, respectively. After the experiments, the permeability of the Katz core at depth 4915.6 ft decreased 26.48%, while the Katz core at depth 4915.9 ft decreased 75.36%. Pressure drop increased significantly in both experiments as soon as the main flush stage started (**Figs. 56** and **57**). This indicates the 9 wt% formic-1 wt% HF can damage the core, and the additional 9 wt% formic-1 wt% HF acid can cause more damage. **Figs. 58** and **59** show the ion concentration in the core effluent samples of coreflood experiment No. 10 and 11. At the end of preflush stage, more than 15,000 ppm Ca was observed, which indicates the possible $CaF_2$ precipitation was formed in the core

during the main flush stage. **Figs. 60** and **61** show the CT numbers of the cores before and after the stimulation for coreflood experiment No. 10 and 11. Fig. 60 showed that the CT numbers increased after the acidizing job at the location of 2.3 in. from the core inlet, which indicates the location of $CaF_2$ precipitation. Fig. 61 shows the CT numbers increased at the location 0.5 to 1 in. and 2.1 to 3 in. from the core inlet. This also shows that additional 9 wt% formic-1 wt% HF acid can cause more damage. In coreflood No. 12, the concentration of HF in the main flush was decreased to 0.5 wt% and the volume was 3 PV. The permeability of the Katz core at depth 4903.1 ft (1st sand) increased 47.31%.

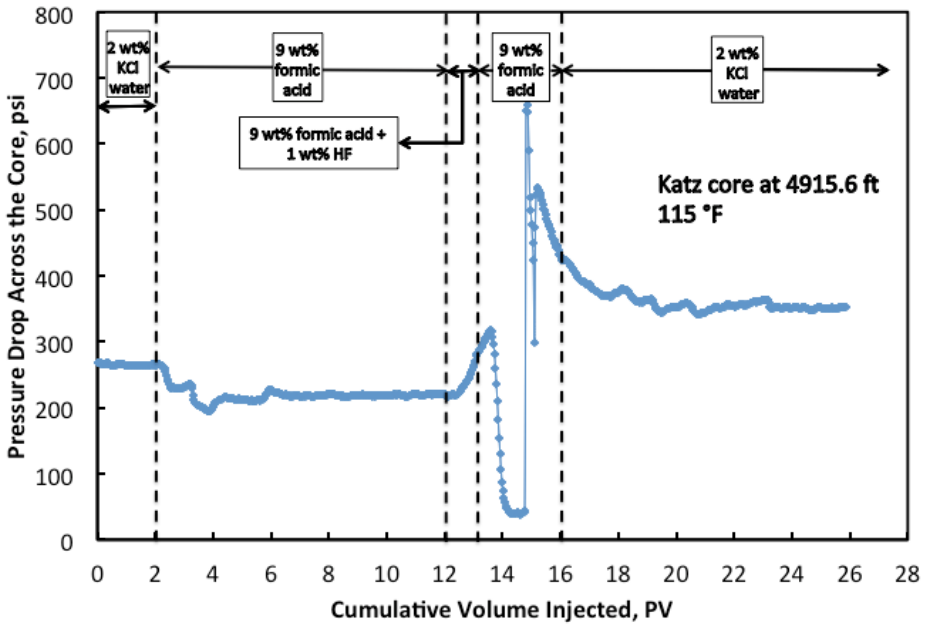


**Fig. 56—Pressure drop across the Katz core at 4915.6 ft, 5 $cm^3$/min, 1 PV 1 wt% HF.**

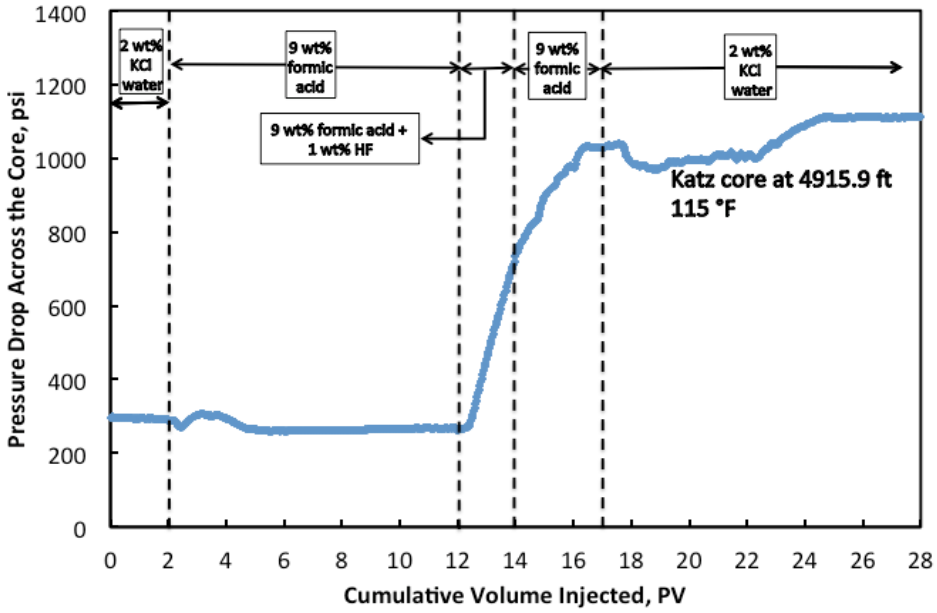


**Fig. 57—Pressure drop across the Katz core at 4915.9 ft, 5 cm$^3$/min, 2 PV 1 wt% HF.**

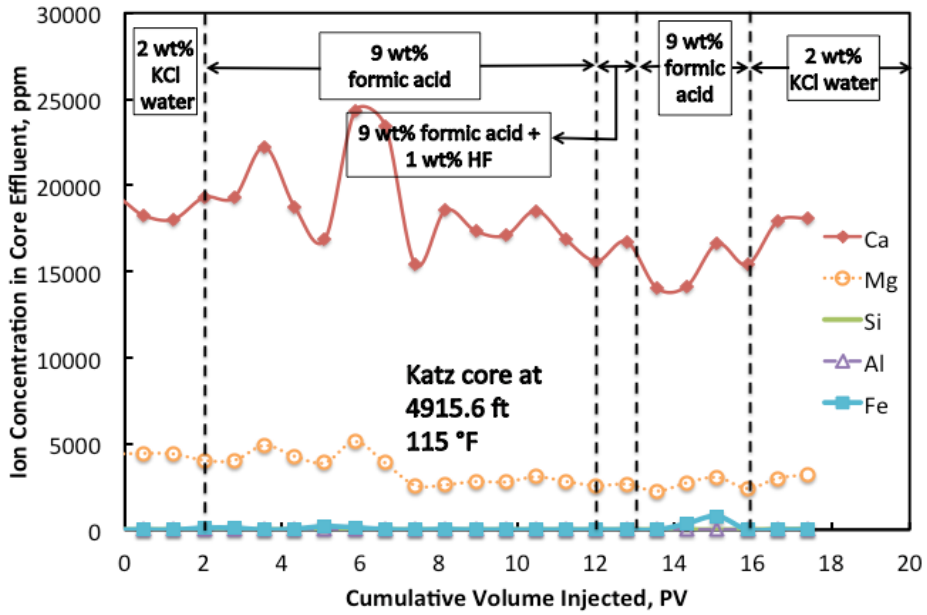


**Fig. 58—Ion concentration in the core effluent samples of Katz core at 4915.6 ft. Flow rate was 5 cm$^3$/min, 1 PV 1 wt% HF.**

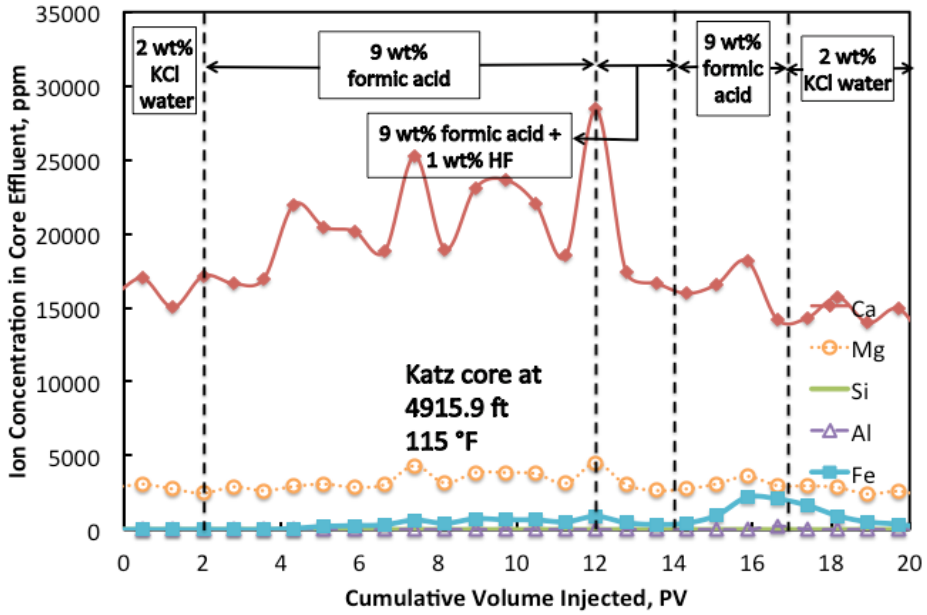


**Fig. 59—Ion concentration in the core effluent samples of Katz core at 4915.9 ft. Flow rate was 5 cm$^3$/min, 2 PV 1 wt% HF.**

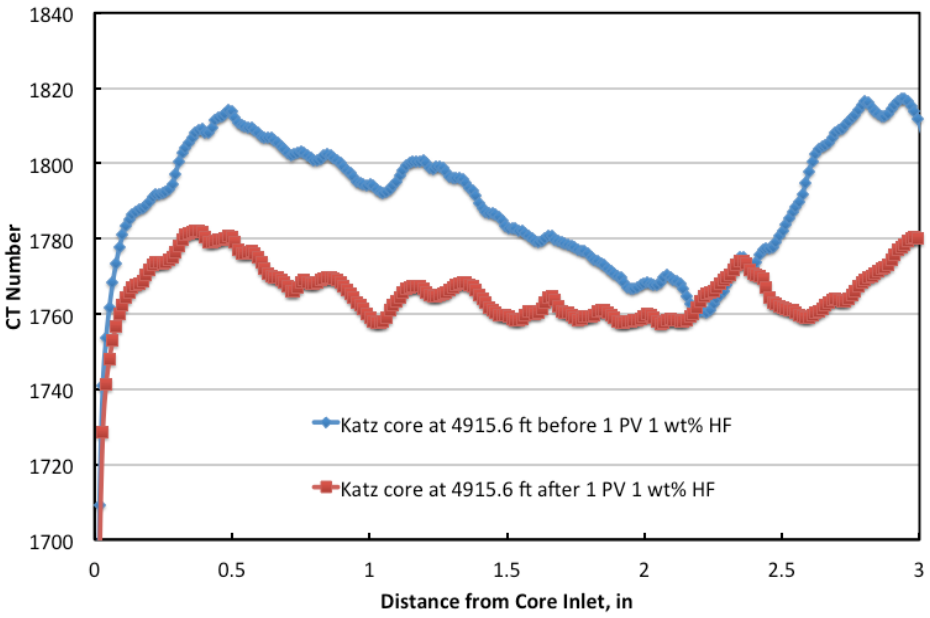


**Fig. 60—CT number across the Katz core at 4915.6 ft after the coreflood test with 5 cm$^3$/min 1 PV of 1 wt% HF at 115°F.**

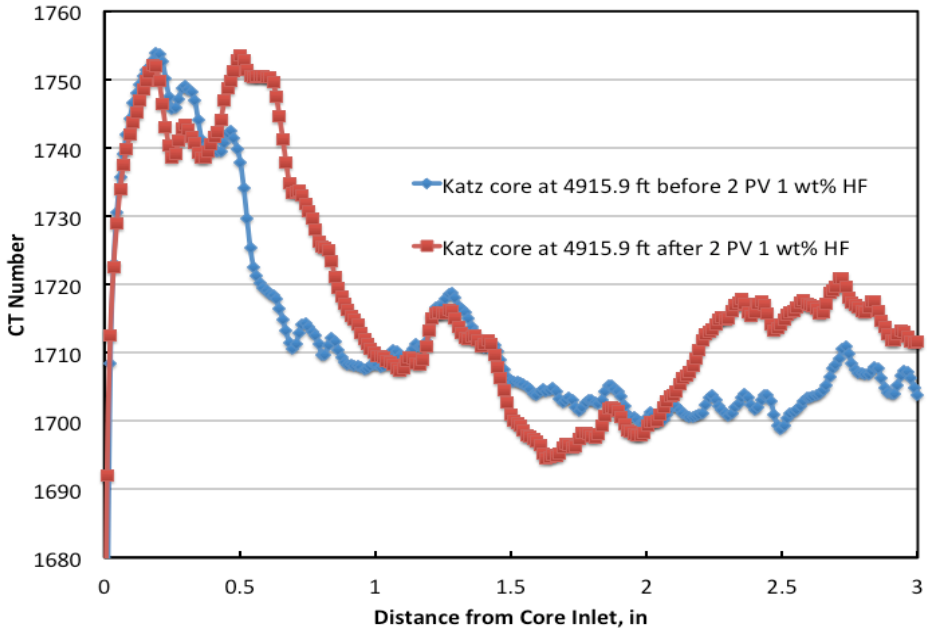


**Fig. 61—CT number across the Katz core at 4915.9 ft after the coreflood test with 5 $cm^3$/min 2 PV of 1 wt% HF at 115°F.**

**Figs. 62** through **64** show the pressure drop, the ion concentration in the core effluent samples, and the CT numbers through the cores before and after the stimulation for coreflood experiment No. 12. No significant precipitation was observed in Fig. 64. When the volume of the 9 wt% formic-0.5 wt% HF in the main flush stage decreased to 1.5 PV, the permeability of the Katz core at 5126.7 ft (3rd sand) only increased 5.55%. **Figs. 65** through **67** showed the pressure drop, the ion concentration in the core effluent samples, and the CT numbers through the cores before and after the stimulation for coreflood experiment No. 13 respectively.

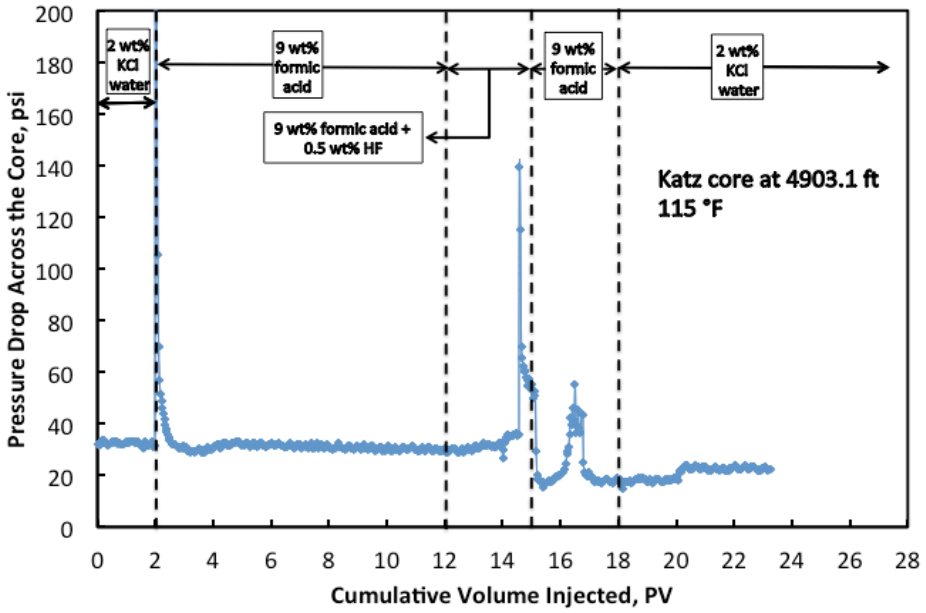


**Fig. 62—Pressure drop across the Katz core at 4903.1 ft, 5 cm$^3$/min, 3 PV 0.5 wt% HF.**

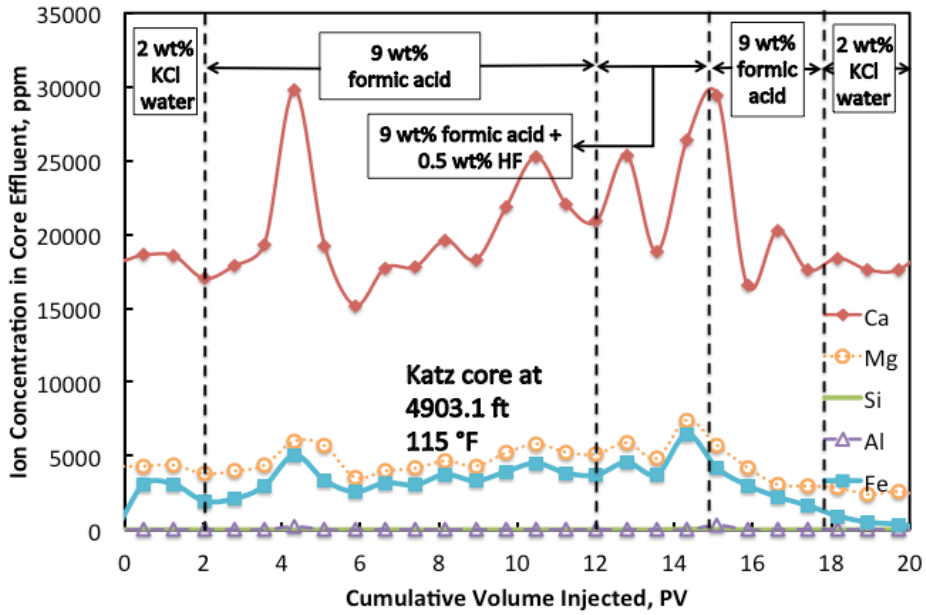


**Fig. 63—Ion concentration in the core effluent samples of Katz core at 4903.1 ft. Flow rate was 5 cm$^3$/min, 3 PV 0.5 wt% HF.**

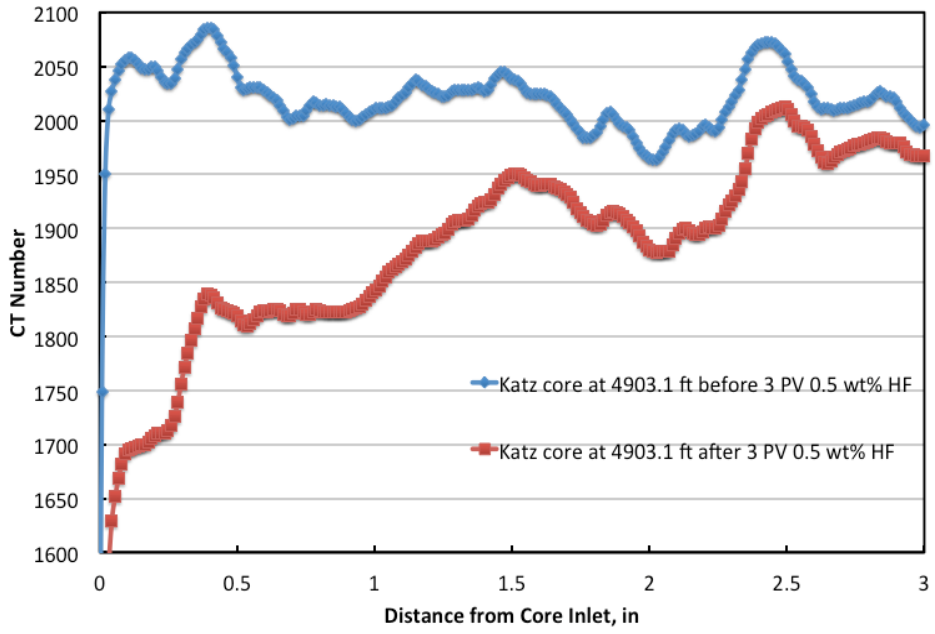


**Fig. 64—CT number across the Katz core at 4903.1 ft after the coreflood test with 5 cm$^3$/min 3 PV of 0.5 wt% HF at 115°F.**

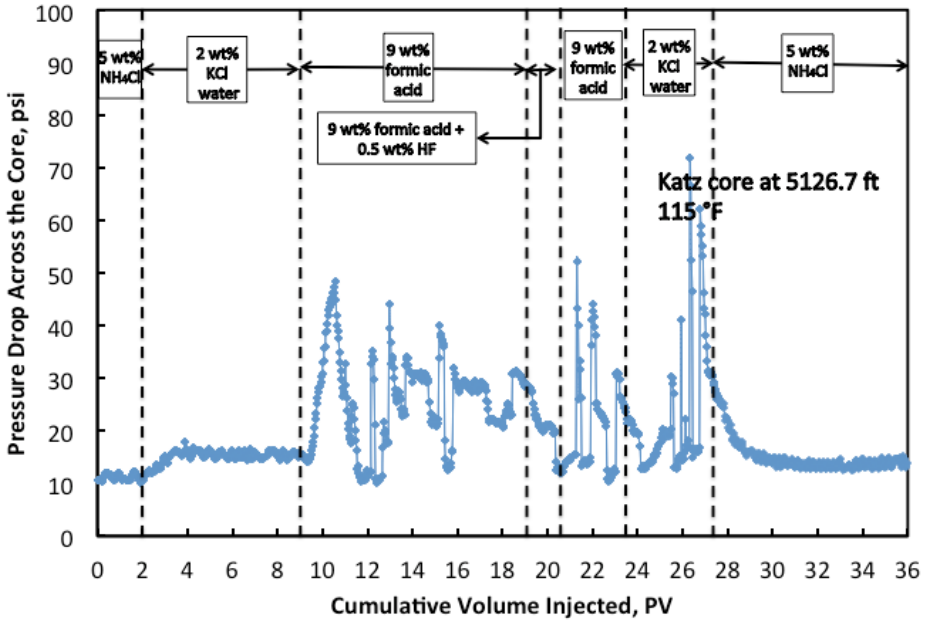


**Fig. 65—Pressure drop across the Katz core at 5126.7 ft, 5 cm$^3$/min, 1.5 PV 0.5 wt% HF.**

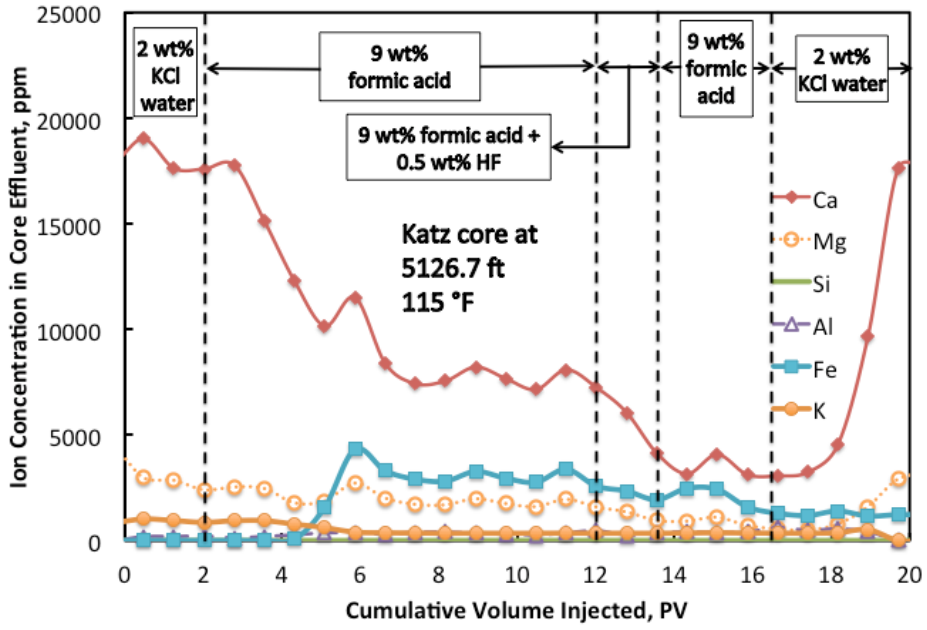


**Fig. 66—Ion concentration in the core effluent samples of Katz core at 5126.7 ft. Flow rate was 5 cm$^3$/min, 1.5 PV 0.5 wt% HF.**

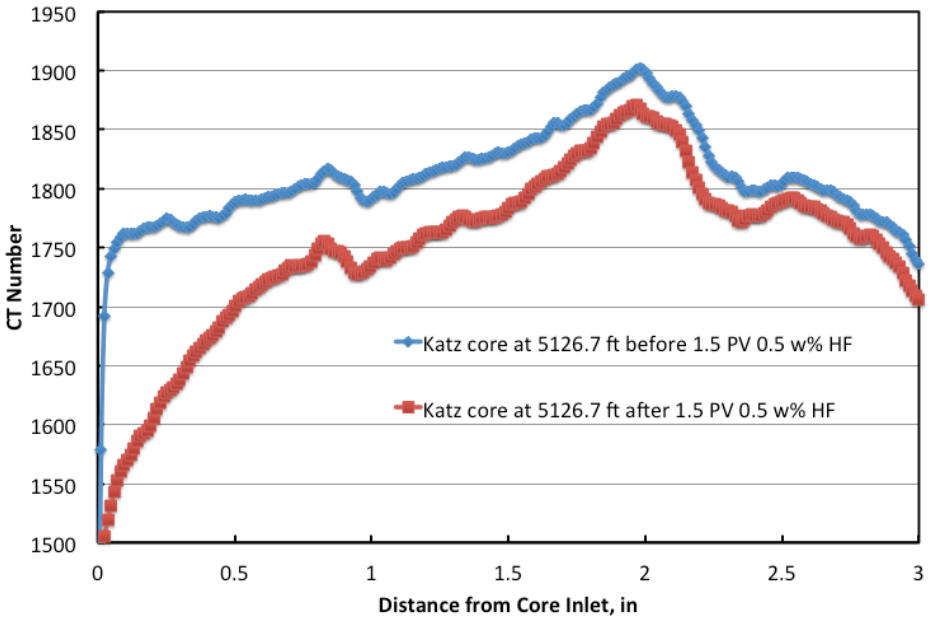


**Fig. 67—CT number across the Katz core at 5126.7 ft after the coreflood test with 5 cm$^3$/min 1.5 PV of 0.5 wt% HF at 115°F.**

Coreflood experiment No. 14 (using Katz core at depth 4948.4 ft, 2nd sand) had the same main flush as Coreflood No. 12. The only difference between these two experiments occurred before the preflush; the Katz core at depth 4948.4 ft has Katz residual oil in it, while the Katz core at 4903.1 ft is clean. To saturate the core with oil, after the Dean-Stark experiment, the core was saturated with the synthetic brine by using the vacuum pump for four hours. Then the Katz crude oil was injected into the core at various flow rates until no brine was observed from the outflow; the flow rate was increased by sequence from 0.1, 0.2, 0.5, 1, 2, to 3 $cm^3$/min. the total amount of brine in the outflow is 7.6 ml. After the synthetic brine (connate water) was injected into the core at the same sequence of the flow rate until no oil was observed from the outflow, the total amount of oil in this step was 1.2 ml. The total pore volume of Katz core at depth 4948.4 ft is 11.2 ml, making the residual oil saturation is 57.14%. After the acid job, the effective permeability of the synthetic brine increased 85.34%. This indicates that the residual oil in the core has no adverse effect to the new acidizing plan. **Figs. 68** through **70** showed the pressure drop, the ion concentration in the core effluent samples, and the CT numbers through the cores before and after the stimulation for coreflood experiment No. 14, respectively.

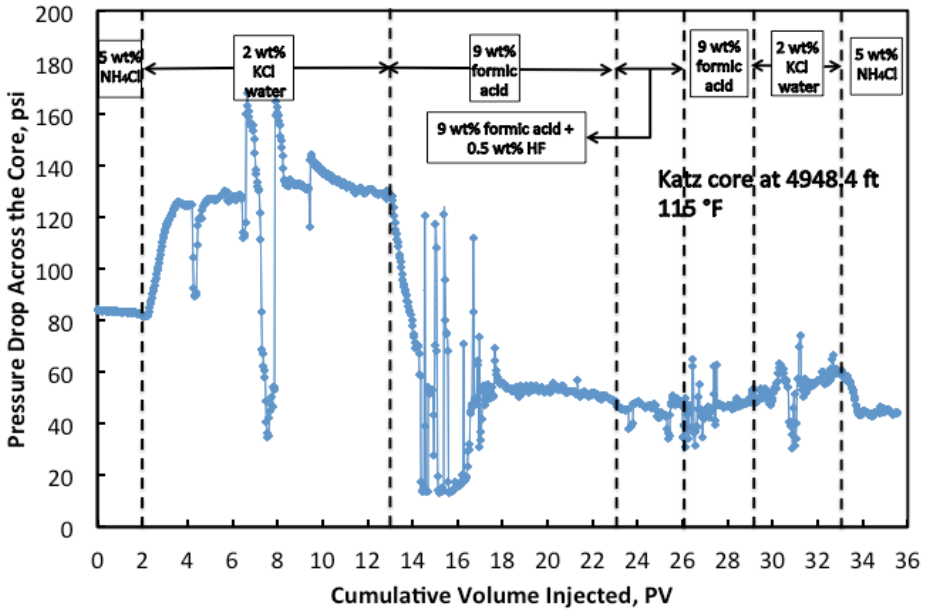


**Fig. 68—Pressure drop across the Katz core at 4948.4 ft, 5 cm$^3$/min, 3 PV 0.5 wt% HF. The core was flushed by Katz crude oil and synthetic brine before the stimulation.**

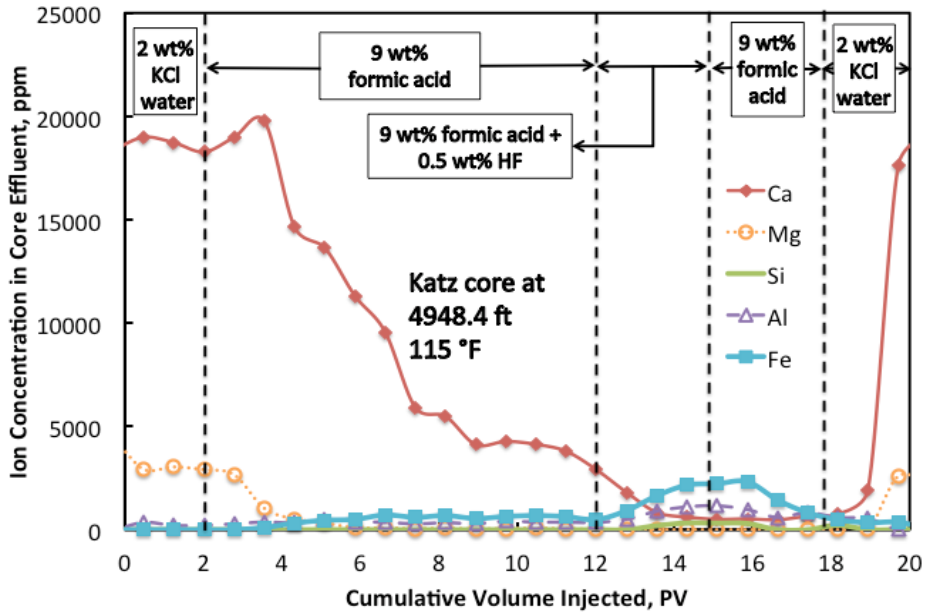


**Fig. 69—Ion concentration in the core effluent samples of Katz core at 4948.4 ft. Flow rate was 5 cm$^3$/min, 3 PV 0.5 wt% HF. The core was flushed by Katz crude oil and synthetic brine before the stimulation.**

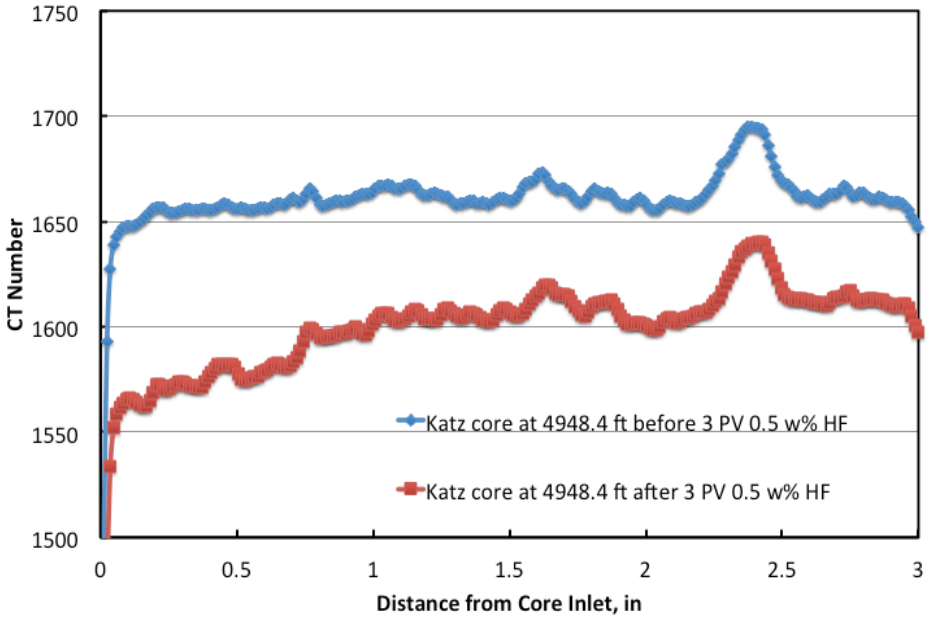


**Fig. 70—CT number across the Katz core at 4948.4 ft after the coreflood test with 5 $cm^3$/min 3 PV of 0.5 wt% HF at 115°F. The core was flushed by Katz crude oil and synthetic brine before the stimulation.**

Coreflood experiment No. 15 (using Katz core at depth 5138.4 ft, 3rd sand) was designed to test if the lower concentration of HCl (5 wt%) can damage the core. The proposed coreflood experiment has 5 steps as follows:

1. White water Xylene Spearhead: 3.1 PV
2. FWS-5% $NH_4Cl$ water spacer + additives: 1.6 PV
3. Second Preflush (5 wt% HCl acid): 3 PV
4. Main (9 wt% formic acid, 1 wt% HF): 3 PV
5. Postflush (9 wt% formic acid+ FWS-5% NH4Cl water spacer + additives): 4 PV

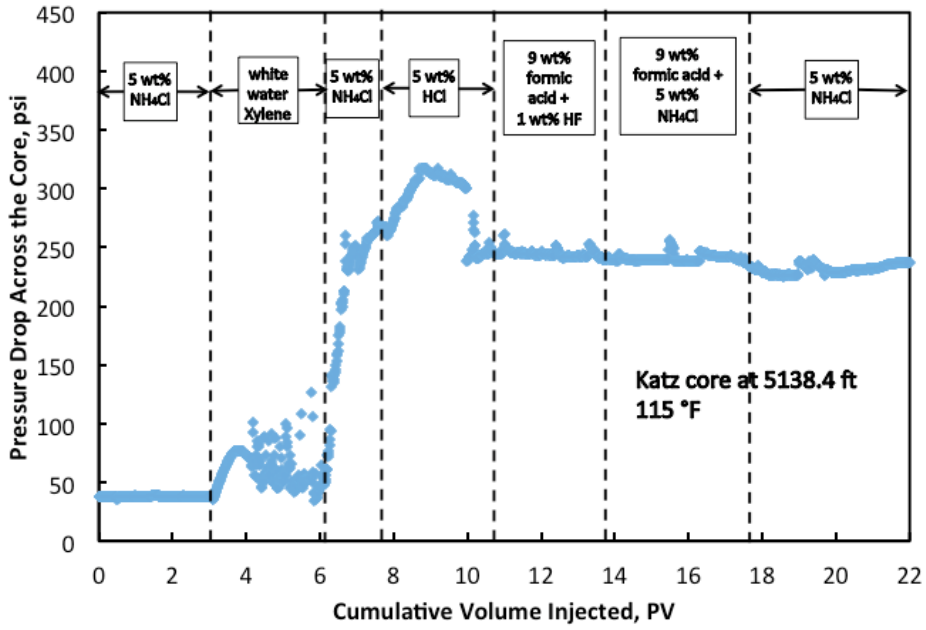


**Fig. 71— Pressure drop across the Katz core at 5138.4 ft, 5 $cm^3$/min, 3 PV 5 wt% HCl followed by 3 PV 1 wt% HF.**

**Fig. 71** shows the pressure drop across the core. The initial permeability is 16.71 md and the final permeability is 2.76 md. The permeability of the core decreased 83.5%.

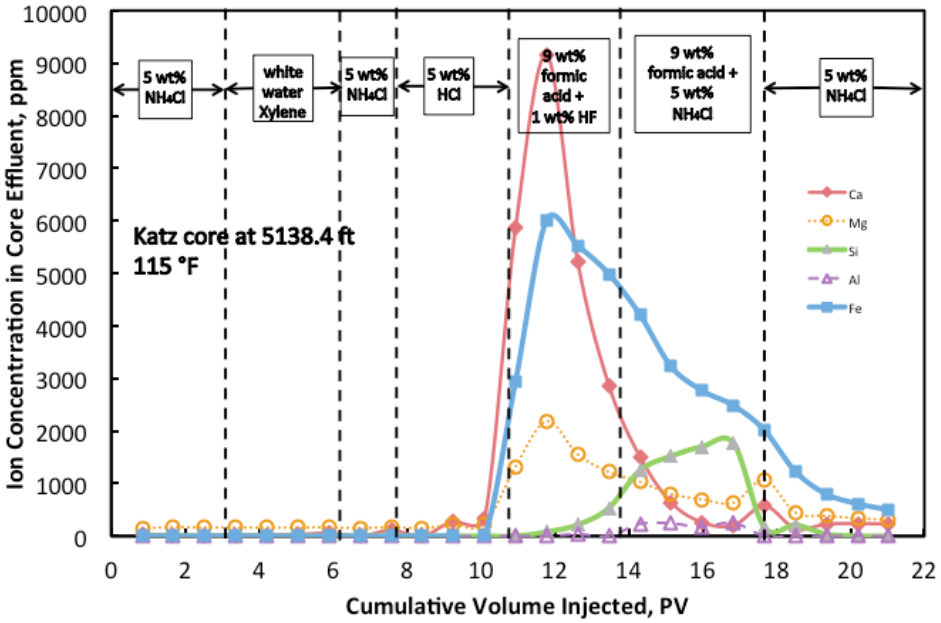


**Fig. 72—Ion concentration in the core effluent samples of Katz core at 5138.4 ft. Flow rate was 5 cm$^3$/min, 3 PV 5 wt% HCl followed by 3 PV 1 wt% HF.**

The ICP results show that on the 5 wt% HCl stage, a lot of Ca, Fe, and Mg were dissolved from the core (**Fig. 72**). This means HCl was dissolving carbonate, dolomite and siderite. The 1 wt% HF in the main flush can cause damage to the core when HCl did not remove all the Ca, Fe, and Mg. The ICP results also show that Si has the peak in the 9 wt% formic acid with the 5 wt% $NH_4Cl$ stage. Because of the dead volume of the coreflood system, the effluent was postponed. The Si was actually dissolved in the 9 wt% formic acid with the 1 wt% HF stage.

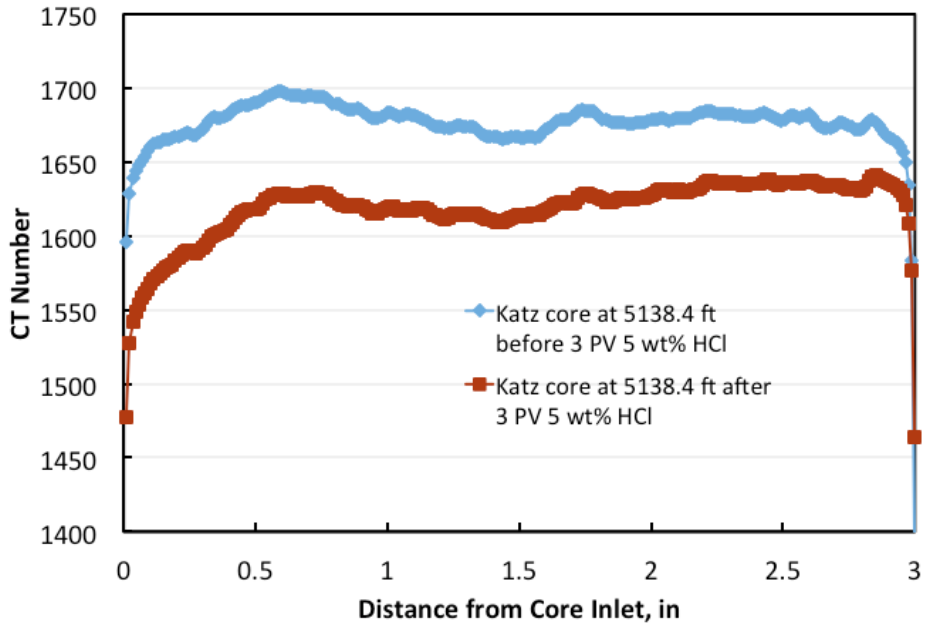


**Fig. 73—CT number across the Katz core at 4948.4 ft after the coreflood test with 5 cm$^3$/min 3 PV 5 wt% HCl followed by 3 PV 1 wt% HF.**

**Fig. 73** shows the CT numbers through the cores before and after the stimulation for coreflood experiment No. 15. Two reasons can cause the density of the core decrease after the acidizing job. HCl dissolves carbonate, dolomite and siderite or HF dissolves the clays or both. However, the core still got damaged and there are also two possible reasons. The 3 PV 5 wt% HCl did not remove all the carbonate, dolomite and siderite and in the HF stage, formic acid dissolves Ca, Mg, and Fe and produces precipitation. Another reason can be HCl reacts with the illite and precipitate amorphous silica gel which can block the pore throat and damage the core. In this case the acidizing plan No. 15 is not recommend.

## *4.4 Conclusions*

A series of coreflood experiments have been performed on cores from the Katz formation and outcrops with similar mineralogy composition as the Katz formation. The original acidizing plans were tested, and a new acidizing plan with formic-HF acid in the main flush was proposed and tuned.

1. The original acidizing plan is damaging the Katz formation in all three pay zones. The 15 or 20 vol% HCl is causing problems when reacting with illite.
2. The stimulation had the best result when using 3 PV of 9 wt% formic-0.5 wt% HF in the main flush. Decreasing the main flush volume will be detrimental to the results.
3. Residual oil in the core has no adverse effect to the new acidizing plan.
4. The new acidizing plan can prevent the damaged caused by the original acidizing plan for the Katz field.

# 5 KATZ FIELD CASE STUDY (FIELD STUDY)

## *5.1 Introduction*

Two candidates were chosen in this project and they are KSU 122 and KSU 132. Both of these two wells are injection wells and the locations are shown in Fig. 31.

### 5.1.1 Candidate Well

#### *5.1.1.1 KSU 122*

There are three pay zones and they are called the 1st, 2nd, and 3rd Sand. The 2nd Sand is divided into two sub-zones and they are called the 2A/2B and 2C from top to bottom. The 3rd Sand is also divided into two sub-zones and they are called the Upper 3rd Sand and the Lower 3rd Sand. The KSU 122 was chosen in our project because each pay zone of the well is well isolated by packers and it is easier if only one pay zone wants to be stimulated. Only the Upper 3rd Sand was stimulated in this project and its total depth is 44 ft, which is from 5071 to 5115 ft.

#### *5.1.1.2 KSU 132*

Similar with KSU 122, only the Upper 3rd Sand of KSU 132 was stimulated in this project and the total depth is 64 ft, which is from 5063 to 5127 ft.

### 5.1.2 Acidizing History of the 3rd Sand

#### *5.1.2.1 KSU 122*

KSU 122 was acidized on 3/18/2011, which is the initial completion. 84 gal of 15% HCl acid was spotted at 5115 ft. After that a packer was set at the depth of 5004 ft.

#### *5.1.2.2 KSU 132*

04/02/2010—Initial Completion

There are three perforations of KSU 132 and they are at 4816 to 4828 ft, 4880 to 4914 ft, and 5080 to 5124 ft.

Stage 1 (5080 to 5124 ft) – Pumped 1250 gal treated water, 1250 gal 15% Ferchek SC acid, 1000 gal treated water with ball diverters, 1250 gal 15% Ferchek SC acid, flush with 2400 gal treated water;

Stage 2 (4880 to 4914 ft) – Pumped 1200 gal treated water, 1000 gal 15% Ferchek SC acid, 1000 gal treated water with ball diverters, shut down job due to communication;

Squeeze Perfs 4880 to 4914 ft;

Stage 2 Repeat (4880 to 4914 ft) – Pumped 1250 gal treated water, 1000 gal 15% Ferchek SC acid, 1000 gal treated water with ball diverters, 1000 gal 15% Ferchek SC acid, flush with 2000 gal treated water;

Stage 3 (4816 to 4828 ft) – 1100 gal treated water, 750 gal 15% Ferchek SC acid, flush with 2000 gal treated water.

07/23/2014—Slick Water Acid Fracturing

The following amount of fluids were pumped in to the KSU 132 by sequence: 40 bbls Xylene, 60 bbls slick water, 48 bbls acid, 40 bbls gel, 30 bbls Xylene, 40 bbls gel, 20 bbls slick water, 60 bbls gel, 48 bbls acid, flushed with 100 bbls fresh water.

06/03/2015—Recompletion

Perfs: 4815 ft, 4816 to 4828 ft, 4880 to 4914 ft, 4935 to 4955 ft, 4972 to 4986 ft, 5063 to 5079 ft, 5080 to 5124 ft, and 5125 to 5127 ft.

Stage 1 (5063 to 5124 ft) – Pumped 3100 gal acid and 200 bbls of treated water

Stage 2 (4935 to 4986 ft) – Pumped 1700 gal acid and 100 bbls of treated water

Stage 3 (4815 to 4828 ft) – Pumped 650 gal acid and 200 bbls of treated water

[Note: There is no other information on the quality of acid or composition of the treated water. There was a xylene flush before each stage.]

### 5.1.3 Mineral Composition of the 3rd Sand

#### *5.1.3.1 KSU 122*

The only core samples available for the whole field were from KSU 231 and KSU 326. KSU 231 is much closer in the location with the candidate well KSU 122, however its mineralogy composition is still not a good reference for KSU 122.

**Fig. 74** shows the locations of KSU 122 and KSU 231 with KSU 221, KSU 220, and KSU121 in between. The red line connected these five wells. The distance between these wells are shown in the figure. **Fig. 75** shows the cross section for well KSU 231, KSU 221, KSU 220, KSU121, and KSU 122. Green color represents shale/oil saturation; yellow color represents sand; dark blue color represents limestone. Distinctive lithological contrast between the KSU 231 and KSU 122 was observed in terms of percentage of sand to shale compositions in the Upper 3rd Sand and Lower 3rd Sand. By inference from logs, lithofacies bedding frequencies is higher in KSU 231 in the Upper

3rd Sand compared to KSU 122. The lithological contrast is so much that KSU 231 mineralogy cannot be used to model the mineralogy of KSU 122.

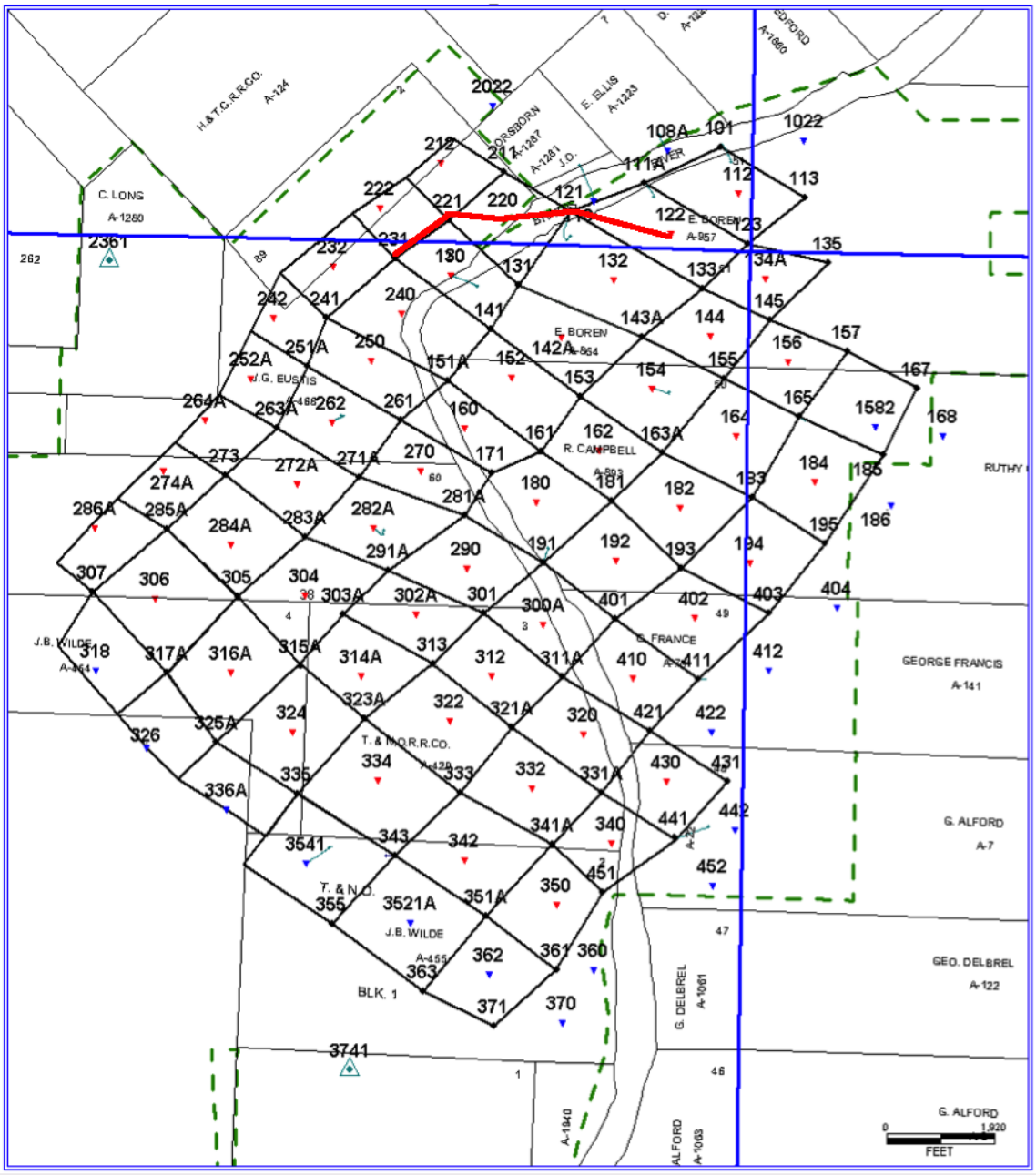


**Fig. 74—Locations of KSU 122 and KSU 231 with KSU 221, KSU 220, and KSU 121 in between. The red line connects these five wells.**

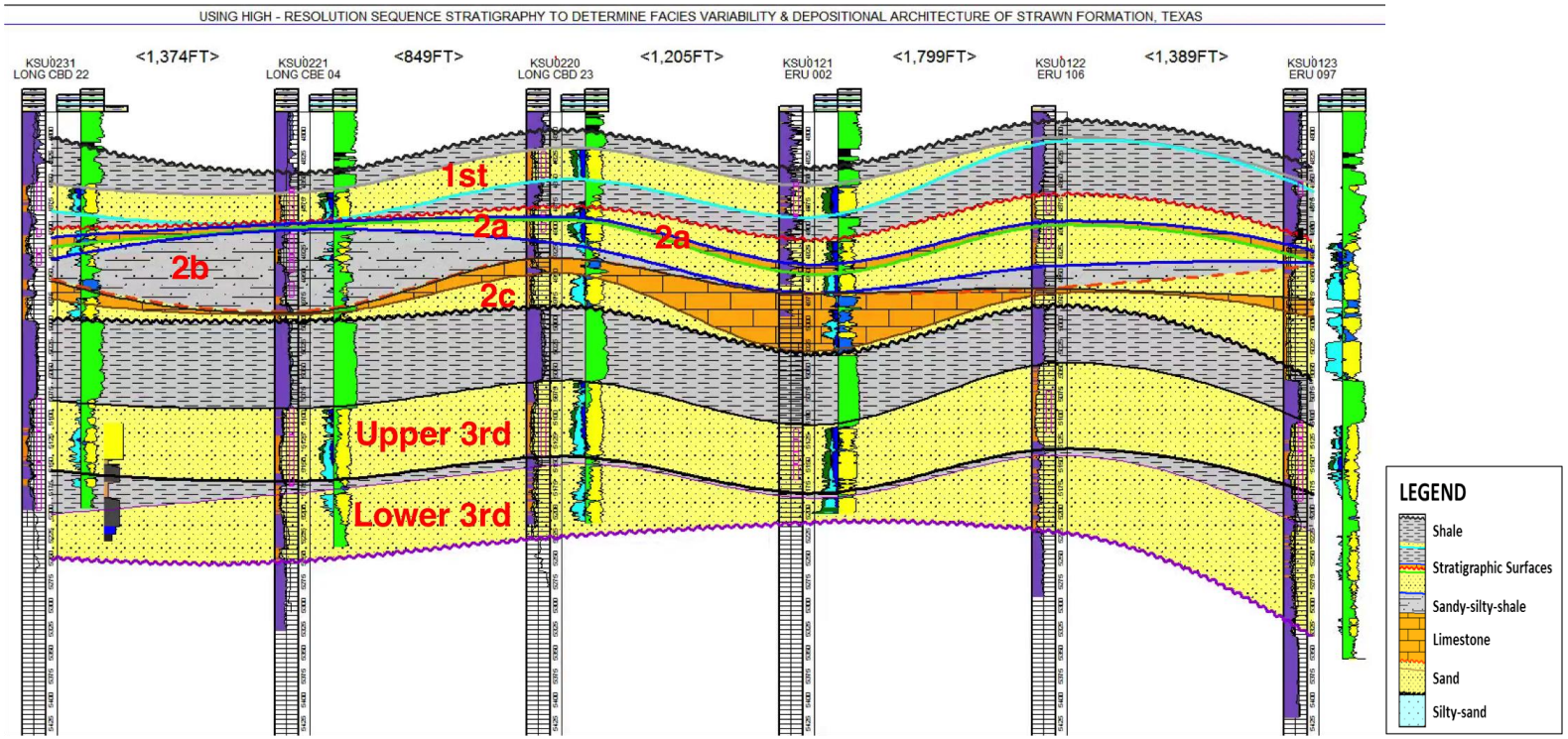


**Fig. 75—Cross section for well KSU 231, KSU 221, KSU 220, KSU 121, and KSU 122. Green color represents shale/oil saturation; yellow color represents sand; dark blue color represents limestone. The 1st, 2a, 2b, 2c, upper 3rd, and lower 3rd Sand are also marked in the figure.**

### *5.1.3.2 KSU 132*

Fig. 31 shows that the distance between KSU 132 and KSU 231 is only a little bit shorter than the distance of KSU 122 and KSU 231. **Fig. 76** shows distinctive lithological contrast between the KSU 231 and KSU 132 was observed in terms of percentage of sand to shale compositions in the Upper 3rd Sand and Lower 3rd Sand.

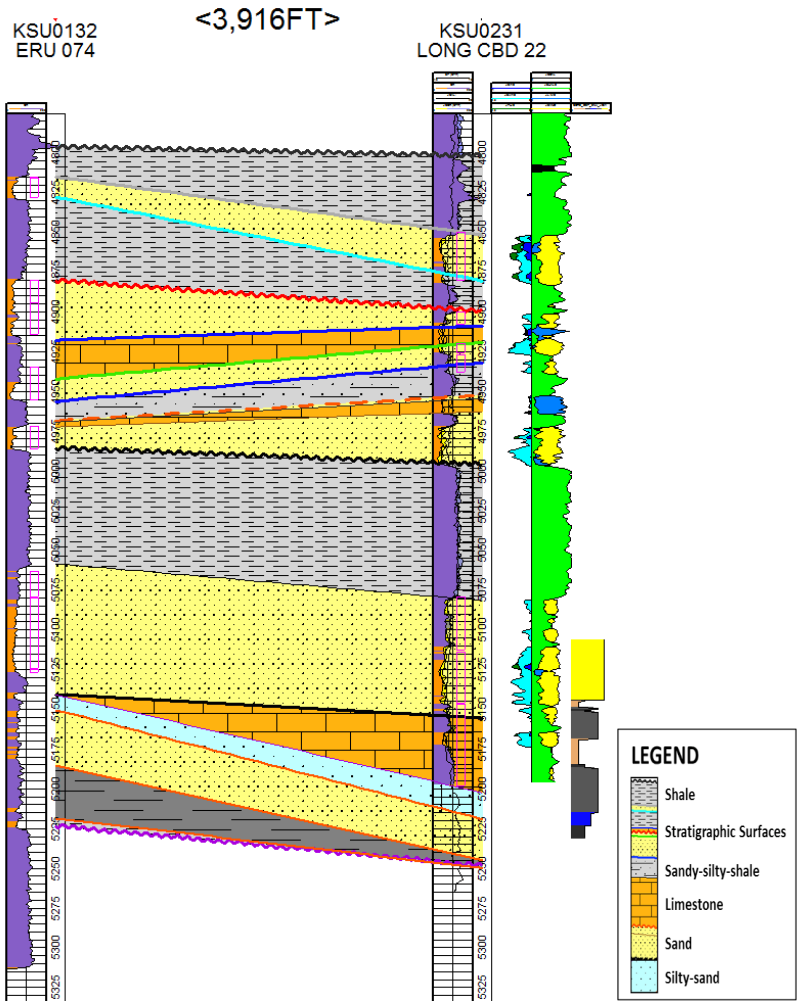


**Fig. 76—Cross section for well KSU 231 and KSU 132. Green color represents shale/oil saturation; yellow color represents sand; dark blue color represents limestone.**

### 5.1.4 Acidizing Plan

The proposed acidizing plan from chapter 4 has 6 steps and they are shown as follows:

1. Pump 18.7 gal/ft white water Xylene Spearhead (Pump 9.4 gal/ft into formation, let it soak overnight, continue to pump the remainder of the fluid systems.)
2. Pump 9.4 gal/ft Slick, FWS-5% $NH_4Cl$ water spacer + additives

   1000 g fluid includes:

   - 50 g $NH_4Cl$
   - 2 ml water wetting surfactant
   - 948 g water
3. Preflush (9 wt% Formic acid): 59 gal/ft

   1000 g fluid includes:

   - 30 g $NH_4Cl$
   - 93.75 g 96 wt% Formic acid
   - 2 ml water wetting surfactant
   - 2 ml FE-360 (Reducer) Iron reducer, AS-2A: 2g/1000g
   - 1 ml corrosion inhibitor (Plexhib 100): 1 gpt
   - 871.25 g water
4. Main flush (9 wt% Formic acid, 0.5 wt% HF): 18 gal/ft

   1000 g fluid includes:

   - 30 g $NH_4Cl$
   - 93.75 g 96 wt% Formic acid

- 7.5 g of ABF
- 12.5 g of 36.5% HCl solution
- 2 ml water wetting surfactant
- 2 ml FE-360 (Reducer) Iron reducer, AS-2A: 2g/1000g
- 1 ml corrosion inhibitor (Plexhib 100): 1 gpt
- 851.25 g water

5. Postflush (9 wt% Formic acid): 18 gal/ft

   1000 g fluid includes:

   - 30 g $NH_4Cl$
   - 93.75 g 96 wt% Formic acid
   - 2 ml water wetting surfactant
   - 2 ml FE-360 (Reducer) Iron reducer, AS-2A: 2g/1000g
   - 1 ml corrosion inhibitor (Plexhib 100): 1 gpt
   - 871.25 g water

6. Pump FWS-5% $NH_4Cl$ water spacer + additives, the volume is the volume of the tubing from surface to the bottom of the 3$^{rd}$ Sand (in total 1062 gal which equals to 19 gal/ft).

   1000 g fluid includes:

   - 50 g $NH_4Cl$
   - 2 ml water wetting surfactant
   - 948 g water

   Soaking for 2 hours before injecting the $NH_4Cl$ water spacer.

#### *5.1.4.1 KSU 122*

The target zone is the Upper 3rd Sand, which has the depth of 44 ft. In this case the volume of the fluids in each step were proposed as follows:

1. White water Xylene Spearhead: 823 gal
2. FWS-5% $NH_4Cl$ water spacer + additives: 414 gal
3. Preflush (9 wt% Formic acid): 2596 gal
4. Main flush(9 wt% Formic acid, 0.5 wt% HF): 792 gal
5. Postflush (9 wt% Formic acid): 792 gal
6. FWS-5% $NH_4Cl$ water spacer + additives: 1056 gal

However, due to the budget, the proposed acidizing job was modified as follows:

1. White water Xylene Spearhead: 823 gal
2. FWS-5% $NH_4Cl$ water spacer + additives: 414 gal
3. Preflush (9 wt% Formic acid): 950 gal
4. Main flush(9 wt% Formic acid, 0.5 wt% HF): 792 gal
5. Postflush (9 wt% Formic acid): 594 gal
6. FWS-5% $NH_4Cl$ water spacer + additives: 1056 gal

All fluids were injected by using the tubing string directly. Coil tubing was not considered because of the small diameter and low flow rate.

#### *5.1.4.2 KSU 132*

The target zone is the Upper 3rd Sand, which has the depth of 64 ft. In this case the volume of the fluids in each step are as follows:

1. White water Xylene Spearhead: 1197 gal

2. FWS-5% $NH_4Cl$ water spacer + additives: 420 gal
3. Preflush (9 wt% Formic acid): 3780 gal
4. Main flush (9 wt% Formic acid, 0.5 wt% HF): 1150.8 gal
5. Postflush (9 wt% Formic acid): 1150.8 gal
6. FWS-5% $NH_4Cl$ water spacer + additives: 1058.4 gal

All fluids were injected by using the tubing string directly. Coil tubing was not considered because of the small diameter and low flow rate.

### 5.1.5 Preparation Experiment

Because all the fluids were injected into the target zone through the tubing string, a local service company did the corrosion test.

Two solutions containing 9 wt% of formic acid and 9 wt% of formic acid with 0.5 wt% HF were prepared and heated to 120°F. The corrosion inhibitor Plexhib 100 was added into both acid systems in the concentration of 1 gpt. One entire section of the tubing was immersed in the each of the acid for 24 hours. The tubing sections were dried in the oven and weighted before and after the soaking and the weight increased slightly. The inside layer of the tubing section is the fiberglass and the outside of the tubing section is the exterior coating. The coating on the exterior of the pipe began to separate from the pipe. However in the real acid injection case, acid shouldn't be able to reach and react with the outside of the pipe. In this case, this issue may not cause any problem. Acid was able to penetrate between the outside coating and the steel, which are believed not fully removed by using the oven after the soaking procedure. This might be the reason of the increased weight of the tubing section (Wiggins 2015). So both 9 wt% of

formic acid and 9 wt% of formic acid with 0.5 wt% HF acid system would not cause problem when adding the1 gpt of the Plexhib 100.

## *5.2 Stimulation Performance*

### 5.2.1 KSU 122

The water-alternative-gas procedure started from June 2011. The modified acid job was on 04/28/2016. **Fig. 77** shows the $CO_2$ injection rate, water injection rate, casing pressure, tubing pressure, and line pressure from July 2015 to March 2017 for KSU 122. The $CO_2$ injection rate increased slightly after the acid job. With the same tubing pressure, the $CO_2$ injection rate increased from about 1800 bbl to 3000 bbl and maintained there ever since. In this case, the acidizing job did improve the performance of KSU 122.

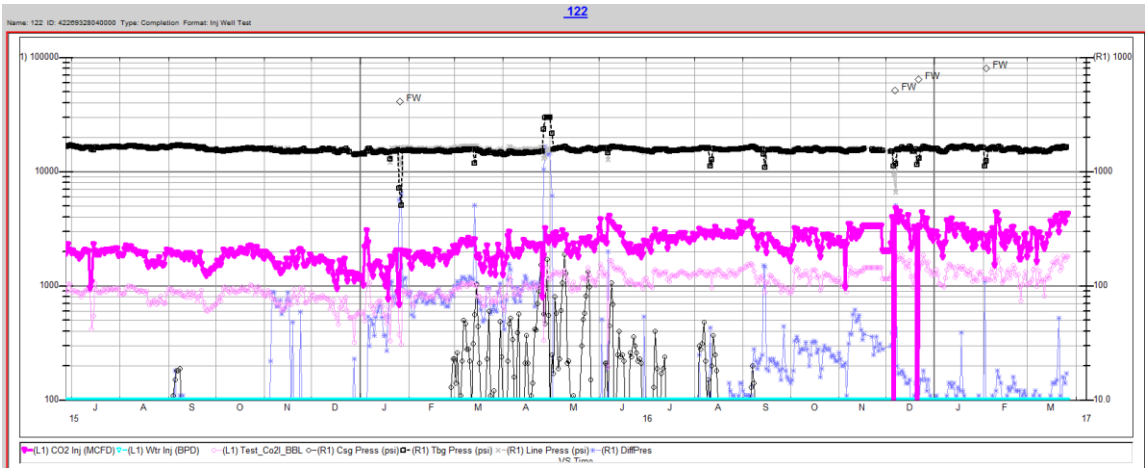


**Fig. 77—$CO_2$ injection rate, water injection rate, casing pressure, tubing pressure, and line pressure from July 2015 to March 2017 for KSU 122.**

### 5.2.2 KSU 132

The water-alternative-gas procedure started from June 2010. The acid job was on 07/28/2016. **Fig. 78** shows the $CO_2$ injection rate, water injection rate, casing pressure, tubing pressure, and line pressure from July 2015 to March 2017 for KSU 132.

The initial response after the stimulation shows positive results as injection increased by double previous rates. However over the course of the month, rates began declining and eventually leveled off back to prestimulation numbers. When opening the sleeves to put the well back on injection for every zone (since the acid job was only performed on the 3$^{rd}$ sand only) the total rates were higher and maintained higher until injection of water started. On February 2017 the well has been back on $CO_2$ injection and the injection rates look to be up again. The testing results show that the acid job helped over the long haul. Comparing the data on March 2017 with March 2016, with a lower tubing pressure, the injection rate of $CO_2$ kept almost the same. This means after the acid job the injection index of the well KSU 132 increased and the skin factor decreased. The acid job improved the performance of KSU 132 as well. More acid jobs are recommended in the Katz field.

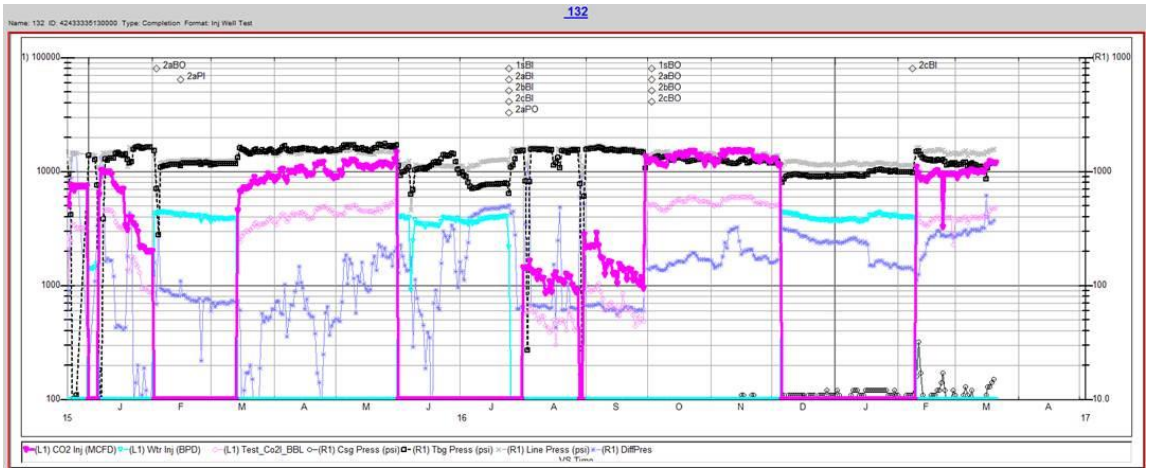


**Fig. 78— $CO_2$ injection rate, water injection rate, casing pressure, tubing pressure, and line pressure from December 2015 to March 2017 for KSU 132.**

## *5.3 Conclusions*

The formic acid/hydrofluoric acid system have been tested on the third sand of well KSU 122 and KSU 132 in the Katz field. For the budget reason, the amount of 9 wt% formic acid in both preflush and post flush was cut for well KSU 122. The performances of both acidizing projects are both positive:

1. The modified acid job improved the performance of KSU 122 and maintained the improvement for more than 11 month. The injection rate of $CO_2$ increased from about 1800 bbl to 3000 bbl by 67%.
2. The acid job improved the performance of KSU 132. Even the well switch from $CO_2$ injection to water injection and then back to $CO_2$ injection, the $CO_2$ injection rate still keeps high.
3. More acid jobs are recommended for the Katz field.

# 6 OVERALL CONCLUSIONS AND FUTURE STUDIES

## *6.1 Overall Conclusions*

### 6.1.1 Al-based Retarded Mud Acid

In this study, a series of solubility tests of Al-based retarded mud acid (15 wt% HCl, 1.5 wt% HF, and 5 wt% $AlCl_3 \cdot 6H_2O$) and mud acid (15 wt% HCl and 1.5 wt% HF) with kaolinite, illite, and bentonite were performed at both 75 and 200°F. Al-based retarded mud acid with different concentration of $AlCl_3 \cdot 6H_2O$ has also been tested. Coreflood tests at 75, 200, and 300°F were also performed and the following conclusions were drawn.

1. $AlCl_3$ can be added into the mud acid system as a retarder to react with clay minerals at 75 and 200°F. The retarding effect decreased as temperature increased.
2. At 75°F, the higher the $AlCl_3$ concentration is in the Al-based retarded mud acid system, the less clays it can dissolve.
3. $^{19}F$ NMR showed that $AlF_3$ and $AlF_4^-$ in the spent acid were the only two aluminum fluoride complexes, $AlF_4^-$ slowly hydrolyzes with $H^+$ to release HF, which keep the low $F^-$ concentration in the system.
4. $^{19}F$ NMR results also showed that more $F^-$ can complex with Al in the Al-based retarded mud acid system than in the mud acid system, which could lead to a deeper penetration of the acid into the formation.

5. No $AlF_3$ precipitate was observed in any of the Al-based retarded mud acid solubility tests at both 75 and 200°F.
6. At high temperatures, $Si(OH)_4$ precipitates very fast, which might cause formation damage.
7. CT scans showed deeper penetration of Al-based retarded mud acid than mud acid at 75°F, but the penetration reduced when temperature increased to 200°F.
8. Al-based retarded mud acid can better improve the permeability of a Berea sandstone core than mud acid under 300°F. The lower the temperature is, the better the potential retardation effect of Al-based retarded mud acid could have. The retarding effect diminished at 300°F.

### 6.1.2 Katz Field Case Study

A series of coreflood experiments have been performed on cores from the Katz formation and outcrops with similar mineralogy composition as the Katz formation. The original acidizing plans were tested, and a new acidizing plan with formic-HF acid in the main flush was proposed and tuned.

1. The original acidizing plan is damaging the Katz formation in all three pay zones. The 15 or 20 vol% HCl is causing problems when reacting with illite.
2. The stimulation had the best result when using 3 PV of 9 wt% formic-0.5 wt% HF in the main flush. Decreasing the main flush volume will be detrimental to the results.
3. Residual oil in the core has no adverse effect to the new acidizing plan.

4. The new acidizing plan improved the performance of both KSU 122 and KSU 132.
5. More acid jobs are recommended for the Katz field.

## *6.2 Significance*

### 6.2.1 Al-based Retarded Mud Acid

This study at the first time investigates the mechanism of why $AlCl_3$ can work as a retarder in the Al-based retarded mud acid system and gives the guideline of how this acid system can be applied in the field.

### 6.2.2 Katz Field Case Study

This study at the first time finds the flaw of the original acidizing plan for the Katz field and provides the guidelines for designing the most effective acidizing treatment in the Katz field. Both field tests on well KSU 122 and KSU 132 gave positive results and it is recommended for more wells to improve their performance.

## *6.3 Future Works*

### 6.3.1 Al-based Retarded Mud Acid

1. Investigate the optimal flow rate of the Al-based retarded mud acid when acidizing the Berea sandstone by using coreflood experiment.
2. Investigate the optimal flow rate and temperature of the Al-based retarded mud acid when acidizing the different types of sandstone by using coreflood experiment.

3. Summarize all the experimental data and find the relationship of optimal temperature, optimal flow rate, and mineralogy composition of the formation.

### 6.3.2 Katz Field Case Study

1. If more wells will be drilled in the field, drilling cuttings can be collected and analyzed by XRD. With the well logging data, more accurate and detailed mineralogy information about the Katz formation will known.
2. Five coreflood experiments were done to the Katz cores due to the limited access to the Katz cores and those cores are only from two wells KSU 231 and KSU 326. The mineral composition of Katz formation from different pay zones or even within the same pay zone varies. In this case, KSU 231 and KSU 326 cannot represent the whole Katz formation very well. Therefore when more Katz cores from other wells are available, more coreflood experiments can be done to find the more efficient acid system for each zone of each well.
3. The two field tests are both on injection wells. This acid job can also be applied on the production wells in the future and can be tuned based on the well performance.

# REFERENCES


Abrams, A., Scheuerman, R. F., Templeton, C. C and Richardson, E. A. 1983. Higher-pH Acid Stimulation Systems. J Pet Tech, 35 (12), 2175-2184. SPE-7892-PA. http://dx.doi.org/10.2118/7892-PA.

Al-Dahlan, M. N., Nasr-El-Din, H. A., and Al-Qahtani, A. A. 2001. Evaluation of Retarded HF Acid Systems. Presented at the SPE International Symposium on Oilfield Chemistry, Houston, Texas, 13-16 February. SPE-65032-MS. http://dx.doi.org/10.2118/65032-MS.

Al-Harbi, B. G., Al-Dahlan, M. N., Al-Khaldi, M. H., Al-Harith, A. M., and Abadi, A. K. 2013. Evaluation of Organic Hydrofluoric Acid Mixtures for Sandstone Acidising. Presented at the International Petroleum Technology Conference, Beijing, China, 26-28 March. IPTC-16967-MS. http://dx.doi.org/10.2523/16967-MS.

Al-Harbi, B. G., Al-Khaldi, M. H., AlDossary, K. A. 2011. Interactions of Organic-HF Systems with Aluminosilicates: Lab Testing and Field Recommendations. Presented at the SPE European Formation Damage Conference, Noordwijk, Netherlands, 7-10 June. SPE-144100-MS. http://dx.doi.org/10.2118/144100-MS.

Akin, S. and Kovscek, A. R. 2003. Computed Tomography in Petroleum Engineering Research. *Geol. Soc. London Spec. Publ.*, **215**: 23-38, http://dx.doi.org/10.1144/GSL.SP.2003.215.01.03.

Bodor, A., Tóth, I., Bányai, I. et al. 2000. $^{19}F$ NMR Study of the Equilibria and Dynamics of the $Al^{3+}/F^-$ System. *Inorg. Chem.* **39** (12): 2530-2537. http://dx.doi.org/10.1021/ic991248w.

Brosset, C. and Orring, J. 1943. Study on the Consecutive Formation of Aluminium Fluoride Complexes. *Svensk kemisk tidskrift.* **55**: 101-116.

Da Motta, E. P., Miranda, C. R., Anjos, S. M. C., Ribeiro, J. A., and Chaves, E. 1996. Acidizing Wells With Acetic/HF Acid Mixtures to Minimize Cement Dissolution. Presemted on the SPE Formation Damage Control Symposium, Lafayette, Louisiana, 14-15 February. SPE-31080-MS. http://dx.doi.org/10.2118/31080-MS.

Economides M. J., Hill A. D., Ehlig-Economides C., Zhu D. 1965. *Petroleum Production System.* 2nd edition. ISBN 9780137031580.

Finney, W. F., Wilson, E., Callender, A. et al. 2006. Reexamination of Hexafluorosilicate Hydrolysis by $^{19}F$ NMR and pH Measurement. *Environ. Sci. Technol.* **40** (8): 2572-2577. http://dx.doi.org/10.1021/es052295s.

Gdanski, R. D. 1985. $AlCl_3$ Retarded HF Acid for More Effective Stimulation. *Oil &Gas J.* **83** (43): 111-115.

Gdanski, R. D. 1998. Kinetics of Tertiary Reactions of Hydrofluoric Acid on Aluminosilicates. *SPE Prod & Oper* **13** (2): 75-80. SPE-31076-PA. http://dx.doi.org/10.2118/31076-PA.

Gdanski, R. D. 1999. Kinetics of the Secondary Reaction of HF on Alumino-Silicates. *SPE Prod & Oper* **14** (4): 260-268. SPE-59094-PA. http://dx.doi.org/10.2118/59094-PA.

Gdanski, R. D. 2000. Kinetics of the Primary Reaction of HF on Alumino-Silicates. *SPE Prod & Oper* **15** (4): 279-287. SPE-66564-PA. http://dx.doi.org/10.2118/66564-PA.

Gdanski, R. D. and Shuchart, C. E. 1996. Newly Discovered Equilibrium Controls HF Stoichiometry. *J. Pet Technol.* **48** (2): 145-149. SPE-30456-JPT. http://dx.doi.org/10.2118/30456-JPT.

Gidley, J. L. 1985. Acidizing Sandstone Formations: A Detailed Examination of Recent Experience. Presented at the SPE Annual Technical Conference and Exhibition, Las Vegas, Nevada, 22-26 September. SPE-14164-MS. http://dx.doi.org/10.2118/14164-MS.

Ji, Q., Zhou, L., Nasr-El-Din, H. A. 2015. Acidizing Sandstone Reservoirs With Aluminum-Based Retarded Mud Acid. *SPE J.* SPE-169395-PA. http://dx.doi.org/10.2118/169395-PA. (In press: posted 1 December 2015)

Mahmoud, M. A., Nasr-El-Din, H. A., and De Wolf, C. A. 2015. High-Temperature Laboratory Testing of Illitic Sandstone Outcrop Cores With HCl-Alternative Fluids. *SPE Prod & Oper* **30** (1): 43-51. SPE-147395-PA. http://dx.doi.org/10.2118/147395-PA.

Nasr-El-Din, H. A., Al-Dahlan, M. N., As-Sadlan, A. M. et al. 2002. Iron Precipitation During Acid Treatments Using HF-Based Acids. Presented at the International

Symposium and Exhibition on Formation Damage Control, Lafayette, Louisiana, 20-21 February. SPE-73747-MS. http://dx.doi.org/10.2118/73747-MS.

Nasr-El-Din, H. A., Hopkins, J. A., Shuchart, C. E. et al. 1998. Aluminum Scaling and Formation Damage Due to Regular Mud Acid Treatment, Presented at the SPE Formation Damage Control Conference, Lafayette, Louisiana, 18-19 February. SPE-39483-MS. http://dx.doi.org/10.2118/39483-MS.

Reyes, E. A., Smith, A. L., and Beuterbaugh, A. 2013. Properties and Applications of an Alternative Aminopolycarboxylic Acid for Acidizing of Sandstones and Carbonates. Presented at the SPE European Formation Damage Conference and Exibition, Noordwijk, Netherlands, 5-7 June. SPE-165142-MS. http://dx.doi.org/10.2118/165142-MS.

Shuchart, C. E. 1997. Chemical Study of Organic-HF Blends Leads to Improved Fluids. Presented at the International Symposium on Oilfield Chemistry, Houston, Texas, 18-21 February. SPE-37281-MS. http://dx.doi.org/10.2118/37281-MS.

Shuchart, C. E., and Gdanski, R. D. 1996. Improved Success in Acid Stimulations with a New Organic-HF System. Presented at the European Petroleum Conference, Milan, Italy, 22-24 October. SPE-36907-MS. http://dx.doi.org/10.2118/36907-MS.

Shuchart, C. E. and Buster, D.C. 1995. Determination of the Chemistry of HF Acidizing with the Use of $^{19}F$ NMR Spectroscopy. Presented at the SPE International Symposium on Oilfield Chemistry, San Antonio, Texas, 14-17 February. SPE-28975-MS. http://dx.doi.org/10.2118/28975-MS.

Simon, D.E. and Anderson, M.S. 1990. Stability of Clay Minerals in Acid. Presented at the SPE Formation Damage Control Symposium, Lafayette, Louisiana, 22-23 February. SPE-19422-MS. http://dx.doi.org/10.2118/19422-MS.

Smith, C.F. and Hendrickson, A.R. 1965. *Hydrofluoric Acid Stimulation of Sandstone Reservoirs*. Original edition. ISBN 978-1-55563-865-8.

Smith, D. J., Kelly, T. R., Schmidt, D. L. et al. 2012. Katz (Strawn) Unit Miscible $CO_2$ Project: Design, Implementation, and Early Performance. Presented at the SPE Improved Oil Recovery Symposium, Tulsa, Oklahoma, 14-18 April. SPE-154023-MS. http://dx.doi.org/10.2118/154023-MS.

Thomas, R.L., Nasr-El-Din, H.A., Mehta, S. et al. 2002. The Impact of HCl to HF Ratio on Hydrated Silica Formation During the Acidizing of a High Temperature Sandstone Gas Reservoir in Saudi Arabia. Presented at the SPE Annual Technical Conference and Exhibition, San Antonio, Texas, 29 September-2 October. SPE-77370-MS. http://dx.doi.org/10.2118/77370-MS.

Thomas, R.L., Nasr-El-Din, H.A., Lynn J.D. et al. 2001. Precipitation During the Acidizing of a HT/HP Illitic Sandstone Reservoir in Eastern Saudi Arabia: A Laboratory Study. Presented at the SPE Annual Technical Conference and Exhibition, New Orleans, Louisiana, 30 September-3 October. SPE-71690-MS. http://dx.doi.org/10.2118/71690-MS.

Wang, B., Jiang, W., Liu, X., and Feng, P. 2000. Acidizing High-Pressure Water Injection Wells Using a New Low-Damage Acetic/HF Acid System. Presented at the International Oil and Gas Conference and Exhibition, Beijing, China, 7-10

November. SPE-64776-MS. http://dx.doi.org/10.2118/64776-MS.

Wehunt, C. D., Van Arsdale, H., Warner, J. L., and Ali, S.A. 1993. Laboratory Acidization of an Eolian Sandstone at 380°F. Presented at the SPE International Symposium on Oilfield Chemistry, 2-5 March, New Orleans, Louisiana. SPE-25211-MS. http://dx.doi.org/10.2118/25211-MS.

Wiggins, H. 2015. Miscellaneous Analysis. Chemplex, Snyder, Texas (10/14/2015).

Yang, F., Nasr-El-Din, H.A., and Al-Harbi, B.M. 2012. Acidizing Sandstone Reservoirs Using HF and Formic Acids. Presented at the SPE International Symposium and Exhibition on Formation Damage Control, Lafayette, Louisiana, 15-17 February. SPE-150899-MS. http://dx.doi.org/10.2118/150899-MS.

Zhou, L. and Nasr-El-Din, H.A. 2013. Interactions of Sandstone Acid Systems with Aluminosilicates. Presented at the SPE International Symposium on Oilfield Chemistry, Woodlands, Texas, 8-10 April. SPE-164050-MS. http://dx.doi.org/10.2118/164050-MS.

# APPENDIX A

If 1000 g mud acid or Al-based retarded mud acid need to be prepared, the composition of the acid will be as follows:

Mud Acid: 15 wt% HCl + 1.5 wt% HF

Fine Control Acid: 15 wt% HCl + 1.5 wt% HF + 5 wt% $AlCl_3 \cdot 6H_2O$

The concentration of HCl is 36.46 wt% and the concentration of $AlCl_3$ solution is Bé=32° which is equivalent to 50 wt%.

The details of the calculation are as follows:

1000 g fine control acid contains 150 g HCl, 15 g HF, and 50 g $AlCl_3 \cdot 6H_2O$.

$$n_{HCl} = \frac{150\ g}{36.5\ g/mol} = 4.095\ mol$$

$$n_{HF} = \frac{15\ g}{20\ g/mol} = 0.75\ mol$$

$$n_{AlCl_3 \cdot 6H_2O} = \frac{50\ g}{241.5\ g/mol} = 0.207\ mol$$

Use ABF (ammonium bifluoride, $NH_4HF_2$) and HCl to generate 0.75 mol of HF.

$$NH_4HF_2 + HCl \leftrightarrow 2HF + NH_4Cl$$

So 0.75 mol HF needs 0.375 mol $NH_4HF_2$ and 0.375 mol HCl to generate.

The total weight of ABF we need is:

$$M_{NH_4HF_2} = 0.375\ mol \times 57 \frac{g}{mol} = 21.38\ g$$

The total amount of HCl we need is:

$$n_{HCl\ total} = 4.095\ mol + 0.375\ mol = 4.47\ mol$$

The total weight of HCl we need is:

$$M_{HCl\ total} = 4.47\ \text{mol} \times 36.5 \frac{g}{mol} = 163.16\ g$$

The total weight of 36.46 wt% HCl solution is:

$$M_{HCl\ Solution} = \frac{163.16\ g}{0.3646} = 447.50\ g$$

$AlCl_3$ solution was provided by Halliburton and the concentration is 50 wt% which is equivalent to Bé=32º . The weight of $AlCl_3$ solution is:

$$M_{AlCl_3\ Solution} = \frac{50\ g}{0.5} = 100\ g$$

The weight of water is:

$$M_{H_2O} = 1000\ g - M_{NH_4HF_2} - M_{HCl\ Solution} - M_{AlCl_3\ Solution}$$

$$= 1000\ g - 21.38\ g - 447.5\ g - 100\ g = 431.12\ g$$

For the mud acid, the calculation will be exactly same except there is no $AlCl_3$ solution. So the weight of water is:

$$M_{H_2O} = 1000\ g - M_{NH_4HF_2} - M_{HCl\ Solution} = 1000\ g - 21.38\ g - 447.5\ g = 531.12\ g$$

# APPENDIX B

Formulas of the three original acidizing plans for the field are as follows:

Acidizing plan A (for the producers):

- Pump 50 gal/ft (4,500 gal) 15 vol% HCl + additives
- Fresh water system (FWS) - 2 wt% KCl water + additives

Acidizing plan B (for the injectors, during water flooding):

- Pump 40 bbl (1680 gal) white water Xylene Spearhead (Pump 20 bbl (840 gal) into perforations, let soak for 30 minutes, continue to pump the remainder of the fluid systems.)
- Pump 20 bbl (840 gal) Slick, FWS - 2 wt% KCl water spacer + additives
- Pump 60 bbl (2,520 gal) Linear 40 ppg (2 wt% KCl water plus additives) pad
- Pump 48 bbl (2,000 gal) 20 vol% HCl Acidtol 80:20 - HCl:Xylene-Dispersion
- Pump 40 bbl Linear 80 ppg guar gel Diverter (FWS-2 wt% KCl water + additives)
- Pump 40 bbl water white Xylene Spearhead + additives
- Pump 20 bbl (880 gal) Slick, FWS-2 wt% KCl water + additives
- Pump 60 bbl (2520 gal) Linear 40 ppg (2 wt% KCl water plus additives) pad
- Pump 48 bbl (2,000 gal) 20 vol% HCl Acidtol 80:20 – HCl:Xylene-Dispersion
- Pump 100 bbl, Slick water flush, 2 wt% KCl + additives & overflush

- Be prepared to hook-up to injection mode as soon as possible after stimulation job ends and continue pumping the injection fluids.

Acidizing plan C (for the injectors, during $CO_2$ flooding):

- Pump 50 bbl of Fresh Water Treated Pre-Flush (FWT PF)
- Pump 40 bbl white water Xylene Spearhead (Pump 20 bbl into perforations, let soak for 30 minutes, continue to pump the remainder of the fluid systems.)
- 36 bbl (1,500 gal) 20 vol% HCl Acidtol 80:20 –HCl:Xylene-Dispersion
- 36 bbl (1,500 gal) FWS (2 wt% KCl water plus additives) spacer
- 48 bbl (2,000 gal) Linear 60 ppg Diverter (FWS 2 wt% KCl + additives)
- 36 bbl (1,500 gal) FWS (2 wt% KCl water + additives) spacer
- 36 bbl (1,500 gal) 20 vol% HCl Acidtol 80:20 - HCl:Xylene-Dispersion
- Overflush w/100 bbl (4200 gal) FWS 2 wt% KCl water + additives)
- Flush with 50 bbl of fresh water treated flush fluid
- Be prepared to hook-up to injection mode as soon as possible after stimulation job ends and continue pumping injection fluids.

# APPENDIX C

The following procedure is used to calculate the amount of fluid needs to inject into the core in the lab as inject 50 gal/ft of the same fluid into the wellbore.

The wellbore conditions are:

- Diameter of the wellbore Dw: 7.875 in.
- Depth of fluid penetration (assumption) Lp: 12 in.
- Injection amount to the wellbore $Q_i$: 50 gal/ft
- Average porosity (assumption) ϕ: 15%

The core conditions are:

- Core diameter Dc: 1.5 in.
- Core length Lc: 3 in.
- Average porosity (assumption) ϕ: 15%
- Injection volume to the core Qc

The coreflood experiments were performed at the same temperature and pressure condition as the wellbore condition. So the density of the fluid keeps the same. Based on mass balance, the volume should also balance.

$$\frac{Q}{\left(\pi\left(\frac{Dw}{2}+L_p\right)^2-\pi\left(\frac{Dw}{2}\right)^2\right)\phi} = pore\ volume = \frac{Q_c}{\pi(\frac{D_c}{2})^2 L_c \phi} \quad (12)$$

Based on Eq. 12, 50 gal/ft of the fluid in the wellbore condition is 8.56 PV, which equals to 111.6 ml fluid. Vise versa, still based on Eq. 12, if 10 PV of fluid was the optimum volume tested in the lab condition, then 59 gal/ft of the fluid should pump into the formation.

# APPENDIX D

Formulas of the three original acidizing plans for the coreflood experiment are as follows. The steps of diverter were skipped because our cores are low permeability cores, the guar gel will block the pores of the cores and fail the coreflood experiments.

Acidizing plan A: Initial acidizing plan for new perforation well

1. Main flush: pump 8.56 PV 15% HCl + Additives

   1000 ml fluid includes:

   - 2 ml of I-112, Corrosion inhibitor (Plexhib 116): 2g/1000g
   - 2 ml of NE-212 (Plexbreak 116) NEFL (non-emulsified iron control HCl): 2g/1000g
   - 4 ml of FE-360 (Reducer) Iron reducer, AS-2A: 4g/1000g
   - 992 ml of 15% HCl

2. Post flush: 2% KCl

   1000 ml fluid includes:

   - 2 ml of choline chloride (Clayplex 600)
   - 0.25 ml Biocide (Plexcide 24L): 1g/4000g
   - 997.25 ml water

Acidizing plan B: Acidizing during the water injection

Well information:

Diameter of the wellbore: 7.875 in

Main flush: 20 vol% HCl Acid injection

1. Pump 3.2 PV white water Xylene Spearhead (Pump 1.6 PV into perforations, let soak for 30 minutes, continue to pump the remainder of the fluid systems.)
2. Pump 1.6 PV Slick, FWS-2% KCl water spacer + additives

   1000 ml fluid includes:

   - 2 ml of choline chloride (Clayplex 600)
   - 0.25 ml Biocide (Plexcide 24L): 1g/4000g
   - 1 ml non-ionic surfactant (Plexsurf 210E)
   - 2.5 ml guar gel (Plexgel 907L-EB)
   - 50 ml EGMBE
   - 944.75 ml water
3. Pump 3.8 PV 20% HCl Acidtol 80:20-HCl: Xylene-Dispersion

   1000 ml fluid includes:

   - 730 ml 20% HCl
   - 50 ml EGMBE
   - 10 ml HCl-Xylene-Dispersion (Acidlink 711)
   - 2 ml I-112, Corrosion inhibitor (Plexhib 116)
   - 4 ml of FE-360 (Reducer) Iron reducer, AS-2A: 4g/1000g
   - 200 ml water white Xylene
4. Pump 3.2 PV water white Xylene Spearhead + additives

   1000 ml fluid includes:

   - 950 ml water white Xylene
   - 50 ml EGMBE

5. Pump 1.6 PV Slick, FWS-2% KCl water + additives

   1000 ml fluid includes:

   - 2 ml of choline chloride (Clayplex 600)
   - 0.25 ml Biocide (Plexcide 24L): 1g/4000g
   - 1 ml non-ionic surfactant (Plexsurf 210E)
   - 2.5 ml guar gel (Plexgel 907L-EB)
   - 50 ml EGMBE
   - 944.75 ml water

6. Pump 3.8 PV 20% HCl Acidtol 80:20-HCl: Xylene-Dispersion

   1000 ml fluid includes:

   - 730 ml 20% HCl
   - 50 ml EGMBE
   - 10 ml HCl-Xylene-Dispersion (Acidlink 711)
   - 2 ml I-112, Corrosion inhibitor (Plexhib 116)
   - 4 ml of FE-360 (Reducer) Iron reducer, AS-2A: 4g/1000g
   - 200 ml water white Xylene

7. Pump 8 PV, Slick water flush, 2% KCl + additives & overflush

   1000 ml fluid includes:

   - 2 ml of choline chloride (Clayplex 600)
   - 0.25 ml Biocide (Plexcide 24L): 1g/4000g
   - 1 ml non-ionic surfactant (Plexsurf 210E)
   - 2.5 ml guar gel (Plexgel 907L-EB)

- 50 ml EGMBE
- 944.75 ml water

Acidizing plan C: Acidizing during the $CO_2$ injection

Diameter of the wellbore: 7.875 in

Fluid penetration: 12 in (Assumption)

Main flush: 20 vol% HCl Acid injection

1. Pump 4 PV of Fresh Water Treated Preflush (FWT PF)
2. Pump 3.2 PV white water Xylene Spearhead (Pump 1.6 PV into perforations, let soak for 30 minutes, continue to pump the remainder of the fluid systems.)
3. Pump 2.9 PV 20% HCl Acidtol 80:20-HCl: Xylene-Dispersion

   1000 ml fluid includes:

   - 730 ml 20% HCl
   - 50 ml EGMBE
   - 10 ml HCl-Xylene-Dispersion (Acidlink 711)
   - 2 ml I-112, Corrosion inhibitor (Plexhib 116)
   - 4 ml of FE-360 (Reducer) Iron reducer, AS-2A: 4g/1000g
   - 200 ml water white Xylene
4. Pump 2.9 PV Fresh Water System (2% KCl water plus additives) Spacer

   1000 ml fluid includes:

   - 2 ml of choline chloride (Clayplex 600)
   - 0.25 ml Biocide (Plexcide 24L): 1g/4000g
   - 1 ml non-ionic surfactant (Plexsurf 210E)

- 2.5 ml guar gel (Plexgel 907L-EB)
- 50 ml EGMBE
- 944.75 ml water

5. Pump 2.9 PV Fresh Water System (2% KCl water plus additives) Spacer

   1000 ml fluid includes:

   - 2 ml of choline chloride (Clayplex 600)
   - 0.25 ml Biocide (Plexcide 24L): 1g/4000g
   - 1 ml non-ionic surfactant (Plexsurf 210E)
   - 2.5 ml guar gel (Plexgel 907L-EB)
   - 50 ml EGMBE
   - 944.75 ml water

6. Pump 2.9 PV 20% HCl Acidtol 80:20-HCl: Xylene-Dispersion

   1000 ml fluid includes:

   - 730 ml 20% HCl
   - 50 ml EGMBE
   - 10 ml HCl-Xylene-Dispersion (Acidlink 711)
   - 2 ml I-112, Corrosion inhibitor (Plexhib 116)
   - 4 ml of FE-360 (Reducer) Iron reducer, AS-2A: 4g/1000g
   - 200 ml water white Xylene

7. Overflush w/ 8 PV FWS 2% KCl water + additives)

   1000 ml fluid includes:

   - 2 ml of choline chloride (Clayplex 600)

- 0.25 ml Biocide (Plexcide 24L): 1g/4000g
- 1 ml non-ionic surfactant (Plexsurf 210E)
- 2.5 ml guar gel (Plexgel 907L-EB)
- 50 ml EGMBE
- 944.75 ml water

8. Flush with 4 PV of Fresh Water Treated Flush Fluid

# APPENDIX E

| Property | Value | Unit |
|---|---|---|
| Medium | Carbon dioxide | |
| State of aggregation | Overcritical fluid | |
| Pressure | 2400 | psi |
| Temperature | 105 | Degree Fahrenheit |
| Density | 794.7099378 | $kg / m^3$ |
| Specific Enthalpy | 284.3550178 | kJ / kg |
| Specific Entropy | 1.236118044 | kJ / kg K |
| Specific isobar heat capacity | 2.557956267 | kJ / kg K |
| Specific isochor heat capacity | 0.927728071 | kJ / kg K |
| Isobar coefficient of thermal expansion | 8.550562356 | $10^{-3}$ (1 / K) |
| Heat conductance | 89.30515422 | $10^{-3}$ (W / m * K) |
| Dynamic viscosity | 70.533104 | $10^{-6}$ (Pa s) |
| Kinematic viscosity | 0.088753268 | $10^{-6}$ $m^2$ / s |
| Thermal diffusivity | 0.442829231 | $10^{-7}$ $m^2$ / s |
| Coefficient of compressibility Z | 0.3502548 | |
| Speed of sound | 450.1027911 | m / s |

Table 11—Property of $CO_2$ at reservoir condition